European Journal of Medicinal Chemistry xxx (2017) 1–32

Contents lists available at ScienceDirect

European Journal of Medicinal Chemistry

journal homepage: http://www.elsevier.com/locate/ejmech

Research paper

NB 06: From a simple lysosomotropic aSMase inhibitor to tools for elucidating the role of lysosomes in signaling apoptosis and LPS-induced inflammation

Markus Blaess [a, b], Nelly Bibak [a], Ralf A. Claus [b, c], Matthias Kohl [a], Gabriel A. Bonaterra [d], Ralf Kinscherf [d], Stefan Laufer [e], Hans-Peter Deigner [a, f, *]

[a] Furtwangen University, Medical and Life Sciences Faculty, Institute of Precision Medicine, Jakob-Kienzle-Str. 17, D-78054 Villingen-Schwenningen, Germany
[b] Clinic for Anesthesiology and Intensive Care, Jena University Hospital, Am Klinikum 1, D-07747 Jena, Germany
[c] Center for Sepsis Control and Care (CSCC), Jena University Hospital, Am Klinikum 1, D-07747 Jena, Germany
[d] Institute of Anatomy and Cell Biology, Department of Medical Cell Biology, University of Marburg, Robert-Koch-Straße 8, D-35032 Marburg, Germany
[e] Pharmaceutical Institute, Department of Pharmaceutical Chemistry, University of Tuebingen, Auf der Morgenstelle 8, D-72076 Tuebingen, Germany
[f] Fraunhofer Institute IZI, Leipzig, EXIM Department, Schillingallee 68, D-18057 Rostock, Germany

ARTICLE INFO

Article history:
Received 1 May 2017
Received in revised form
29 August 2017
Accepted 13 September 2017
Available online xxx

Keywords:
Cellular ceramide quantification
Lysosomotropic compounds
LPS induced inflammation
Lysosomal signaling
Lysosome
aSMase inhibitor

ABSTRACT

Ceramide generation is involved in signal transduction of cellular stress response, in particular during stress-induced apoptosis in response to stimuli such as minimally modified Low-density lipoproteins, TNFalpha and exogenous C_6-ceramide. In this paper we describe 48 diverse synthetic products and evaluate their lysosomotropic and acid sphingomyelinase inhibiting activities in macrophages. A stimuli-induced increase of C_{16}-ceramide in macrophages can be almost completely suppressed by representative compound NB 06 providing an effective protection of macrophages against apoptosis. Compounds like NB 06 thus offer highly interesting fields of application besides prevention of apoptosis of macrophages in atherosclerotic plaques in vessel walls. Most importantly, they can be used for blocking pH-dependent lysosomal processes and enzymes in general as well as for analyzing lysosomal dependent cellular signaling. Modulation of gene expression of several prominent inflammatory messengers IL1B, IL6, IL23A, CCL4 and CCL20 further indicate potentially beneficial effects in the field of (systemic) infections involving bacterial endotoxins like LPS or infections with influenza A virus.

1. Introduction

Apoptosis is a mandatory process in development and control of biological systems and organisms. It takes place under physiological conditions, is accompanying cell growth, cell division and differentiation and is essential for tissue homeostasis and immune response of organisms [1]. Macrophages and smooth muscle cells in the vessel wall are able to internalize cholesterol and modified LDL (mLDL) via scavenger receptors (scavenger receptor class A (SRA I/II/III)) [2,3]. Once macrophages are saturated with (minimally) modified (oxidatively/enzymatically) Low-Density Lipoproteins (mmLDL), they transform into foam cells. Foam cells, however, located in larger gatherings in the vessel wall, form fatty streaks and significantly contribute to plaque formation. Minor injuries result in fibrous plaque containing foam cells or smooth muscle cells, respectively fragments from apoptosis or necrosis. In further steps, a complex injury to the vessel wall with a necrotic core is emerging, finally leading as unstable plaque, to thrombosis or infarction [2]. Macrophages are particularly interesting as a test system for acid sphingomyelinase (aSMase) inhibitors, as they play a crucial role in the development of atherosclerosis and represent a potential therapeutic target for compounds under investigation. In cell culture experiments apoptotic rates of human macrophages correlate with the mmLDL concentration applied [4]. Oxidized phospholipids in mmLDL induce apoptotic signaling in arterial smooth muscle cells via activation of aSMase [5]. In addition to mmLDL, TNFalpha is a prototype activator of aSMase, increasing

* Corresponding author. Furtwangen University, Medical and Life Sciences Faculty, Institute of Precision Medicine, Jakob-Kienzle-Str. 17, D-78054 Villingen-Schwenningen, Germany.
E-mail address: hans-peter.deigner@hs-furtwangen.de (H.-P. Deigner).

https://doi.org/10.1016/j.ejmech.2017.09.021
0223-5234/

concentration of ceramide in cells and inducing apoptosis [6,7]. Unlike mmLDL-stimulated acid sphingomyelinase, neutral sphingomyelinase (nSMase) plays an important role in increasing ceramide levels in lipid extracts of cells. Ceramides with fatty acids of varying chain lengths bound as amides, are components of the sphingomyelin cycle and are well established signaling molecules. Activation of SMases and subsequent ceramide generation is involved in signal transduction of cellular stress response, in particular during stress-induced apoptosis. Sphingomyelin as a substrate of these pathways is a physiologically inert phosphosphingolipid abundant in all eukaryotic cell types [8–10].

(C_{16}-) ceramide with its raft- and transport-vesicles forming characteristics links both pathways [11]. A lysosomotropic compound lacks a direct effect on free enzymes, it is rather an inhibitor of all lysosome-dependent signaling pathways as well as lysosomal luminal enzymes, transporters and structures depending on an acidic pH value. It thus can be used as an enzyme cross-inhibitor of the lysosome for blocking pH-dependent lysosomal processes. Based on this concept, further conclusions on pro-apoptotic stimuli such as mmLDL, TNFalpha, exogenous C_6-ceramide and synthetic ceramide analogues (1R)-(E)-(2-methyl-oxazol-4-yl)-hexadec-2-ene-1-ol (HPL-1R36N) and 4-[(1R)-(E)-1-Hydroxy-3-phenyl-allyl]-(2RS,4R)-2-phenyl-thiazolidin-3-carbonic acid-*t*-butyl ester (HPL-39N) [12] as well as from inhibitor treatment (NB 06 (**23**)) [4] could be derived; in fact they all require an intact lysosome. An active compound not only engages with classic metabolic processes such as proteolysis and degradation of membrane lipids, but also alters presentation of lipid antigens since lysosomal lipid-binding proteins are necessary to present lipid or glycolipid antigens, such as e.g. the four MHC-I-like glycoproteins CD1a-d [13].

Chlorpromazine (**15**), imipramine (**1**) and desipramine (**2**) are used therapeutically as neuroleptics (**15**) or anti-depressants (**1**, **2**) in panic disorder, bulimia and agoraphobia with panic attacks [14]. High concentrations of weakly basic compounds promote detachment of aSMase from intralysosomal membranes and thus, allow proteolytic degradation of this enzyme [15]. The release of the active enzyme from the inner lysosomal membrane and an enhanced proteolytic degradation was suggested as a cause for inactivation. At a concentration of 20 μM, **2** initiates dissociation of 50% of aSMase from the lysosomal membrane-bound substrate sphingomyelin. Complete dissociation is achieved at 50 μM [16]. Since the mid-eighties, compounds like **2** have been known as irreversible inhibitors of aSMase (EC 3.1.4.12) [17,18]. Compound **2** reduces or suppresses enzyme activity, thus completely mimicking a Niemann-Pick syndrome in intact cells when administered at non-cytotoxic concentrations. Neither **15** nor **2** show a similar peeling effect on other acidic lysosomal lipid hydrolases [18,19]. Starting from known lysosomotropic aSMase inhibiting compounds **2** and **15**, we designed and prepared a group of 48 congeners introducing novel structures into potent inhibitors. Synthetic products were characterized in macrophages with regard to anti-apoptotic effects, lysosomotropic activities and aSMase inhibition, using well-known aSMase inhibitors like **1**, **2**, **15** and amitriptyline (**88**) as references. Based on methylamine - a common prerequisite for effective inhibitors (weak base, pKa >6, lipophilic) [15,20], our structural variations comprise: a) introduction of ring systems with varying lengths of carbon chains linking the aliphatic *N*,*N*-dimethylamine and the ring nitrogen, b) 4-methoxy or 3,4-dimethoxy substitution of the phenylethyl moiety, c) replacement of the endocyclic nitrogen by carbon and introduction of an adjacent exocyclic nitrogen ring, d) replacement of the hetero atoms in the ring system (sulfur by oxygen, switch from 10*H*-phenothiazines to 4*H*-phenoxazines) and e) steric restriction of free rotational elements by fusion to additional ring systems or by introduction of carbon double bonds. Unlike previous studies on approved pharmaceutical compounds and their classification as “Functional inhibitors of aSMase” [15,20] based on a structure-activity relationship model (SARM) using three connection-specific values (pKa, log P, steric hindrance factor of the most basic nitrogen atom), the focus here was on a rational design and a targeted variation of distinct structural features for investigating biological activities related to lysosomotropic effects. Due to common prerequisites for the effectiveness towards aSMase (i.e. weak base, pKa >6, lipophilic) parallels to structure-activity relationships found by Kornhuber are inevitable [15,20]. Our results, however, provide accurate statements about partial structures responsible for the (in) efficacy of a compound as lysosomotropic as well as an aSMase inhibitor. Special attention is paid also to the symmetry of compounds (**132** (NB 45)), blockade of basic nitrogen (e.g. **53** (NB 22)) as well as strong increase in lipophilicity due to e.g. fluorine substitution (**113** (NB 32)). Hybridization experiments elucidating time-dependent gene expression effects in human Mono-Mac 6 cells stimulated with the bacterial endotoxin LPS, also in presence of the active lysosomotropic compound **23** (NB 06), have been performed. The results provide further insights into modulating properties of lysosomotropic compounds on gene expression of various inflammatory messengers (interleukins and cytokines).

2. Results and discussion

2.1. Chemistry

Compounds **1**, **2** and **15** are already known as lysosomotropic compounds active as aSMase inhibitors [17,18]. Therefore, in initial syntheses tricyclic compounds **1**, **2** and **15** are modified by incorporating additional *N*-methyl amine moieties like 4-methoxy- or 3,4-dimethoxy-phenylethyl residues. To investigate structure-activity-relationships, compounds with varying ring systems and a shorter aliphatic carbon chain (carbazole (**19**), diphenylamine (**31**), 10*H*-phenothiazine (**41**) and 10*H*-phenoxazine (**36**)), were prepared. Depending on the ring structure, final compounds IVa/b were synthesized using Scheme 1A (6,11-dihydro-5*H*-benzo[b][1] benzazepine (7-ring)), 10*H*-phenothiazines, 10*H*-phenoxazines or Scheme 1B (carbazoles). Each synthesis consists of three steps: spacer attachment to a compound containing a heterocycle (step A), *N*-Alkyl spacer demethylation with 1-chloroethyl chloroformate (ACE-Cl), a reagent for selective *N*-dealkylation of tertiary amines [21] (step B) and finally an *N*-Alkyl spacer substitution (step C). Final compounds based on the same intermediates III are designated as compounds IVa/IVb in Scheme 1/Table 2 in Material and Methods. An overview of inserted residues is given in Scheme 1C. More synthetic details with regard to each subgroup of compounds presented here are provided in the Experimental section.

2.2. aSMase enzyme inhibition and anti apoptotic potential in vital cells (PBMC)

Starting from known aSMase inhibitors **2** and **15** [17,18] a total number of 48 compounds were prepared and tested on PBMCs subjected to aSMase stimulation and mmLDL-induced apoptosis, **2** and **15** were used as reference compounds. Based on results obtained in these experiments, molecules to be synthesized next were designed and a compound library generated. Selected active compounds were further investigated as for biological effects in cell lysates, on TNFalpha-induced apoptosis, ceramide pattern and levels as determined in the lipid extracts of cells, as well as in transcription and gene expression experiments.

Apoptosis assay: PBMC were pre-incubated with 2 μM of each compound for 30 min, then mmLDL (27 μg/mL) or TNFalpha (3 ng/mL) was added, cells incubated 4 h and stained with YO-PRO®-1

Please cite this article in press as: M. Blaess, et al., NB 06: From a simple lysosomotropic aSMase inhibitor to tools for elucidating the role of lysosomes in signaling apoptosis and LPS-induced inflammation, European Journal of Medicinal Chemistry (2017), https://doi.org/10.1016/j.ejmech.2017.09.021

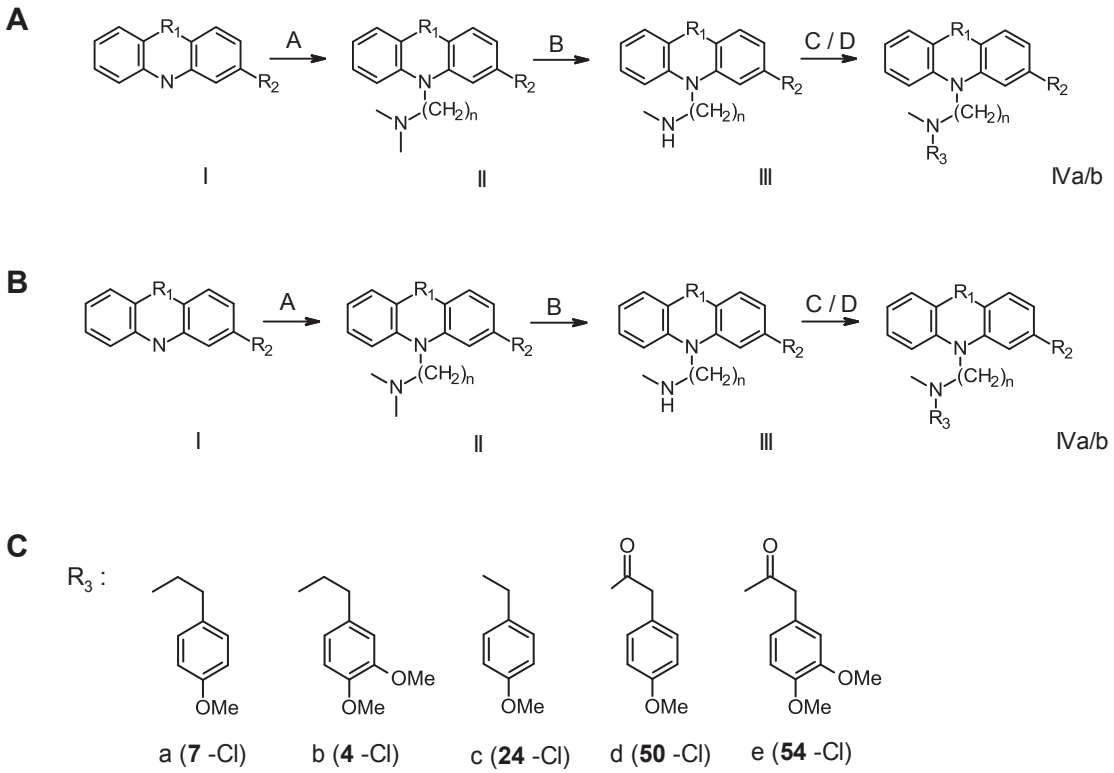

Scheme 1. (A) Synthesis of compounds based on 6,11-dihydro-5*H*-benzo[b][1]benzazepine (7-ring compounds), 10*H*-phenothiazine (**36**), 10*H*-phenoxazine (**41**) (6-ring compounds with hetero atoms) and (B) carbazole (**19**) (5-ring compounds) and (C) inserted residues. Reagents and conditions: (A) 1) *n*-BuLi, dry toluene, −78 °C, 2) *n*-BuLi, dry toluene, $N(CH_3)_2(CH_2)_nCl$, triisobutylalumane (triisobutylaluminum/TIBA), reflux, 24–48 h; (B) 1) $CH_3CHClOCOCl$, triethylamine, CH_2Cl_2, reflux, 1–2 h, 2) MeOH, reflux, 1–3 h; (C) **amines**: *n*-BuLi, dry THF or dry toluene, −78 °C; a-c in dry toluene, TIBA, reflux, 24–48 h (D) **amides**: dry THF, 0 °C or 1,2-dichloroethane, RT; d-e in dry toluene, TIBA, reflux, 24–48 h. Scheme 1A is also applicable to diphenylamine (**31**) derivatives. Abbreviations: I (starting compound), II, III (intermediate compounds), IVa/IVb final compounds based on a common reactant.

(apoptotic cells) and Hoechst 33342 (all cells). Each 4-well plate contained control, apoptotic stimulus, compound and compound plus apoptotic stimulus (n = 3).

aSMase activity assay: PBMC were pre-incubated 30 min with 50, 10, 2 and 0.5 μM of each compound, 27 μg/mL mmLDL was added and incubated for 2 h. Each 24-well plate contained a control, mmLDL (twice) and up to 4 compounds per plate in final concentrations of 50 μM without and 50, 10, 2 and 0.5 μM with mmLDL treatment. aSMase activity in the recovered cell lysates was determined with a semi-automated HPLC method (development see Supplementary data) based on a fluorescently-labeled reactant sphingomyelin (BODIPY FL C_5-sphingomyelin) and product (BODIPY FL C_5-ceramide). The resulting amount of BODIPY FL C_5-ceramide formed is proportional to ceramide, conversion rates were kept less than 15% of the substrate. Residual enzyme activity [%] is calculated by (1 − (conversion rate aSMase, compound/conversion rate aSMase, mmLDL)) x 100. Maximum concentration of 50 μM corresponds to the concentration of reference compound **2**, where 100% of the aSMase is separated from the lysosomal membrane and membrane-bound substrate sphingomyelin [16]. In our experiments, aSMase activity in cells disappeared after 2 h of incubation [17]. Due to primary cell culture (different donors and response) a transformation of readings into a relative scale of 0% (control, spontaneous apoptosis) to 100% (maximum effect mmLDL or TNFalpha) is required. Percentages obtained describe the strength of a compound to reduce the maximal apoptotic effect; accordingly minor values indicate more effective compounds. Results on apoptosis, $IC_{50,aSMase}$, calculated lipophilicity value log P of all tested 50 compounds are given, together with the structures, in Table 1, sorted by ring system/lead compound.

Potential of aSMase inhibition and anti-apoptotic effects: The analysis of results shown in Table 1 (plotted in Supplementary Data Fig. 5) reveals a correlation between aSMase inhibition and anti-apoptotic effects. Since aSMase is an important enzyme in the formation of mmLDL-induced apoptosis, relevant to lysosomal sphingolipid metabolism and activated by mmLDL [4], an anti-inflammatory effect of **2** and **1** or related structures appeared likely. To probe this hypothesis, IC_{50} concentrations and apoptosis rates of imipramine derivatives in response to mmLDL (27 μg/mL) and TNFalpha stimulation (3 ng/mL), were compared. By using compounds with low IC_{50}, we found that the apoptosis rate could significantly be reduced. For mmLDL treated macrophages, IC_{50} concentrations of NB-compounds correlate very well with their anti-apoptotic activities. Most of the compounds displayed show an anti-apoptotic and aSMase-inhibitory effect similar to **1**, which was used as a reference [17]. Having observed this, the low anti-apoptotic activity of **51** (NB 14) and a complete lack of activity of **52** (NB 17), however, is striking. Transition from a tertiary amine (active compound) to an amide (inactive compound) obviously is accompanied by a significant loss of activity, even enhanced further by shortening the distance between ring nitrogen and amide nitrogen (**51**: n = 3, propyl, **52**: n = 2, ethyl). This observation is consistent with the premise of aliphatic, nucleophilic, electron-rich amine nitrogen in the side chain for lysosomotropic/aSMase inhibitory effects of a compound. Similar to mmLDL, TNFalpha-induced apoptosis can be reduced by inhibitors of aSMase,

Please cite this article in press as: M. Blaess, et al., NB 06: From a simple lysosomotropic aSMase inhibitor to tools for elucidating the role of lysosomes in signaling apoptosis and LPS-induced inflammation, European Journal of Medicinal Chemistry (2017), https://doi.org/10.1016/j.ejmech.2017.09.021

Table 1
Chemical structures, relative proportions of apoptotic human macrophages undergoing 27 μg/mL mmLDL or 3 ng/mL TNFalpha treatment, $IC_{50,aSMase}$ of 27 μg/mL mmLDL stimulated human macrophages and calculated log P-values of synthesized carbazoles, 1,2,3,4-tetrahydrocarbazoles, indoles, 10*H*-phenothiazins, 10*H*-phenoxazins, 6,11-dihydro-5*H*-dibenzo[2,1-b:1′,2′-e][7]annulenes, 6,11-dihydro-5*H*-dibenzo[2,1-b:1′,2′-e][7]annulenes, napthalenes, (3*E*)-4-[(Z)-prop-1-enyl]-3-vinyl-1,2,5,6-tetrahydro-1-benzazocines, benzoxazinones, quinazoline-2,4-diones as well as of reference compounds **1** and **15** are shown. Percentages of apoptotic cells (apc) are given in a relative scale of 0−100%. Maximal effect (100%) is achieved by stimuli mmLDL or TNFalpha at conditions specified. Minimum effect (0%) is obtained in untreated control cells (corrected for spontaneous apoptosis). Given percentages thus describe how effectively a compound reduces the maximal pro-apoptotic effect of mmLDL or TNFalpha. Data are shown as means ± *SE*, n = 3. Abbreviations: apc − percentage apoptotic cells, n.d. − not determined.

carbazoles

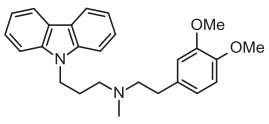

22 (NB 05)
apc_{mmLDL}= 24 ± 4 %; $apc_{TNFalpha}$= 41 ± 3 %
$IC_{50,aSMase}$= 14 ± 4 μM; log P= 6,31 ± 0,56

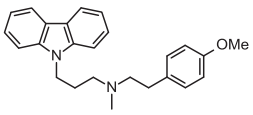

23 (NB 06)
apc_{mmLDL}= 33 ± 5 %; $apc_{TNFalpha}$= 19 ± 5 %
$IC_{50,aSMase}$= 13 ± 3 μM; log P= 6,49 ± 0,56

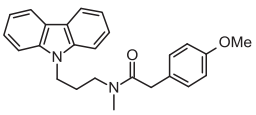

53 (NB 22)
apc_{mmLDL}= 100 ± 1 %; $apc_{TNFalpha}$= n. d.
$IC_{50,aSMase}$= > 250 μM; log P= 5,26 ± 0,58

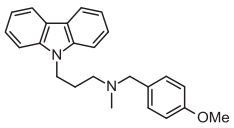

25 (NB 30)
apc_{mmLDL}= 17 ± 4 %; $apc_{TNFalpha}$= n. d.
$IC_{50,aSMase}$= 29 ± 3 μM; log P= 6,21 ± 0,56

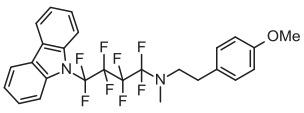

113 (NB 32)
apc_{mmLDL}= 80 ± 6 %; $apc_{TNFalpha}$= n. d.
$IC_{50,aSMase}$= > 250 μM; log P= 13,47 ± 1,03

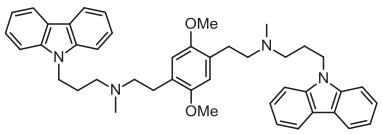

132 (NB 45)
apc_{mmLDL}= 7 ± 5 %; $apc_{TNFalpha}$= n. d.
$IC_{50,aSMase}$= 10 ± 3 μM; log P= 10,84 ± 0,63

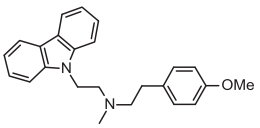

28 (NB 25)
apc_{mmLDL}= 9 ± 6 %; $apc_{TNFalpha}$= 55 ± 5 %
$IC_{50,aSMase}$= 6 ± 2 μM; log P= 6,27 ± 0,56

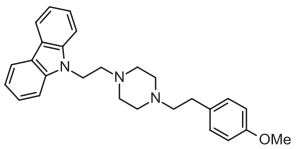

99 (NB 18)
apc_{mmLDL}= 14 ± 5 %; $apc_{TNFalpha}$= 16 ± 5 %
$IC_{50,aSMase}$= 33 ± 3 μM; log P= 5,60 ± 0,60

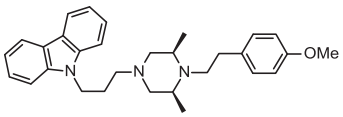

105 (NB 19)
apc_{mmLDL}= 25 ± 4 %; $apc_{TNFalpha}$= 0 ± 1 %
$IC_{50,aSMase}$= 9 ± 1 μM; log P= 6,80 ± 0,59

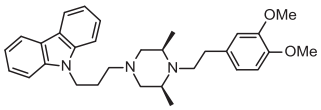

104 (NB 42)
apc_{mmLDL}= 35 ± 6 %; $apc_{TNFalpha}$= n. d.
$IC_{50,aSMase}$= 141 ± 5 μM; log P= 6,62 ± 0,60

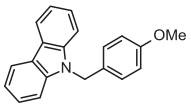

30 (NB 29)
apc_{mmLDL}= 14 ± 3 %; $apc_{TNFalpha}$= 30 ± 4 %
$IC_{50,aSMase}$= 156 ± 2 μM; log P= 5,10 ± 0,54

indoles

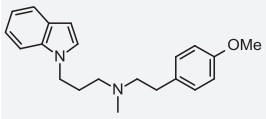

62 (NB 23)
apc_{mmLDL}= 84 ± 5 %; $apc_{TNFalpha}$= n. d.
$IC_{50,aSMase}$= 21 ± 4 μM; log P= 4,92 ± 0,36

1,2,3,4-tetrahydrocarbazoles

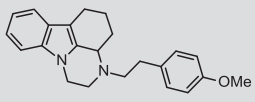

120 (NB 43)
apc_{mmLDL}= 19 ± 5 %; $apc_{TNFalpha}$= n. d.
$IC_{50,aSMase}$= > 250 μM; log 5,55 ± 0,82

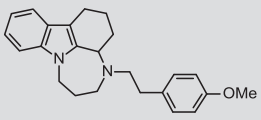

130 (NB 44)
apc_{mmLDL}= 25 ± 5 %; $apc_{TNFalpha}$= n. d.
$IC_{50,aSMase}$= 15 ± 3 μM; log P= 6,00 ± 0,82

10*H*-phenothiazines

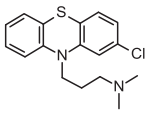

15 (chlorpromazine)
apc_{mmLDL}= n. d.; $apc_{TNFalpha}$= n. d.
$IC_{50,aSMase}$= 11 ± 1 μM; log P= 5,36 ± 0,27

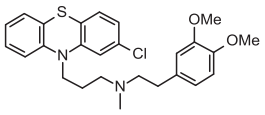

18 (NB 03)
apc_{mmLDL}= 31 ± 6 %; $apc_{TNFalpha}$= 18 ± 5 %
$IC_{50,aSMase}$= 12 ± 3 μM; log P= 7,29 ± 0,37

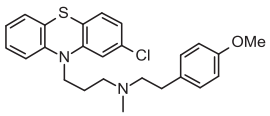

17 (NB 04)
apc_{mmLDL}= 71 ± 4 %; $apc_{TNFalpha}$= n. d.
$IC_{50,aSMase}$= 134 ± 8 μM; log P= 7,47 ± 0,34

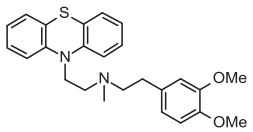

48 (NB 07)
apc_{mmLDL}= 72 ± 9 %; $apc_{TNFalpha}$= n. d.
$IC_{50,aSMase}$= > 250 μM; log P= 6,27 ± 0,37

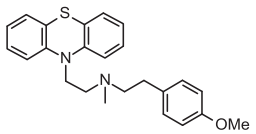

49 (NB 08)
apc_{mmLDL}= 25 ± 6 %; $apc_{TNFalpha}$= 25 ± 5 %
$IC_{50,aSMase}$= 15 ± 5 μM; log P= 6,45 ± 0,36

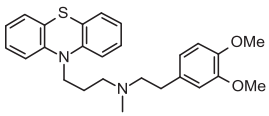

44 (NB 40)
apc_{mmLDL}= 52 ± 5 %.; $apc_{TNFalpha}$= n. d.
$IC_{50,aSMase}$= 16 ± 3 μM; log P= 6,56 ± 0,36

Please cite this article in press as: M. Blaess, et al., NB 06: From a simple lysosomotropic aSMase inhibitor to tools for elucidating the role of lysosomes in signaling apoptosis and LPS-induced inflammation, European Journal of Medicinal Chemistry (2017), https://doi.org/10.1016/j.ejmech.2017.09.021

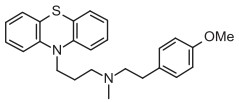

45 (NB 39)

apc_{mmLDL}= 100 ± 5 %; $apc_{TNFalpha}$= n. d.

$IC_{50,aSMase}$= 9 ± 1 μM; log P= 6,74 ± 0,35

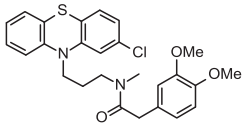

54 (NB 09)

apc_{mmLDL}= 41 ± 5 %; $apc_{TNFalpha}$= n. d.

$IC_{50,aSMase}$= > 250 μM; log P= 6,10 ± 0,40

10*H*-phenoxazines

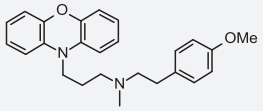

40 (NB 20)

apc_{mmLDL}= 25 ± 5 %; $apc_{TNFalpha}$= 43 ± 4 %

$IC_{50,aSMase}$= 25 ± 2 μM; log P= 4,85 ± 0,51

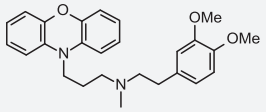

39 (NB 37)

apc_{mmLDL}= 36 ± 6 %; $apc_{TNFalpha}$= n. d.

$IC_{50,aSMase}$= 13 ± 3 μM; log P= 4,67 ± 0,53

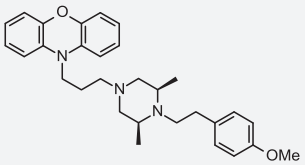

109 (NB 36)

apc_{mmLDL}= 10 ± 5 %; $apc_{TNFalpha}$= n. d.

$IC_{50,aSMase}$= 43 ± 5 μM; log P= 5,16 ± 0,58

6,11-dihydro-5*H*-benzo[b][1]benzazepines

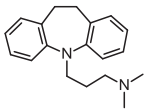

1 (imipramine)

apc_{mmLDL}= 15 ± 4 %.; $apc_{TNFalpha}$= 16 ± 3 %

$IC_{50,aSMase}$= 5 ± 2 μM; log P= 4,47 ± 0,38

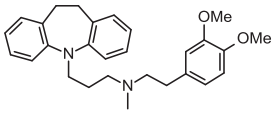

5 (NB 01)

apc_{mmLDL}= 73 ± 6 %; $apc_{TNFalpha}$= n. d.

$IC_{50,aSMase}$= 31 ± 8 μM; log P= 6,39 ± 0,42

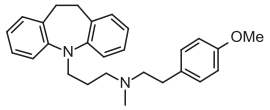

8 (NB 02)

apc_{mmLDL}= 36 ± 6 %; $apc_{TNFalpha}$= 30 ± 4 %

$IC_{50,aSMase}$= 16 ± 1 μM; log P= 6,57 ± 0,41

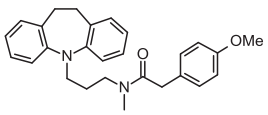

51 (NB 14)

apc_{mmLDL}= 69 ± 5 %; $apc_{TNFalpha}$= n. d.

$IC_{50,aSMase}$= 107 ± 4 μM; log P= 5,35 ± 0,44

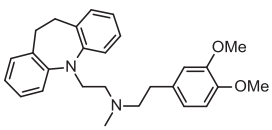

13 (NB 15)

apc_{mmLDL}= 30 ± 6 %; $apc_{TNFalpha}$= 58 ± 5 %

$IC_{50,aSMase}$= 14 ± 0 μM; log P= 6,06 ± 0,43

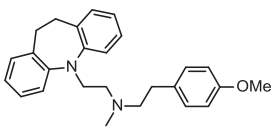

14 (NB 16)

apc_{mmLDL}= 49 ± 7 %.; $apc_{TNFalpha}$= 35 ± 4 %

$IC_{50,aSMase}$= 17 ± 1 μM; log P= 6,24 ± 0,42

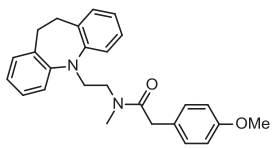

52 (NB 17)

apc_{mmLDL}= 94 ± 5 %; $apc_{TNFalpha}$= 90 ± 4 %

$IC_{50,aSMase}$= > 250 μM; log P= 5,02 ± 0,45

6,11-dihydro-5*H*-dibenzo[2,1-b:1',2'-e][7]annulenes

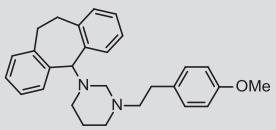

87 (NB 24)

apc_{mmLDL}= 27 ± 4 %; $apc_{TNFalpha}$= 17 ± 3 %

$IC_{50,aSMase}$= 11 ± 4 μM; log P= 6,60 ± 0,42

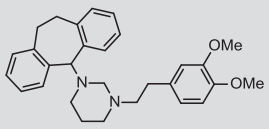

86 (NB 47)

apc_{mmLDL}= n. d.; $apc_{TNFalpha}$= n. d.

$IC_{50,aSMase}$= 22 ± 3 μM; log P= 6,32 ± 0,49

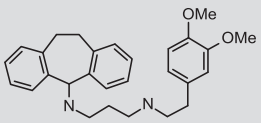

84 (NB 41)

apc_{mmLDL}= 43 ± 5 %; $apc_{TNFalpha}$= n. d. %

$IC_{50,aSMase}$= 39 ± 4 μM; log P= 5,35 ± 0,38

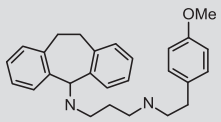

85 (NB 46)

apc_{mmLDL}= n. d.; $apc_{TNFalpha}$= n. d.

$IC_{50,aSMase}$= 17 ± 2 μM; log P= 5,53 ± 0,37

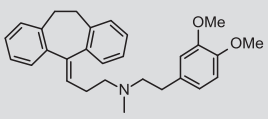

90 (NB 38)

apc_{mmLDL}= 79 ± 5 %; $apc_{TNFalpha}$= n. d.

$IC_{50,aSMase}$= 10 ± 4 μM; log P= 8,07 ± 0,37

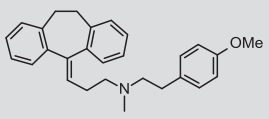

91 (NB 31)

apc_{mmLDL}= 10 ± 4 %; $apc_{TNFalpha}$= n. d.

$IC_{50,aSMase}$= 10 ± 2 μM; log P= 8,25 ± 0,35

4*H*-1,4-benzoxazin-3-ones

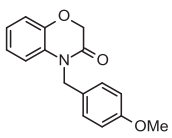

73 (NB 26)

apc_{mmLDL}= 100 ± 2 %; $apc_{TNFalpha}$= n. d.

$IC_{50,aSMase}$= > 250 μM; log P= n. d.

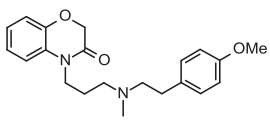

78 (NB 48)

apc_{mmLDL}= n. d.; $apc_{TNFalpha}$= n. d.

$IC_{50,aSMase}$= 38 ± 4 μM; log P= n. d.

Please cite this article in press as: M. Blaess, et al., NB 06: From a simple lysosomotropic aSMase inhibitor to tools for elucidating the role of lysosomes in signaling apoptosis and LPS-induced inflammation, European Journal of Medicinal Chemistry (2017), https://doi.org/10.1016/j.ejmech.2017.09.021

naphthalenes

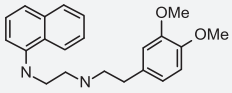

67 (NB 10)
apc_{mmLDL}= 65 ± 4 %; $apc_{TNFalpha}$= n. d.
$IC_{50,aSMase}$= 112 ± 6 μM; log P= n. d.

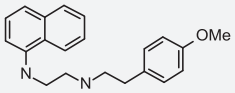

68 (NB 11)
apc_{mmLDL}= 87 ± 6 %; $apc_{TNFalpha}$= n. d.
$IC_{50,aSMase}$= 116 ± 8 μM; log P= n. d.

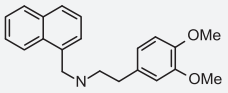

64 (NB 12)
apc_{mmLDL}= 86 ± 5 %; $apc_{TNFalpha}$= n. d.
$IC_{50,aSMase}$= 96 ± 6 μM; log P= n. d.

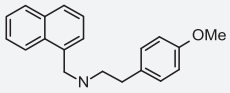

65 (NB 13)
apc_{mmLDL}= 100 ± 1 %; $apc_{TNFalpha}$= n. d.
$IC_{50,aSMase}$= 240 ± 9 μM; log P= n. d.

quinazoline-2,4-diones

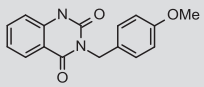

70 (NB 27)
apc_{mmLDL}= 57 ± 7 %; $apc_{TNFalpha}$= 59 ± 6 %
$IC_{50,aSMase}$= > 250 μM; log P= n. d.

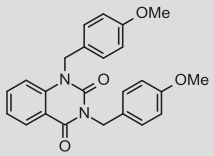

71 (NB 28)
apc_{mmLDL}= 4 ± 2 %; $apc_{TNFalpha}$= n. d.
$IC_{50,aSMase}$= > 250 μM; log P= n. d.

(3E)-4-[(Z)-prop-1-enyl]-3-vinyl-1,2,5,6-tetrahydro-1-benzazocines

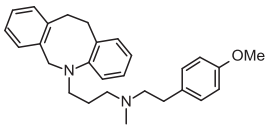

95 (NB 21)
apc_{mmLDL}= 8 ± 5 %; $apc_{TNFalpha}$= 2 ± 5 %
$IC_{50,aSMase}$= 17 ± 2 μM; log P= 6,89 ± 0,41

open B-cycles

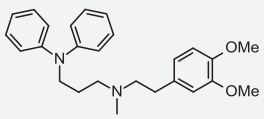

34 (NB 35)
apc_{mmLDL}= 59 ± 4 %; $apc_{TNFalpha}$= n. d.
$IC_{50,aSMase}$= 56 ± 5 μM; log P= 6,01 ± 0,40

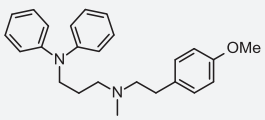

35 (NB 34)
apc_{mmLDL}= 35 ± 5 %; $apc_{TNFalpha}$= n. d.
$IC_{50,aSMase=}$ > 250 μM; log P= 6,19 ± 0,40

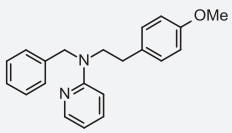

75 (NB 33)
apc_{mmLDL}= 85 ± 5 %; $apc_{TNFalpha}$= n. d.
$IC_{50,aSMase}$= > 250 μM; log P= 5,34 ± 0,35

further supporting the concept that apoptosis-inducing TNFalpha signaling, at least partially, is associated with aSMase [4].

Lysosome-specific chemical properties: The phenomenon underlying the effect of a compound on activity of aSMase in the lysosome is called lysosomotropism. Lysosomal membranes are much more permeable to uncharged compounds (such as weak organic bases) than to charged compounds (ions, protonated weak organic bases). After a passage through the lysosomal membrane, weak organic bases are protonated in the lysosome due to lower pH of 5 present there; charged compounds then can't escape the lysosome and thus accumulate [15]. Known pK_a values of therapeutics (9.30 (**15**), 9.40 (**88**), 9.50 (**1**) and 10.20 (**2**)) indicate an accumulation of these compounds in the lysosome. The physiological pH of active lysosomes thus causes that active compounds with pK_a values higher than 6.0 are protonated at least to 99% within the lysosomal compartment (calculated using Henderson-Hasselbalch equation (IUPAC Compendium of Chemical Terminology)) [22]. 1,3-diamino propane or 1,4-diamino-butane is assumed to be a structural element serving as the mandatory structural prerequisite for the lysosomotropic property of a compound. Basic characteristics can, however, also be introduced via heterocycles (piperazine, oligohydrated diazepine or pyrazine).

Symmetry, ring system, substitution pattern, log P, $IC_{50,aSMase}$ and apoptotic cells: The graphical plot of the proportion of apoptotic cells obtained after administration of compounds containing various heterocycles (Supplementary Data Table 2B) against $IC_{50,aSMase}$, exhibits no favorable ring structure. The size of the central B ring can vary from five to eight atoms with no apparent impact on biological activity. Among six ring systems investigated, the oxygen in the B-ring can be replaced by sulfur and the C-ring can be omitted without losing effectivity (**62** (NB 23)). Unlike the majority of the congeneric compounds, **17** (NB 04) and **35** (NB 34) however, proved significantly less active. **17** (NB 04) is a halogenated compound bearing a chlorine atom at position 2 of the phenothiazine ring. In **35** (NB 34), the B-ring of the carbazole ring system is formally cleaved to give two phenyl rings of a diphenylamine which can freely rotate in space. Interestingly, **18** (NB 03) and **34** (NB 35) can be converted back into active compounds when 3,4-dimethoxylation is applied.

In order to penetrate a lipid membrane, a compound requires adequate lipophilicity while too much lipophilicity may lead to solubility problems in the aqueous environment of the cytosol and in cell culture medium. To investigate a possible relationship between log P and $IC_{50,aSMase}$, log P values of compounds derived from

Please cite this article in press as: M. Blaess, et al., NB 06: From a simple lysosomotropic aSMase inhibitor to tools for elucidating the role of lysosomes in signaling apoptosis and LPS-induced inflammation, European Journal of Medicinal Chemistry (2017), https://doi.org/10.1016/j.ejmech.2017.09.021

15, **2**, **36**, **41** and **19** were calculated. A majority of compounds display a log P between 4.5 (10*H*-phenothiazines) and 8.5 (amitryptilines). Obviously, log P values do not allow a distinction between active and inactive compounds. Despite its pronounced lipophilicity, **132** (NB 45, 10.84 ± 0.63) is active ($IC_{50,aSMase}$ 10 ± 3 μM), **113** (NB 32, log P 13.47 ± 1.03), however, ($IC_{50,aSMase}$ > 250 μM) inactive. **132** (NB 45) is a symmetric compound containing two large aromatic ring systems, carrying no polar, hydrophilic or ionic substituents, and therefore, is lipophilic, but easily protonatable. In contrast, **113** (NB 32), an octafluorobutyl-variant of **23** (NB 06) where the hydrogen atoms of the propyl-chain are completely replaced by fluorine atoms (and the chain extended by one carbon atom), however, is lipophilic, inactive and almost insoluble. A likely explanation is, that due to decreased basicity of the amine-nitrogen (negative inductive effect of fluorine), the ability to form a hydrochloride is considerably reduced in this compound and the equilibrium is on the side of the non-protonated congener **113** (NB 32), thus causing poor solubility in cytosol and cell culture media. A passage through the lysosomal membrane, protonation in the lysosome and subsequent accumulation in the lysosome is thus unlikely. Lipophilicity (in combination with a protonatable base) therefore, is a prerequisite, however, not a sufficient feature for lysosomotropic aSMase inhibitors. In fact, 4-methoxy-compounds exhibit an increased log P value of additional 0.18, when compared to the 3,4-dimethoxy-compounds. They thus are somewhat more lipophilic (with the exception of **17** (NB 04) and **35** (NB34)) and are also more potent aSMase inhibitors. In case of **45** (NB 39)/**17** (NB 04) an increased lipophilicity (+0.73) is observed due to introduction of a new substituent (halogenation at position 2 of the 10*H*-phenothiazine ring). All compounds synthesized on the basis of *N′*-[2-(3,4-dimethoxyphenyl)ethyl]-*N′*-methyl-propane-1,3-diamine proved to be active aSMase inhibitors, suggesting a broader range of possible ring systems than only *N′*-[2-(4-methoxyphenyl)ethyl]-*N′*-methyl-propane-1,3-diamines. A prediction whether the 3,4-dimethoxy and the 4-methoxy substituted compound, however, is active (**45** (NB 39)/**44** (NB 40)) or inactive **18** (NB03)/**17** (NB04) is almost impossible since no further criteria are available. Steric hindrances is a notable parameter, however, as pointed out by Kornhuber et al. in a SPAR model [15], can here be ruled out.

2.3. Effects of structural modifications on aSMase inhibition

Based on structural modifications in our compound library, we can draw the following conclusions about effects associated with each alteration (tabulation and details see associated content/supplementary data, Supplementary Data Table 2A (motif and variation)): a) replacement of the endocyclic nitrogen by an exocyclic double bond: increasing inhibitory activity (transition to triptylines like **88**), b) elimination of basic aliphatic propylamine side chain: weak or no inhibitory activity, c) length of the alkyl amine: no significant effect (sole exception: phenothiazines **48** (NB 07)/**44** (NB 40)), d) substitution pattern of the aliphatic nitrogen: almost complete loss of activity when replacing 4-methoxy-phenyl ethyl by a 4-methoxy-phenyl acetyl residue (sole exception: imipramine derivative **51** (NB14) preserves weak activity), e) cyclic alkyl amines ((dimethyl)-piperazine containing): improvements in activity in 4-methoxy-substituted compounds (**23** (NB 06)/**105** (NB 19)), loss in 3,4-dimethoxy-substituted compounds (**22** (NB 05)/**104** (NB 42)), f) transition from endo- to exocyclic nitrogen: no alterations observable and g) four ring systems - complete fixation of the aliphatic amine: significant variation is evident in aSMase inhibitory activity, however, not in anti-apoptotic activity (the 6 membered ring fixation reveals inhibitory activity).

Regarding the ring structure (tabulation and details see associated content/Supplementary data, Supplementary Data Table 2B (ring structure)) our data suggest that the properties of the ring system in combination with the substitution pattern of the phenylethyl-methyl-aminopropyl moiety in **17** (NB 04)/**45** (NB 39) and **18** (NB 03)/**44** (NB 40) is crucial for an inhibitory effect. Therefore, no conclusion can be drawn, whether a combination, respectively fusion, leads to an inhibitory active or inactive compound. Active compounds are lysosomotropic compounds that act as indirect inhibitors of aSMase. It is, therefore, not too surprising that a clear structure-activity relationship cannot be derived easily.

2.4. Structure-activity relationship for active compounds

As a result of modifications and comparisons, the following structural features emerge: Lipophilicity of a compound is one factor contributing the inhibitory effect among others. Increasing lipophilicity (log P value) does not necessarily result in an improvement and above a threshold rather plays a minor role in terms of lysosome-dependent aSMase inhibition. An excessive increase of lipophilicity (**113** (NB 32)), however, abolishes activity, likely due to trapping of such agents in the membrane. A basic, aliphatic and protonatable side chain with a length of typically three carbon atoms thus emerged as an essential structural element. Both, acetylation of the nitrogen to the corresponding amide, shortening of the side chain, as well as complete fluorination result in a complete loss of activity; protonation of the linker is no longer possible and the amphiphilic character of the compounds is lost. An amphiphilic character is critical for an enrichment into acidic compartments such as lysosomes of living cells. Log P values > 3.0 thus emerged as necessary but not sufficient prerequisite. These findings are consistent with the SPAR model of Kornhuber [15] defining a high pK_a (6–8.5) and Log P values > 3.0 as prerequisites. To improve estimation, an additional factor (so called “steric hindrance factor”) has been introduced for the most basic nitrogen atom. It refers to the two shortest moieties of the basic, under lysosomal conditions protonatable, nitrogen and the number of non-hydrogen atoms. According to our results presented here, inductive, mesomeric and genuine steric (molecular geometric) effects rather appear responsible for varying activities as aSMase inhibitors of compounds. An observed inactivity of amides **52** (NB 17), **53** (NB 22), **54** (NB 09) and the lack of activity of compound **113** (NB 32), the octafluoro-butyl-variant of **23**, is compatible with this interpretation. Notably, results obtained here are exclusively linked to effects in (primary) cell culture. Application in living organisms will likewise include effects of metabolism, not included here.

2.5. Potential applications of lysosomotropic aSMase inhibitor *23* *(NB 06) as reference compound*

22 (NB05) and **23** (NB06) are the first cellular aSMase inhibitors containing a carbazole ring and a 4-methoxy or (3,4-dimethoxyphenyl)ethyl residue as substituent of the aliphatic amine nitrogen. After considering the structure-activity relationships we investigated the biological impact of **23** in stimulated macrophages in terms of anti-apoptotic characteristics. Starting with an extended measurement of aSMase activity in mmLDL/TNFalpha treated cells to determine concentration and time dependence of the inhibitory/lysosomotropic effect of **23,** a reaction profile of **23** was derived and then compared with the symmetrically substituted 2,5-dimethoxy compound **132** (NB 45). Next, apoptosis prevention by **23** and relation to C_{16}-ceramide suppression was investigated. C_{16}-ceramide is an indicator and endogenous inducer of apoptosis [23]. Further, a hybridization experiment was performed to investigate time-dependent

Please cite this article in press as: M. Blaess, et al., NB 06: From a simple lysosomotropic aSMase inhibitor to tools for elucidating the role of lysosomes in signaling apoptosis and LPS-induced inflammation, European Journal of Medicinal Chemistry (2017), https://doi.org/10.1016/j.ejmech.2017.09.021

lysosomotropic effects on gene expression and bacterial endotoxin/LPS stimulation in human Mono-Mac-6 cells. The emphasis here was placed on changes of inflammatory messenger concentration. To ensure that **23** can enter the cell and the lysosome in sufficient quantities, macrophages were treated prior to stimulus addition. Chloroquine is known to exhibit a lysosomotropic effect (increase of lysosomal pH value) immediately after application to the cell culture medium showing a maximum after 2 min, followed by a sustained plateau phase [24]. A 30 min preincubation of cells with **23** provided sufficient preconditioning prior to stimulation.

2.6. aSMase inhibition, sphingomyelin hydrolysis and lysosomotropic activity

Based on the data of aSMase inhibition in human fibroblasts (25 μM **2**, approx 20% residual aSMase activity after 2 h incubation) [18] and measurement of anti-apoptotic effects of each compound in macrophages (4 h incubation with mmLDL, 27 μg/mL, or TNFalpha, 3 ng/mL), 2 h incubation time and same mmLDL/TNFalpha concentrations were chosen. A preincubation of macrophages (30 min) with 0.5, 2, 10 and 50 μM of **23** or **132** (NB 45) is performed to ensure equilibration of cells with test compounds. In order to exclude solvent effects, DMSO concentrations of 70, 35, 14.07, 2.81 and 0.70 mM were additionally tested, corresponding to final concentrations of DMSO (max 0,5%) in the medium due to dilution of stock solutions of **23** or **132** (NB 45).

Macrophages treated solely with DMSO dilutions corresponding to final concentrations of DMSO as solvent for **23** in the medium do not exhibit any concentration-dependent inhibition of aSMase activity. An inhibitory effect of the solvent DMSO (e.g. with the addition of **23** (Fig. 1A)), could be ruled out. DMSO is largely inert with respect to aSMase activity, rather showing a slightly activating effect on aSMase (Fig. 1A). After incubation of macrophages with apoptosis inducers like mmLDL and TNFalpha, aSMase activity increases to 1.70 ± 0.024 fold (mmLDL) and 1.90 ± 0.016 fold (TNFalpha) of the untreated control. A marginal increase in activity is also obtained in pretreated macrophages up to 2 μM **23**. At concentrations higher than 2 μM, **23** (NB06) begins to inhibit aSMase activity. In a concentration interval from 2 to 50 μM, aSMase activity results in a sigmoidal curve in a first approximation. It extends across the whole concentration interval in absence of aSMase inducing triggers. Our data reveal that TNFalpha is more potent than mmLDL in inducing aSMase activity. TNFalpha-treated macrophages show highest aSMase activity. As a result, higher concentrations of **23** are required to achieve the same inhibitory effect. Accordingly, an mmLDL-induced activation can be intercepted with relatively low concentrations of **23**. Partial induction of aSMase activity in mmLDL or TNFalpha stimulated macrophages veileds the original sigmoidal curve. Since a lysosomotropic effect is expected as the cause of aSMase inhibition, the onset of action very abruptly already occurs at minor concentration increases of **23**. Measuring points at 10 (high activity) and 50 μM (completely inhibited) approved to be too far enough apart to represent the curve properly. Accordingly, concentration- and time-dependence of inhibition in mmLDL-stimulated macrophages were investigated further. To ensure detection of aSMase enzyme activity over the entire time interval (0–2 h) a maximal concentration of 25 μM **23** was chosen. Activity at the beginning of the incubation period with mmLDL (t = 0 min) was of particular interest, since effects of 30 min preincubation with **23** can be observed. At this time, lysosomotropy (according to Hurwitz [18] and Ohkuma [25]) is already well developed. Implementation in 24-well cell culture dishes allows an uniform distribution in 30 min segments for a test batch. Based on preliminary results, time points between 0 and 30 min had not been taken into consideration. Overall, Fig. 1B displays a concentration dependency of the inhibitory effect. Even at higher concentrations of **23** aSMase, activity is not depleted constantly. Activity increases slightly at the beginning to fall towards the end of the observation period, corresponding to values given in Fig. 1A (concentration dependence at 2 h). Strongest activation of aSMase (by mmLDL) is present after 30–60 min of incubation. After that, activity decreases significantly, in particular with regard to the two higher concentrations tested. At the two low concentrations, activity, however, remains significantly increased (2-fold). It is also noteworthy, that at the beginning of incubation with mmLDL or after 30 min with **23,** a slight increase of aSMase activity at concentrations up to 10 μM of **23** was observed. Obviously **23** affects integrity of the lysosomal membrane and activates aSMase. This effect is rather low compared to the activation of aSMase by mmLDL, however, detectable. The symmetrically substituted 2,5-dimethoxy-benzene **132** (NB45) shows a good approximation to a sigmoid curve in a logarithmic concentration plot (Fig. 1C). The inhibition curve of aSMase (Fig. 1A, D) is similar in shape to a titration curve of a weak protolyte (weak bases and acids) (IUPAC Compendium of Chemical Terminology) [22] and is typical for lysosomotropic compounds and their downstream inhibitory effects on lysosomal targets (enzymes; amphiphilic compounds), respectively for processes involving the lysosome as an important compartment [26]. The same type of graph occurs in concentration-dependent inhibition of virally infected cells (Sindbis viruses in BHK-21 cells) by chloroquine [27]. Fig. 1A and C assigns lysosomotropic properties to **23**, Fig. 1C lysosomotropic properties to **132** (NB 45). A direct and immediate action of **23** (NB06) or **18** (NB03) on aSMase on the other hand is undetectable (Fig. 1D). At concentrations of 100 μM **23** (NB06) or **18** (NB03), enzyme activity in the cell lysate remains at control level.

2.7. C_{16}-Ceramide generation and lysosomotropic activity

Initial studies on the effect of acid lysosomal pH on ceramide production had been carried out in 1998 [6], long before the discovery of a unique property of aCERase (the hydrolase − synthase switch) in 2003 [24] or before C_{16}-ceramide was identified as the strongly elevated ceramide species in apoptosis [23]. TNFalpha (10 ng/mL) induces apoptosis in human monocytes (U937 cells) and murine fibroblasts (L-929 cells) via generation of ceramide (measured as total ceramide). Lysosomotropic ammonium chloride prevents TNFalpha- and exogenous C_2-ceramide- (10 μM) induced formation of endogenous ceramide and apoptosis [6]. Our own studies in cultured human fibroblasts indicate that free exogenous ceramide (here C_6-ceramide) induces apoptosis in human fibroblasts and increases (total) ceramide levels in the lipid extract. Using **23**, both, rate of apoptosis stimulated by C_6-ceramide and mmLDL as well as the increase in ceramide levels could be prevented in these cells [4]. In all previous studies, however, only total ceramide levels have been determined using the DAG quantification method, without differentiation of individual ceramide species. Using an improved ceramide analysis and a modified test, we could show that an increase of endogenous C_{16}-ceramide takes place mainly in cells stimulated with mmLDL, TNFalpha or exogenous C_6-ceramide [28]. In parallel, cells were additionally incubated in combination with **23** in order to check, whether **23** is able to prevent an increase of the apoptosis marker C_{16}-ceramide in apoptotically stimulated cells. Due to the primary therapeutic goal of **23** administration, prevention of apoptosis in macrophages located in atherosclerotic plaques, tests were performed in macrophages from primary culture including a 30 min preincubation with **23** prior to stimulation. Using the same experimental approach, it can also be determined whether macrophages respond

Please cite this article in press as: M. Blaess, et al., NB 06: From a simple lysosomotropic aSMase inhibitor to tools for elucidating the role of lysosomes in signaling apoptosis and LPS-induced inflammation, European Journal of Medicinal Chemistry (2017), https://doi.org/10.1016/j.ejmech.2017.09.021

to exogenous C_6-ceramide with a C_{16}-ceramide increase (bridging aSMase) and whether this effect can be blocked by **23**. Notably, treatment with **23** reveals that aSMase activity or an intact lysosome is required for C_{16}-ceramide formation and C_6-ceramide indirectly induces apoptosis in cells. To exclude solvent effects, cells were incubated with (non apoptosis-inducing) C_2-dihydroceramide and with DMSO (data not shown). All other long-chain ceramides were quantified in addition to apoptosis-related C_{16}-ceramide. In cells treated with C_6-ceramide to induce apoptosis, no increased C_6-ceramide levels could be detected. In terms of suppression of apoptosis by **23**, ceramide quantification is focused on C_{16}- and $C_{24:1}$-ceramide (Fig. 1E–H). mmLDL (54 μg/mL), TNFalpha (3 ng/mL) and exogenously added C_6-ceramide (10 μM) all trigger an increase of C_{16}-ceramide levels in macrophages after 4 h incubation. mmLDL and TNFalpha cause an increase of C_{16}-ceramide level by a factor of 2–3 of untreated controls, exogenous C_6-ceramide, however, up to 7-fold. **23** is able to suppress the increase of C_{16}-ceramide levels in macrophages in response to all stimuli to effectively keep it on the control level. Since the increase of C_{16}-ceramide levels is a marker for induction of apoptosis in cells, this test result is a strong indicator that **23** has anti-apoptotic activities and provides effective protection of macrophages against apoptosis via this mechanism. **23** itself shows no significant impact on the C_{16}-ceramide level in macrophages and behaves almost inert, similar to the non-apoptotic C_2-dihydroceramide (Fig. 1G). A just slightly elevated C_{16}-ceramide level of C_6-ceramide-stimulated macrophages preincubated with **23** indicates almost complete inhibition of C_{16}-ceramide synthesis by lysosomal aCERase; apparently, the lysosomotropic effect of 10 μM **23** raising the lysosomal pH is not sufficient to completely block the ATP-independent reverse ceramide synthase activity of aCERase over the entire incubation period; an accumulation of C_{16}-ceramide occurring due to a lack of aCERase activity is an alternate explanation.

2.8. LPS-induced altering in gene expression and lysosomotropic activity of NB 06 (*23*)

Several lysosomal enzymes are key players of the sphingomyelin cycle regulating the sphingolipid rheostat. Nevertheless, an intact lysosome is necessary to present lipid or glycolipid antigens [13]. LPS (*E. coli* serotype 0111:B4) stimulates inflammation-related genes in Mono-Mac-6 cells. When using **23** (NB 06) as a lysosomotropic compound in hybridization experiments, addressing inflammation-related genes provides an insight into lysosome-dependent gene expression. For this purpose, total RNA of LPS- (1 ng/mL) ± 5 μM **23** (pre-incubation 30 min) or 5 μM **23** alone (without LPS) was isolated from Mono-Mac-6 cells after treatment for a period of 1, 2, 4 or 6 h, transcribed, labeled and subjected to microarray analysis. To this end, cDNA was labeled with DY-647-S-NHS-dye and co-hybridized with DY-548-S-NHS-dye labeled cDNA - obtained from untreated Mono-Mac-6 cells (control) - on a LabArraytor human 60-inflammation oligonucleotid-chip (SIRS-Lab GmbH, Jena, Germany) comprising 780 inflammation-related, well-characterized human gene-probes as well as 22 controls.

Overall 374 genes were recognized as differentially expressed (alteration > 1.5-fold) under these conditions (Fig. 2A). Compound **23** itself triggers overall 252 differentially expressed genes over the incubation period, indicating that the lysosome is involved in regulating homeostasis of several inflammation-related genes. The number of altered genes changes across the incubation period. Maximum alteration is found after 2 h (227 genes) followed by 1 h (190 genes), 4 h (151 genes) and, finally, 6 h (119 h) (Fig. 2A). To illustrate groups of altered genes, heatmaps clustering genes of similar behavior were generated (Fig. 2B and C). An improved comparability can be obtained by subtracting the mean value from the normalized intensities. Due to displaying logarithmic data, values shown represent log-fold changes with respect to the overall mean. In the subsequent heatmap a color code is used depicting changes greater than log2 (3) or smaller than −log2 (3) by maximum color intensity. Clustering of probes has been computed using function kmeansGap from our R package “SLmisc” [29]. This function implements k-means clustering where the number of clusters is determined via the gap-statistics [30]. Clustering of all samples was computed using hierarchical clustering with method “complete” and Pearson's sample correlation distance. Gap-statistics identifies 13 distinct gene-clusters. Applying the same procedure on **23** treated cells (Fig. 2B) gap-statistics identifies 4 distinct gene-clusters (Fig. 2C).

Notably, **23** is not completely indifferent in terms of gene expression. A small number of genes (e.g. IFNA13, maximum + 41.95 (1 h), FCGR2B, maximum + 2.93 (4 h) and HSPA1A, maximum + 2.67 (4 h)), all flagged “good”, exhibit a time-dependent up-regulation (green cluster). A group of well-known cytokines and chemokines exhibits profound down-regulation at the end of the observation period (6 h) (blue cluster): CXCL3 (- 4.67), CCL4 (- 7.41), CCL20 (- 5.68), CXCL10 (- 6.70) and CXCL2 (- 5.44) are significantly down-regulated. Inducible prostaglandin-endoperoxide synthase 2 (PTGS2) and intercellular adhesion molecule 1 (ICAM1) also belong to this group of genes. The observed effect, however, is less pronounced (PTGS2: - 2.23, ICAM1: - 1.79) (oligo nucleotide array, Fig. 3D). Four genes were analyzed by real-time PCR in addition (Fig. 3E): CXCL2 (real-time PCR-oligo nucleotide array comparison), IL6 (missing spots on this oligo nucleotide array, but well-known LPS inducible gene in Mono-Mac-6 cells), IL23A and TNFalpha (flagged „found“, weak spot, but classified differentially regulated). When comparing the array and real-time PCR expression profiles of CXCL2, only minor fold-change differences are observed; maximum effect of LPS occurs after 4 h incubation time. Among the genes altered, IL6 exhibits the most powerful increase in mRNA expression (+76.46) followed by CCL4 (+18.52), CXCL3 (+13.52), CXCL2 (+13.17) and IL23A (+10.78). As for apoptosis-related genes, CXCL10 and TNFalpha, as well as the oxidative stress inducible PTGS2 demonstrate just a slight increase in expression (3–5 times control level). **23** is capable to significantly reduce LPS-induced expression of all genes under investigation, at least at one point in time. Fig. 3A–C depicts representative scans of one subarray (4 h incubation time) consisting of four blocks. Genes indicated in Fig. 3D and TNFalpha (Fig. 3E) are marked with arrows in Fig. 3A–C. Accordingly, LPS-up regulated genes presented in Fig. 3A (10 ng/mL LPS) (bright red) turn into light red or green colored genes in Fig. 3B (10 ng/mL LPS + 5 μM **23** (NB 06)) and Fig. 3C (5 μM **23** (NB 06)). Highest quenching effects (fold changes) displayed CXCL2 (9.35, 6 h) and IL23A (6.29, 4 h and 6.51, 6 h). Altered expression of genes on response to **23** are involved into the following biological processes (overview): CXCL3, CXCL2 - neutrophil trafficking, CCL4 - macrophage and NK cell migration; T cell–DC interactions, CCL20 - homeostatic, Th17 responses; B cell and DC homing to gut-associated lymphoid tissue, CXCL10 - inflammatory, Th1 response; Th1, CD8, NK trafficking, apoptosis [31], PTX3 - promoting fibrocyte differentiation, regulating inflammation and complement activation, essential component of humoral innate immunity [32], PTGS2 - inducible enzyme (constitutively expressed in brain and kidney), expression activated in a variety of cells in response to cytokines, mitogens and endotoxins [33], involved in inflammatory processes in tumor progression (in PTGS2 deficient mice) [34], ICAM1 - leukocyte adhesion and leukocyte transendothelial migration (TEM) [35], IL23A - mediating innate and adaptive arms of the immune system (expressing the IL-23 receptor)) [36], IL6 – most inflammatory cytokine [37], and TNFalpha – a multifunctional pro-

Please cite this article in press as: M. Blaess, et al., NB 06: From a simple lysosomotropic aSMase inhibitor to tools for elucidating the role of lysosomes in signaling apoptosis and LPS-induced inflammation, European Journal of Medicinal Chemistry (2017), https://doi.org/10.1016/j.ejmech.2017.09.021

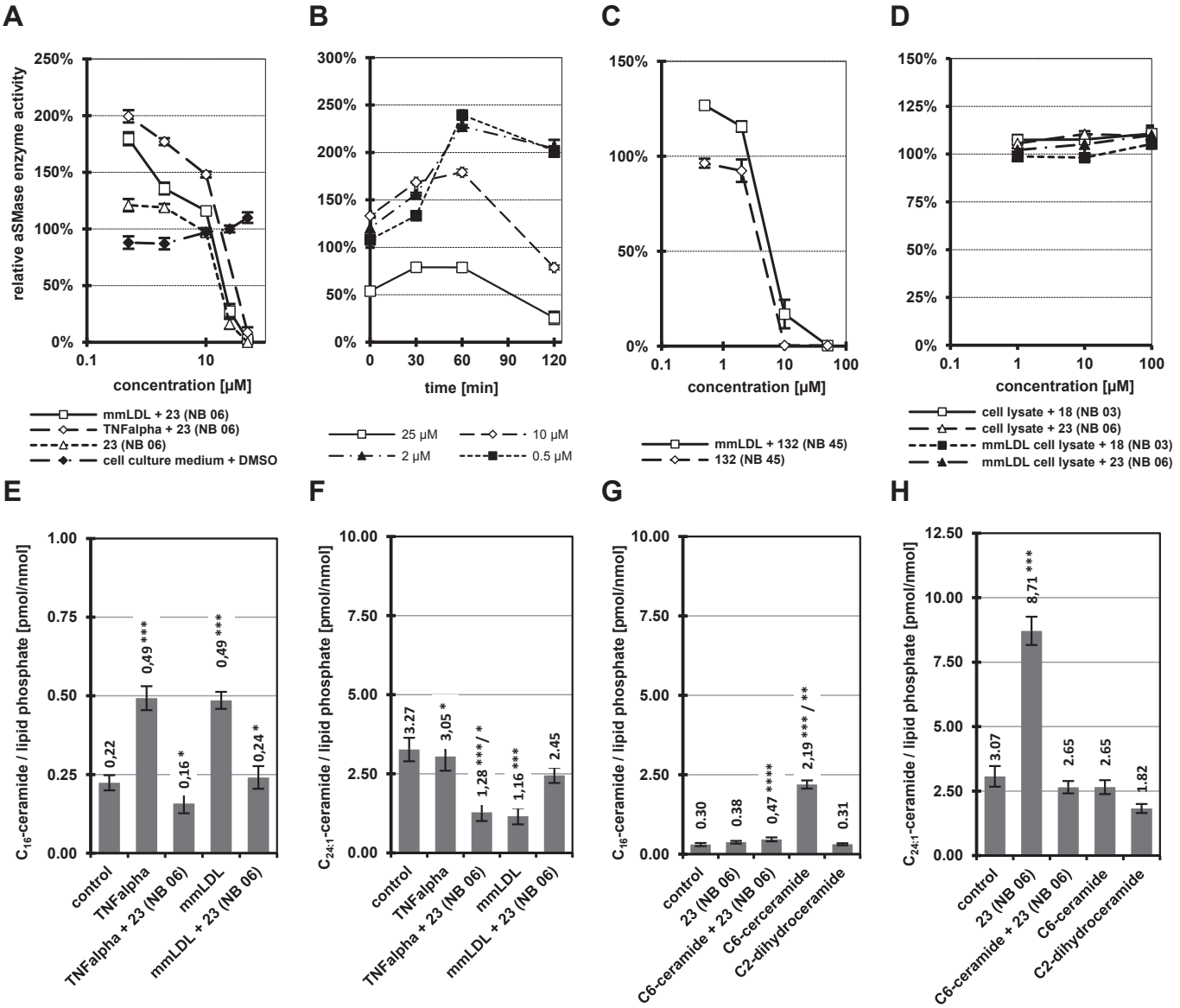

Fig. 1. (A) aSMase inhibitory activity of **23** (NB 06) in human macrophages. Macrophages were stimulated 2 h with 27 µg/mL mmLDL or 3 ng/mL TNFalpha and in combination with 50, 25, 10, 2 and 0.5 µM **23** as well as **23** (preincubation 30 min) and a corresponding DMSO/cell culture medium dilution (testing solvent effects). aSMase activity was determined by measuring the turnover of BODIPY FL C_5-sphingomyelin (substrate) to BODIPY FL C_5-ceramide using HPLC separation and quantification of both BODIPY FL C_5-labeled compounds. Stimulated cells revealed a turnover of 170 ± 2.4% (mmLDL) and 193 ± 1.6% (TNFalpha) of untreated control (at 37 °C). (B) Time dependency of aSMase inhibitory effect using various concentrations of **23**. 30 min pretreatment with final concentrations of 25, 10, 2 and 0.5 µM **23** and stimulation 0, 30, 60 and 120 min with mmLDL (27 µg/mL) stimulated cells (120 min incubation time) revealed a turnover of 188 ± 4.3% of untreated control (at 37 °C). (C) Inhibitory effects of **132** (NB 45) in human macrophages. Macrophages were pretreated 30 min with 50, 10, 2 and 0.5 µM **132** and stimulated 2 h with 27 µg/mL mmLDL according to (B). (D) aSMase inhibitor activity of compounds **18** (NB 03), **23** (NB 06) and **132** (NB 45) in cell lysates of cultured human macrophages. Each compound was added in final concentration of 1, 10 and 100 µM to an aSMase cell lysate w/o mmLDL 27 µg/mL stimulation containing 250–400 µg/mL protein (determined as bovine serum albumin). Turnover of BODIPY FL C5-sphingomyelin is determined as described in (A). (E–H) Induction and quantification of selected individual ceramide species in human macrophages after 4 h stimulation with compounds indicated. If **23** is applied, cells were pre-incubated 30 min with 10 µM **23** prior to stimulation. (E) C_{16}-ceramide and (F) $C_{24:1}$-ceramide level in macrophages after 4 h treatment with 54 µg/mL mmLDL and 3 ng/mL TNFalpha and in combination with 10 µM **23**. (G) C_{16}-ceramide and (H) $C_{24:1}$-ceramide level after treatment with **23**, 10 µM semi-synthetic exogenous C_6-ceramide w/o **23** and 10 µM C_2-dihydroceramide. Ceramide levels were shown as means ± SE, n = 3. One-way ANOVA in combination with post-hoc t-tests and Bonferroni's correction for multiple testing, $P < 0.0001$ (1-way ANOVA); significant with $P < 0.05$: *** versus control, * mmLDL/TNFalpha versus mmLDL/TNFalpha + 23, ** versus C2-dihydroceramide, **** versus exogenous C6-ceramide.

inflammatory cytokine belonging to the tumor necrosis factor super family. These genes are playing a central role in a variety of biological processes such as apoptosis, induction of genes, lipid metabolism, cytokine secretion, cell activation, cell death, cell adhesion, cell differentiation, cell stimulation and cell proliferation [38]. With regard to biological impacts of altered genes and their interactions, **23** in fact interferes with inflammatory responses of Mono-Mac-6 cells and prevents host's response. Interestingly, a modulating effect is already present without triggering inflammation (by LPS). Cytokine as well as chemokine and enzyme homeostasis are influenced by **23** in particular at 6 h incubation time. A 30 min pre incubation period only triggers the well known lysosomotropic effect of **23** without any significant impact on gene expression. No alteration is observable after 2 h with exception of TNFalpha (−3.78). Early inhibition of TNFalpha expression reducing the pool of available TNFalpha in cells, may be a reason for

Please cite this article in press as: M. Blaess, et al., NB 06: From a simple lysosomotropic aSMase inhibitor to tools for elucidating the role of lysosomes in signaling apoptosis and LPS-induced inflammation, European Journal of Medicinal Chemistry (2017), https://doi.org/10.1016/j.ejmech.2017.09.021

preventing a long-lasting induction of ICAM1 expression (1.94 (2 h), 2.88 (4 h) and 2.90 (6 h)), since ICAM1 expression is known to be induced by TNFalpha (in human HUVECs) [35]. IL6 plays a key role in the development and maintenance of autoimmune diseases, cross-talks with IL1B and TNFalpha. Further, it is known that IL1B induces IL6 expression [39]. In fact, the inhibitor **23** diminishes IL1B expression over the entire observation period (−1.70 (1 h), −3.16 (2 h), −5.61 (4 h), −4.57 (6 h)) resulting in a down-regulation of IL6 expression. Unlike IL6 and IL1B, IL23A reveals only a slight down-regulation in response to **23** after 6 h when analyzing PTGS2 and ICAM1. Endotoxin induced expression of PTGS2 and ICAM1 is inhibited by **23** as all other genes analyzed herein.

3. Conclusion

Compounds synthesized show distinct potencies as aSMase inhibitors as determined by inhibition of enzymatic activities in whole cells; structure-activity relationships have been examined. Further active compounds could be added to the known chlorpromazines, imipramines and tricyclic carbazoles: phenoxazines, 11,12-dihydro-6*H*-dibenzo [b, f] azozines and the bicyclic ring system 4*H*-benzo [1,4] oxazin-3-one have been introduced as aSMase inhibitors. No significant further improvement could be obtained with the novel compounds in terms of aSMase inhibition (lower $IC_{50,aSMase}$ concentrations in whole cell assays). Structural variations, however, allowed the definition of groups required for inhibition.

Due to the lack of a direct effect on the free enzyme, compounds such as **23** do not qualify as specific inhibitors of aSMase, rather as inhibitors of enzymes, transporters, structures and signaling pathways dependent upon a luminal acidic pH of the lysosome. Accordingly, **23** can be used for blocking pH-dependent lysosomal processes and enzymes and for the analysis of lysosome-dependent cellular signaling. Lysosomal inhibition reduces cellular apoptosis by blocking synthesis and increase of the endogenous pro-apoptotic messenger C_{16}-ceramide, induced e.g. by mmLDL, TNFalpha and exogenous C_6-ceramide (Fig. 1E and F). In all cases, an intact lysosome is required, playing an important role in formation of C_{16}-ceramide in apoptotic cells. Among ceramide-dependent signaling, C_6-ceramide exhibits special characteristics. On one hand C_6-ceramide induces an increase of endogenous C_{16}-ceramide, on the other hand, it can serve as a substrate in aCERase-mediated generation of sphingosine. Effects of **23** reveal that a bridging of the lysosome by exogenous C_6-ceramide does not occur. Thus, our data indicate that only a specific increase of C_{16}-ceramide in cells is triggered during apoptosis, an observation matching previous results [23]. Upon blocking lysosomes using **23**, $C_{24:1}$-ceramide accumulates due to a lack aCERase turnover in the lysosome. The classical, energy-consuming palmitoyl-CoA serine dihydroceramide pathway of synthesis of long chain ceramides like $C_{24:1}$-ceramide, however, still remains active.

As derived from molecular mechanisms of action, a very important point of our study relates to the scope of potential applications of compounds under investigation. Besides prevention of apoptosis of macrophages in atherosclerotic plaques in vessel walls, compounds like **23** offer additional interesting fields of application. Modulating gene expression of various prominent inflammatory messengers like IL1B, IL6, IL23A, CCL4 and CCL20 show beneficial effects in the field of (systemic) infection involving bacterial endotoxins like LPS, targeting the TLR4 receptor pathway in sepsis [40]. Furthermore, infections with influenza A virus may be addressed by compounds such as **23** since IL6, a key inflammatory cytokine, also associated with virus-induced inflammatory immune response, is up-regulated in murine lung lobes with influenza A (H1N1) virus inflammation and elevated in murine serum samples. High expression levels of IL1B, CCL4 and CXCL10 have been detected, too [41]. Systemic application of compounds such as **23** may reduce the strength of immune responses involving ROS, chemo- and cytokines and may protect infected individuals from high levels of macrophage-derived chemokines and cytokines involved in infiltration of inflammatory cells and severe hemorrhage. With regard to sepsis, application of **23** or similar compounds, therefore, might prevent severe sepsis and organ failure elicited by bacterial endotoxins. Local administration is expected to be more straightforward due to lack of side effects such as xenobiotically induced Niemann-Pick Type C lipidosis (excessive accumulation of sphingomyelin, a known side effect of **15** [19]) or Faber's syndrome (excessive accumulation of ceramide in lysosomal membranes). IL23 is a heterodimer composed of the common p40 sub-unit and the specific p19 sub-unit. Differentially expressed IL23A (Fig. 3E) is encodes the p19 sub-unit of IL23. CCL20, differentially expressed as well (Fig. 3D) and targeting the

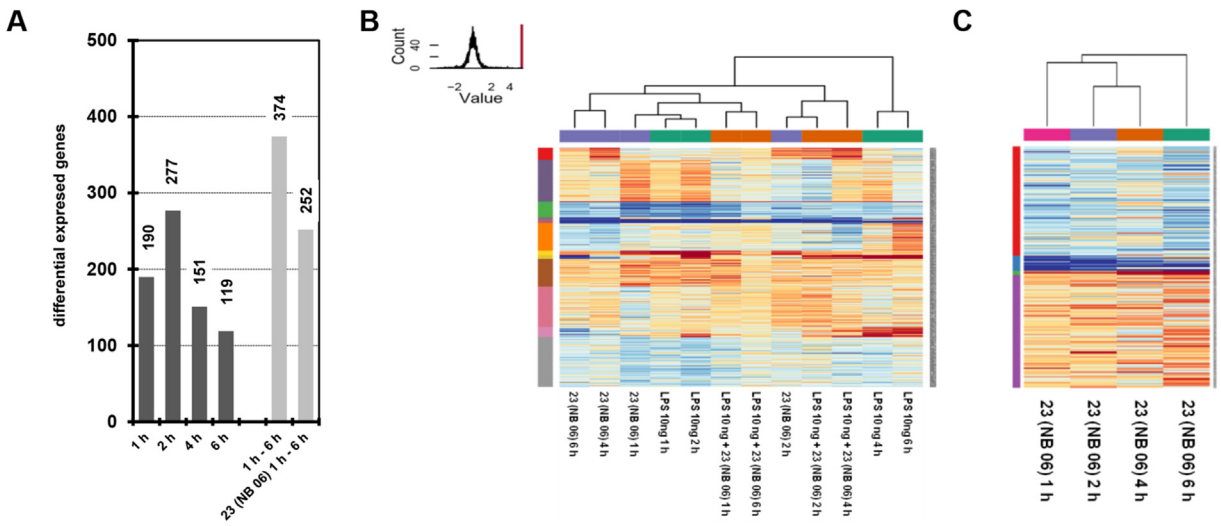

Fig. 2. 23 (NB 06) alters gene expression in Mono-Mac-6 cells. (**A**) Differentially expressed genes in Mono-Mac-6 cells treated 1, 2, 4 or 6 h with 1 ng/mL LPS (*E. coli* serotype 0111:B4) w/o 5 μM **23** (pre-incubation 30 min) or with 5 μM **23** alone (without LPS). Black bars represent the quantity of differentially expressed genes at times indicated. Grey bars indicate overall differentially expressed genes (1 h–6 h) or genes altered by **23**. (**B**) Heatmap and clustering of differentially expressed genes at time points/under conditions indicated. (**C**) Heatmap and clustering of differentially expressed genes affected by **23** at times indicated.

Please cite this article in press as: M. Blaess, et al., NB 06: From a simple lysosomotropic aSMase inhibitor to tools for elucidating the role of lysosomes in signaling apoptosis and LPS-induced inflammation, European Journal of Medicinal Chemistry (2017), https://doi.org/10.1016/j.ejmech.2017.09.021

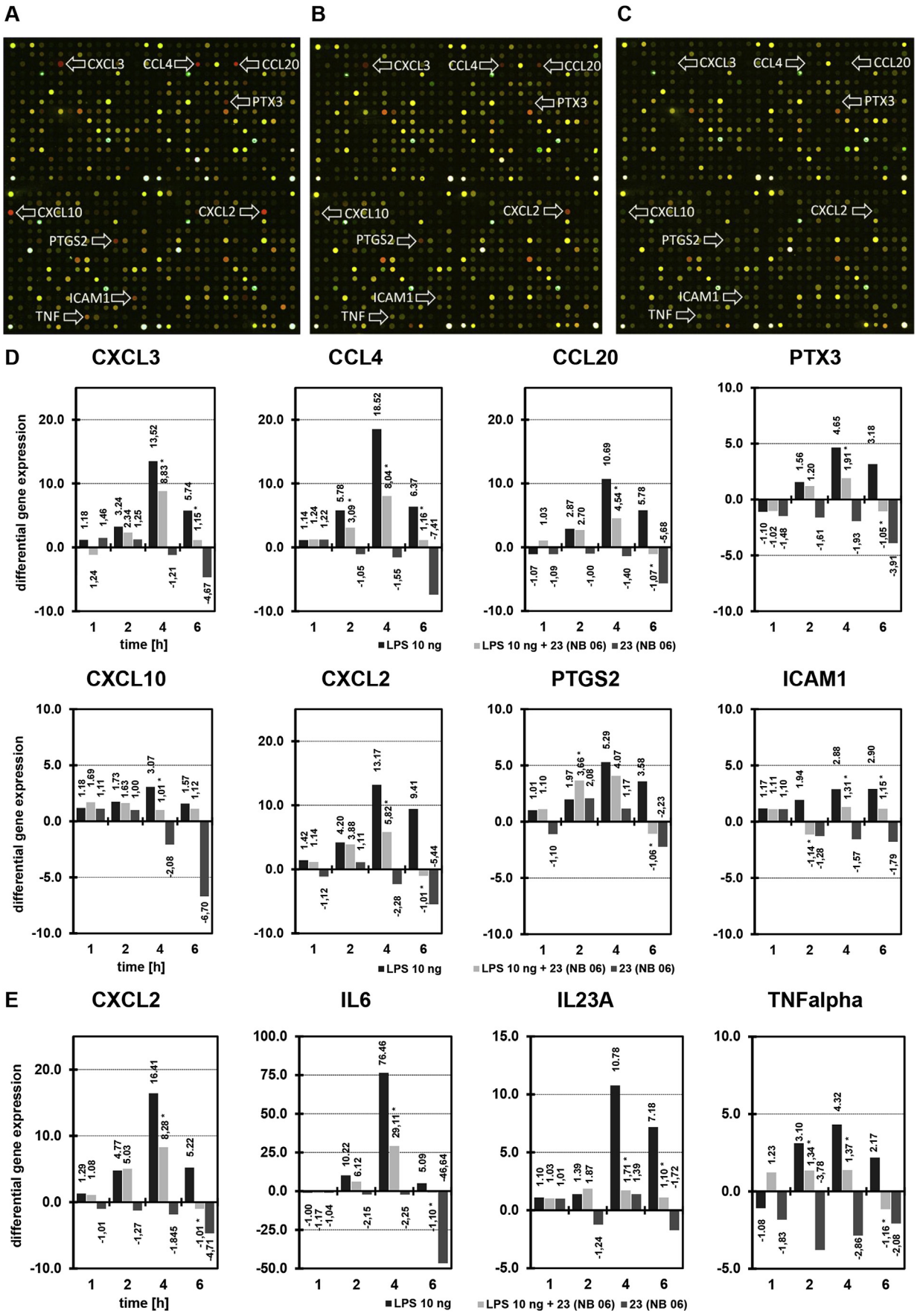

Please cite this article in press as: M. Blaess, et al., NB 06: From a simple lysosomotropic aSMase inhibitor to tools for elucidating the role of lysosomes in signaling apoptosis and LPS-induced inflammation, European Journal of Medicinal Chemistry (2017), https://doi.org/10.1016/j.ejmech.2017.09.021

CCR6 receptor, may recruit more CCR6-presenting cells from peripheral circulation [42]. Since **23** strikingly reduces CCL20 expression (−5.68, 6 h), it may intercept the self-amplifying loop of inflammation.

TNFalpha is highly elevated in many inflammatory conditions involving activated dendritic cells (TIP-DCs), and activated T cells [42]. Compounds like **23** in fact are lowering TNFalpha expression levels significantly over the whole observation period (Fig. 3E) and **23** and compounds activating similar mechanisms exhibit a general potential of reducing inflammatory messengers.

When considering biological characteristics of compounds under investigation several exciting perspectives arise. Given a central role of the lysosome in many diseases (infection by viruses and bacteria, sepsis, malaria, atherosclerosis etc.) mechanisms of these and others could be further elucidated using lysosomotropic compounds. Blocking the lysosome e.g. is a straightforward approach for further analyzing mechanisms of C_{16}-generation in apoptotic cells e.g. in the context of mmLDL-, TNFalpha- and exogenous C_6-ceramide-induced apoptosis. Lysosomal inhibition, however, may be of further potential therapeutic use, in particular with regards to a stimulation of local effects to prevent known systemic side effects.

4. Experimental

4.1. Chemistry and instrumentation

Chemicals and solvents were obtained from Sigma-Aldrich (Taufkirchen, Germany), Alexis (Gruenberg, Germany), Acros (Geel, Belgium), Fluka (Taufkirchen, Germany), Merck (Darmstadt, Germany) or J.T. Baker (Deventer, Netherlands). All chemicals were of reagent grade. If necessary, all solvents were freshly distilled and dried before use. Solvents for HPLC were either freshly distilled or commercially available HPLC grade. Methanol and ethanol were dried using magnesium cuttings, DMF and chloroform using calcium hydride and THF using sodium. All solvents were removed under reduced pressure below 40 °C. Organic phases were dried over anhydrous sodium sulphate. Reactions with *n*-BuLi or $NaBH_4$ were performed in dry glassware under argon atmosphere (Ar). TLC analyses were performed on precoated plastic sheets (POLYGRAM ALOX N/UV254 or POLYGRAM SIL G/UV254 (Macherey-Nagel, Dueren, Germany)) using chloroform-methanol or *n*-hexane-ethyl acetate as eluant. Spots were visualized by UV light at 254 and 366 nm and/or spraying with ethanol-sulfuric acid-acetic acid-*p*-anisaldehyde, 90:3:1:2. Column chromatography was performed using silica gel 60 (0.063–0.2 mm/70–230 mesh ASTM) (Merck, Darmstadt, Germany). Melting points (mp) were determined in open glass capillaries or object slide on a melting point microscope (W. Reichert LABTEC, Wolfratshausen, Germany) and left uncorrected. ^{1}H NMR and ^{13}C NMR spectra were recorded on an AM-360 (360.12 MHz and 90.56 MHz respectively) or WM-250 (250.13 MHz and 62.89 MHz respectively) instrument (Bruker, Karlsruhe, Germany) using $CDCl_3$, CD_3OD or DMSO-d_3 as solvent with TMS as internal standard; IR spectra were recorded on a Perkin-Elmer model PE 1600 FT-IR instrument (Rodgau, Germany); high-resolution mass spectroscopy (HRMS) and EI-mass spectra were performed on a double focused mass spectrometer MAT-311 A (Varian, Darmstadt, Germany), CHNS-elemental analyses were carried out on an automatic micro analyzer Foss-Heraeus vario EL, (Heraeus, Hanau, Germany).

4.2. General synthetic procedures according to Scheme 1 - methods *A* – *D*

4.2.1. Spacer attachment (method *A*)

n-BuLi (1.6 M in hexane) was added slowly at −78 °C under an inert argon atmosphere in dry toluene (70 mL) to a solution of the starting amine and stirred for 1 h. Then *n*-BuLi (1.6 M in hexane) and triisobutylalumane (TIBA) were added slowly under argon at −78 °C to a stirring solution of 2-chloro-*N*,*N*-dimethyl-ethanamine hydrochloride (**10**) or 3-chloro-*N*,*N*-dimethyl-propanamine hydrochloride (**56**) in dry toluene (30 mL), stirring continued 1 h at −78 °C and added slowly to the previously prepared solution of the starting amine; the resulting mixture was refluxed over night. The crude product was obtained after cooling using ice and the product filtered off to remove tetrabutylammonium chloride (TBACl)/TIBA. The residue was extracted with a mixture of ethyl acetate (100 mL) and saturated $NaHCO_3$ solution (20 mL), the organic phase washed with 10 mL brine, dried with anhydrous Na_2SO_4 and concentrated under reduced pressure to obtain a colored, oily product. Finally the oily product was purified by column chromatography (silica gel 60 (0.063–0.2 mm/70–230 mesh ASTM), chloroform-methanol 10:1 and 5:1 (v/v)).

4.2.2. N-Alkyl spacer demethylation (method *B*)

1-Chloroethyl chloroformate (ACE-Cl) was added over a period of 15 min to a stirred solution of the dimethylamine (obtained by method **A**) and *N*,*N*,*N*′,*N*′-Tetramethyl-1,8-naphthalenediamine (proton sponge) (**58**) or triethylamine in 1,2-dichloroethane at 0 °C. The mixture was allowed to warm to RT and then refluxed for 1–2 h. The colored solution was concentrated to one-third of its original volume by distillation. Methanol was added carefully and the color of the mixture faded. After refluxing, methanol was evaporated under vacuum. The crude solid was dissolved in dichloromethane (100 mL), washed with saturated NH_4Cl (20 mL) and finally with brine (10 mL). The organic phase was dried over Na_2SO_4, filtered and the solvent extracted. The obtained oily compound was purified by column chromatography (silica gel 60 (0.063–0.2 mm/70–230 mesh ASTM), chloroform-methanol 3:1 (v/v)) to afford the desired product.

4.2.3. N-Alkyl spacer substitution (method *C*)

To a solution or suspension of the methylamine (obtained by method **B**) in THF/toluene, *n*-BuLi (1.6M in hexane, 1.2 equiv.) was added under argon atmosphere over a period of 15–30 min at −78 °C. After stirring for 1 h, different 2-(chloroethyl)-methoxy-benzenes (1.1 equiv.) in 10 mL toluene and TIBA (1.1 equiv.) were added. The resulting mixture was stirred under reflux for one or two days. To purify the final products, the solution was cooled, diluted with THF or toluene and washed twice with saturated aqueous NH_4Cl (20–30 mL), then once with water (10–20 mL). The organic phase was dried over Na_2SO_4 and solvents evaporated. Final purification was performed by column chromatography (silica gel 60 (0.063–0.2 mm/70–230 mesh ASTM), chloroform-methanol 99:1 (v/v)).

Fig. 3. Differential expression of nine prominently altered genes affected by **23** (NB 06) in Mono-Mac-6 cells undergoing stimulation with LPS. Human Mono-Mac-6 cells were treated (1, 2, 4 or 6 h) with 1 ng/mL LPS (*E. coli* serotype 0111:B4) w/o 5 μM **23** (pre-incubation 30 min) or 5 μM **23** alone (without LPS). Total RNA of treated cells and untreated controls were transcribed and labeled separately, however, co-hybridized on the same array (Lab-Arraytor® human 60-inflammation oligonucleotid chip). Scans of one of three subarrays: (**A**) 1 ng/mL LPS 4 h, (**B**) 1 ng/mL LPS + 5 μM **23** and (**C**) 5 μM **23** treated cells. Nine prominent altered genes (*CXCL3*, *CCL4*, *CCL20*, *PTX3*, *CXCL10*, *CXCL2*, *PTGS2*, *ICAM1* and *TNFalpha*) are indicated. (**D**) Effects of **23** (NB 06) on LPS-dependent, however differentially expressed genes in total RNA of Mono-Mac-6 cells. Time course of *CXCL3*, *CCL4*, *CCL20*, *PTX3*, *CXCL10*, *CXCL2*, *PTGS2* and *ICAM1*: eight prominent and significantly altered genes on LPS stimulated cells by **23**. (**E**) *CXCL2*, *IL6*, *IL23A* and *TNFalpha*: four prominent differentially expressed genes in real-time PCR. Significance is supposed, if numerical value of differential gene expression >1.5. * Significant effect of **23** versus LPS.

Please cite this article in press as: M. Blaess, et al., NB 06: From a simple lysosomotropic aSMase inhibitor to tools for elucidating the role of lysosomes in signaling apoptosis and LPS-induced inflammation, European Journal of Medicinal Chemistry (2017), https://doi.org/10.1016/j.ejmech.2017.09.021

4.2.4. N-Alkyl acetylation (method **D**)

To a solution or suspension of the amine (obtained by method **B**) in 30 mL 1,2-dichloroethane (RT), trimethylamine (3 equiv.) was added and stirring continued for 30 min at RT. A mixture of 2-(4-methoxyphenyl)acetyl chloride (**50**) or 2-(3,4-dimethoxyphenyl) acetyl chloride (**54**) (1 equiv.) in 10 mL toluene and TIBA (1.5 equiv.) was added slowly. The resulting mixture was stirred and refluxed overnight, the reaction then quenched by addition of saturated NH_4Cl and the mixture extracted with toluene (40 mL). The organic layer was dried with Na_2SO_4, filtered and the solvent was evaporated under vacuum. The residue was purified by column chromatography (chloroform-methanol, 99:1 (v/v)).

4.3. Synthetic strategies

4.3.1. Synthesis of imipramine and chlorpromazine derivatives (Scheme 1A/Table 2)

Starting with an iminodibenzyl (**9**) ring structure an initial set of compounds was prepared. **1** is a valuable starting compound for derivatives with carbon chains of n = 3, serving as intermediate compound II (Scheme 1A). To prepare NB 01 (**5**), **1** was first treated with ACE-Cl (step B, Scheme 1A); refluxing in CH_2Cl_2 forms $RN(C{=}O)OCHClCH_3$ as intermediate. Finally, methanol addition and refluxing leads to **2** (85% yield, intermediate compound III, first synthesized in 1960) [43]. 2-(3,4-dimethoxyphenyl) ethanol (**3**) treated with PCl_5 afforded 4-(2-chloroethyl)-1,2-dimethoxy-benzene (**4**) [44]. Finally, **2** (as hydrochloride) was refluxed with *n*-BuLi according to step C (Scheme 1A), **4** and TIBA to give amine **5** (NB 01) (final compound IVa Table 2). To improve yield of **5**, TIBA was added prior to heating (38% yield). NB 02 (**8**) (final compound IVb Table 2) was obtained using 1-(2-chloroethyl)-4-methoxy-benzene (**7**) instead of **4** in step C. **9** was chosen as starting compound I to investigate compounds with a shorter carbon chain (n = 2) linking both nitrogen atoms. Heating **16** with *n*-BuLi and **4** or **7** in presence of TIBA affords at least 10% higher yields than in absence of TIBA.

4.3.2. Synthesis of carbazole and diphenylamine derivatives (Scheme 1A and Table 2)

Carbazole (**19**) was used to synthesize derivatives with potential lysosomotropic/aSMase inhibitory activity and anti-apoptotic effects with a varying ring system. **19** treated with *n*-BuLi, 3-chloro-*N*,*N*-dimethyl-propanamine; hydrochloride (**56**) and 2-chloro-*N*,*N*-dimethyl-ethanamine; hydrochloride (**10**), respectively, in toluene with *n*-BuLi and TIBA, yielded 3-carbazol-9-yl-*N*,*N*-dimethyl-propan-1-amine (**20**) (n = 3) and 2-carbazol-9-yl-*N*,*N*-dimethyl-ethanamine (**26**) (n = 2) (intermediate compounds II, step A). When performing step C with phenylethyl chlorides **4**, **7** or 1-(chloromethyl)-4-methoxy-benzene (**24**), NB 05 (**22**), NB 06 (**23**) and NB 30 (**25**) with a 4-methoxy-benzyl moiety were obtained. Given a good lysosomotropic activity and SMase inhibition of **23** (NB 06) we aimed at improving the yield of the synthesis. The synthesis of **23** was modified using tosylate and iodide, respectively, instead of chloride as leaving groups. First of all, tosylate was prepared using **6** in pyridine with TsCl to give 2-(4-methoxyphenyl) ethyl 4-methylbenzenesulfonate (**29**) and 4-carbazol-9-yl-butan-1-amine (**21**), then **7** was added (43% yield). Replacement of chloride by iodide was accomplished by adding 1 equiv. TIBA to the reaction mixture; initial 31% yield of **23** was improved to 43% (tosylate method) and 41% (TIBA method). To investigate the requirement for a carbon-chain, **19** was directly alkylated with 4-methoxybenzyl chloride (**24**) to give NB 29 (**30**) (step C). In order to study conformational effects and a requirement of a fixed planar ring structure, more flexible diphenylamine (**31**) derivatives were prepared; **31** can be considered as a carbazole analogue with two freely rotatable phenyl groups. Starting with **31** and 3-chloro-*N*,*N*-dimethyl-propanamine hydrochloride (**56**) *N*,*N*-dimethyl-*N*′,*N*′-diphenyl-propane-1,3-diamine (**32**) was obtained (step A, intermediate compound II).

4.3.3. Synthesis of 10H-phenoxazine and thiodiphenylamine (10H-phenothiazine) derivatives (Scheme 1B, Table 2)

NB 37 (**39**) and NB 20 (**40**) were obtained starting from deprotonated **36** via *N*,*N*-dimethyl-3-phenoxazin-10-yl-propan-1-amine (**37**) (intermediate compound II, step A). Analogue reactions were carried out starting from **41** (10*H*-phenothiazine) to obtain compounds for comparing inhibitory activities between **41**, **19** and **36** derivatives (Scheme 1B). These derivatives allow an observation of the impact of an exchange of oxygen by sulfur in the polycyclic aromatic moiety or hydrogen atoms instead of chlorine in derivatives of **15** as well as a variation in carbon chain length. Accordingly, **41** in combination with **56** or **10** leads to *N*,*N*-dimethyl-3-phenothiazin-10-yl-propan-1-amine (**42**) (n = 3) or *N*-methyl-3-phenothiazin-10-yl-propan-1-amine (**46**) (n = 2) respectively (step A). Phenothiazine derivatives NB 40 (**44**) (n = 3), and NB 07 (**48**) (n = 2) were obtained using **43** or **47** subsequent treatment of **4**, NB 39 (**45**) and NB 08 (**49**) using **7** in step C. To obtain a less protonatable exocyclic nitrogen (transition from amine to acetamide), acetamide analogues (compared to previously synthesized compounds) **8** (NB 02), **14** (NB 16), **17** (NB 04), **23** (NB 06) were synthesized. Intermediate compounds III were treated with triethylamine, **50** and TIBA in 1,2-dichloroethane 24–48 h to give the acetamides NB 14 (**51**), NB 17 (**52**) and NB 22 (53). NB 09 (**55**) was achieved using **54** as reactant. Table 2 summarizes starting compounds, intermediates II and III and yields of the syntheses of imipramine, 10,11-Dihydro-dibenzo[b,f]azepine, 10*H*-phenothiazine 4*H*-Phenoxazines Carbazole and Diphenylamine derivatives in ascending order (compound number).

4.3.4. Synthesis of seven- and eight-membered ring systems (Scheme 2)

Seven-membered ring systems with minor structural alterations were synthesized to assess the influence of the endocyclic nitrogen, the replacement of nitrogen against an exocyclic carbon double bond and of a hexahydro-pyrimidine moiety as a second ring structure instead of a simple carbon chain. 5-Chlorodibenzosubrane (**82**) and **88** were chosen as starting material. **82** was added to a mixture of 1,3-diaminopropane deprotonated with 0.5 equiv. *n*-BuLi afforded **83a** as product (step D, Scheme 2B). Work-up with EtOAc instead of toluene followed by column chromatography using acidic silica gel yielded the acetylated form of the expected product **83a**. Besides, an unexpected product arised and was identified as **83b** by HH-COSY, CH-COSY and NOE (Scheme 2B). According to method **C**/step C **83a** was alkylated with **4** and **7** respectively obtaining NB 41 (**84**) and NB 46 (**85**). Purification using silica gel with active acidic residues and methanol containing formaldehyde as solvent leads to compounds NB 47 (**86**) and NB 24 (**87**). Both compounds contain a methyl bridge between the two exocyclic amines leading to hexahydro-pyrimidine ring in **86** and **87** (structures confirmed by NOE, HH-COSY and CH-COSY (Supplementary Data Fig. 2A and B)). Finally, the eight-membered ring NB 21 (**95**) was obtained using the three step method of 6,11-dihydro-5*H*-benzo[b][1]benzazepines starting with 5,6,11,12-tetrahydrodibenz[*b*,*d*]azocine hydrochloride (**92**) and **56** (Scheme 2C).

4.3.5. Synthesis of piperazine or dimethylpiperazine residues containing compounds

Syntheses depicted below make use of backbones like **23** (NB 06) and **40** (NB 20) e. g. **19** and **36**. Unlike the syntheses outlined before, more sophisticated ways of preparing compounds had to be

Please cite this article in press as: M. Blaess, et al., NB 06: From a simple lysosomotropic aSMase inhibitor to tools for elucidating the role of lysosomes in signaling apoptosis and LPS-induced inflammation, European Journal of Medicinal Chemistry (2017), https://doi.org/10.1016/j.ejmech.2017.09.021

Table 2
Compounds derived on 6,11-dihydro-5*H*-benzo[b][1]benzazepine (7-ring compounds), 10*H*-Phenothiazine (**36**), 10*H*-Phenoxazine (**41**) (6-ring compounds with hetero atoms), carbazole (**19**) (5-ring compounds) and diphenylamine (**31**). Synthesis according to Scheme 1 using identical abbreviations: I (starting compound), II, III (intermediate compounds), IVa/IVb final compounds based on a common reactant.

final compound	lead compound/ scheme	starting compound I	carbon chain	intermediate compound II/yield	Intermediate compound III/yield	final compound IVa/yield	final compound IVb/yield
5/NB 01 **8**/NB 02	Imipramine **B**	–	n = 3	**1** $R_1 = C_2H_4$ R_2 = H	**2**, 85% $R_1 = C_2H_4$ R_2 = H	**5**, 38% $R_1 = C_2H_4$ R_2 = H, R_3 = b	**8**, 39% $R_1 = C_2H_4$ R_2 = H, R_3 = a
13/NB 15 **14**/NB 16	10,11-Dihydro-dibenzo[*b*,*f*] azepine **B**	Iminodibenzyl (**9**) $R_1 = C_2H_4$ R_2 = H	n = 2	**11**, 91% $R_1 = C_2H_4$ R_2 = H	**12**, 81% $R_1 = C_2H_4$ R_2 = H	**13**, 28% $R_1 = C_2H_4$ R_2 = H, R_3 = b	**14**, 30% $R_1 = C_2H_4$ R_2 = H, R_3 = a
18/NB 03 **17**/NB 04	10*H*-phenothiazine **B**	–	n = 3	**15** R_1 = S, R_2 = Cl	**16**, 77% R_1 = S R_2 = Cl	**18**, 37% R_1 = S R_2 = Cl, R_3 = b	**17**, 36% R_1 = S R_2 = Cl, R_3 = a
22/NB 05 **23**/NB 06	Carbazole **A**	Carbazole (**19**) R_2 = H	n = 3	**20**, 82% R_2 = H	**21**, 87% R_2 = H	**22**, 39% R_1 = H R_3 = b n = 3	**23**, 41% R_2 = H R_3 = a
25/NB 30	Carbazole **A**	Carbazole (**19**) R_2 = H	n = 3	**20**, 82% R_2 = H	**21**, 87% R_2 = H	**25**, 33% R_2 = H R_3 = c	
28/NB 25	Carbazole **A**	Carbazole (**19**) R_2 = H	n = 2	**26**, 88% R_2 = H	**27**, 76% R_2 = H	**28**, 25% R_2 = H R_3 = c n = 2	
30/NB 29	Carbazole **A**	Carbazole (**19**) R_2 = H	n = 0	–	–	**30**, 41% R_2 = H R_3 = c n = -	
34/NB 35 **35**/NB 34	open B-cycle **A**	Diphenylamine (**31**) R_2 = H	n = 3	**32**, 71% R_2 = H	**33**, 71% R_2 = H	**34**, 24% R_2 = H R_3 = b	**35**, 25% R_2 = H R_3 = a
39/NB 37 **40**/NB 20	4*H*-Phenoxazine **B**	Phenoxazine (**36**) R_1 = O R_2 = H	n = 3	**37**, 82% R_1 = O R_2 = H	**38**, 73% R_1 = O R_2 = H	**39**, 23% R_1 = O R_2 = H, R_3 = b n = 3	**40**, 35% R_1 = O R_2 = H, R_3 = a n = 3
44/NB 40 **45**/NB 39	10*H*-phenothiazine **B**	Thiodiphenyl amine (**41**) R_1 = S, R_2 = H	n = 3	**42**, 82% R_1 = S R_2 = H	**43**, 74% R_1 = S R_2 = H n = 3	**44**, 32% R_1 = S R_2 = H, R_3 = b n = 3	**45**, 31% R_1 = S R_2 = H, R_3 = a n = 3
48/NB 07 **49**/NB 08	10*H*-phenothiazine **B**	Thiodiphenyl amine (**41**) R_1 = S, R_2 = H	n = 2	**46**, 83% R_1 = S R_2 = H n = 2	**47**, 72% R_1 = S R_2 = H n = 2	**48**, 33% R_1 = S R_2 = H, R_3 = b n = 2	**49**, 33% R_1 = S R_2 = H, R_3 = a
51/NB 14	Imipramine **B**		n = 3	**1** $R_1 = C_2H_4$ R_2 = H	**2**, 85% $R_1 = C_2H_4$ R2 = H	**51**, 25% $R_1 = C_2H_4$ R_2 = H, R_3 = d	
52/NB 17	10,11-Dihydro-dibenzo[*b*,*f*] azepine **B**	Iminodibenzyl (**9**) $R_1 = C_2H_4$ R_2 = H	n = 2	**11**, 91% $R_1 = C_2H_4$ R_2 = H	**12**, 81% $R_1 = C_2H_4$ R_2 = H	**52**, 33% $R_1 = C_2H_4$ R_2 = H, R_3 = d	
53/NB 22	Carbazole **A**	Carbazole (**19**) R_2 = H	n = 3	**20**, 82% R_2 = H	**21**, 87% R_2 = H	**53**, 33% R_2 = H R_3 = d	
55/NB 09	10*H*-phenothiazine **B**	–	n = 3	**15** R_1 = S, R_2 = Cl	**16**, 77% R_1 = S, R_2 = Cl	**55**, 37% R_1 = S R_2 = H, R_3 = e	

applied. Preparing NB 18 (**99**) required some changes in the sequence of steps. Starting with method **C**, **7** is coupled with 1-(2-hydroxyethyl)-piperazine (**96**) to form [4-[(4-methoxyphenyl) methyl]piperazin-1-yl]methanol (**97**); **97** is halogenated with PCl_5 to give 1-(chloromethyl)-4-[(4-methoxyphenyl)methyl]piperazine (**98**). Applying method **A** (step C) on **19** and **98** yield **99** (NB 18, 23%) (Scheme 3A). Applying this procedure to **36**, the desired 10*H*-phenoxazine derivative could not be isolated. To prepare 2,6-dimethylpiperazine (**102**) containing derivatives of **19** and **36**, an approach starting with method **A** (step D) was chosen. Alkylation with 1-bromo-3-chloro-propane (**100**) yielded 9-(3-chloropropyl) carbazole (**101**) and 10-(3-chloropropyl)phenoxazine (**106**) respectively. After adding water, **102**, respectively K_2CO_3 to **101** in DMF, rimcazole (**103**) was obtained [45]. When using **106,** 10-[3-[(3S,5R)-3,5-dimethylpiperazin-1-yl]propyl]phenoxazine (**107**) is formed in 40% yield (step E). Coupling **103** with **4** or **7** (method **C**, step F) afforded NB 42 (**104**) and NB 19 (**105**). When subjecting **107** to method **C** in combination with **4** NB, 36 (**109**) was isolated (Scheme 3A).

*4.3.6. Synthesis of NB 32 (4-carbazol-9-yl-1,1,2,2,3,3,4,4-octafluoro-N-[2-(4-methoxyphenyl)-ethyl]-N-methyl-butan-1-amine) (**113**)*

Various tests with carbazole derivative **23** (NB 06) have shown that metabolism in mammals involves dealkylation at the nitrogen atom in mammals [4]. In order to improve metabolic stability in organisms, hydrogen atoms of the carbon chain were exchanged for fluorine and ultrasound was applied to facilitate exchange

Please cite this article in press as: M. Blaess, et al., NB 06: From a simple lysosomotropic aSMase inhibitor to tools for elucidating the role of lysosomes in signaling apoptosis and LPS-induced inflammation, European Journal of Medicinal Chemistry (2017), https://doi.org/10.1016/j.ejmech.2017.09.021

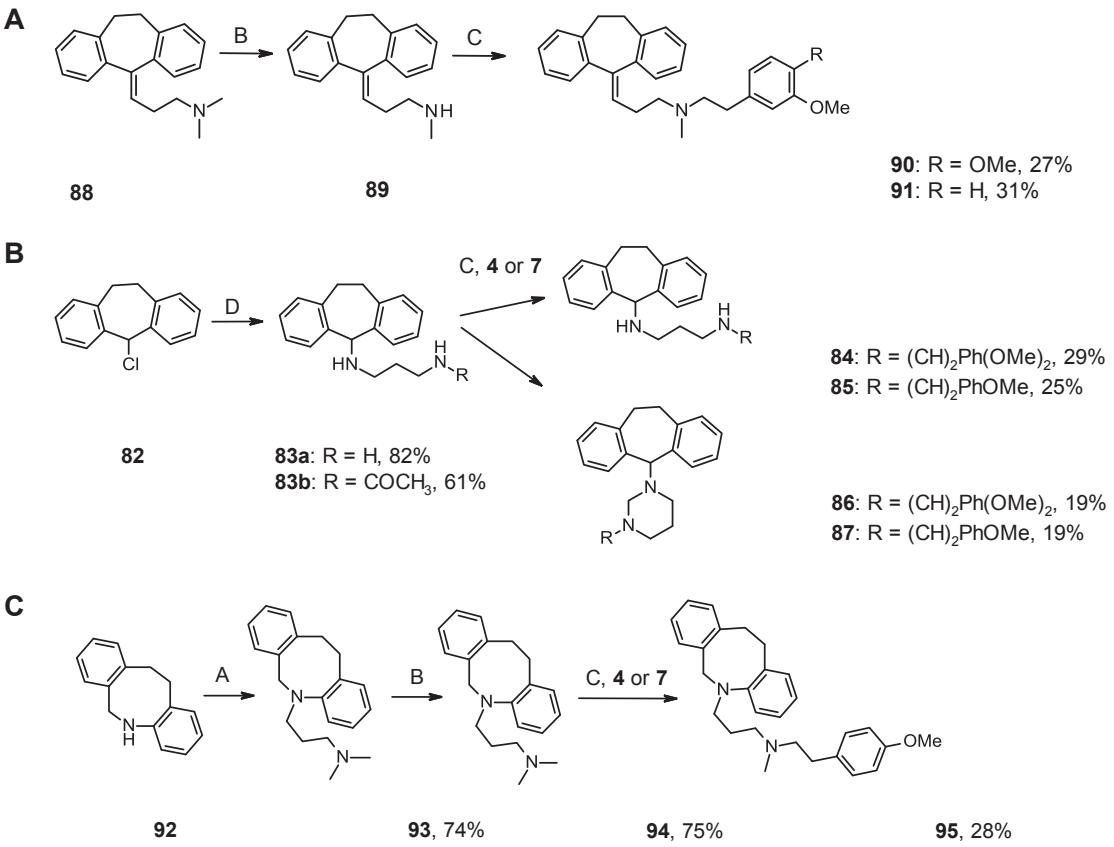

Scheme 2. Synthesis of compounds with seven- and eight-membered ring systems. Reagents and conditions: (A) 1) *n*-BuLi, dry toluene, −78 °C, 2) *n*-BuLi, dry toluene, $N(CH_3)_2(CH_2)_nCl$, TIBA, reflux, 24–48 h; (B) 1. ACE-Cl, CH_2Cl_2, reflux, 2 h, 2. MeOH, reflux, 4 h; (C) *n*-BuLi, dry THF, −78 °C, **4** or **7** in dry toluene, TIBA, reflux, 48 h; (D) 1,3-diaminopropane, *n*-BuLi, toluene, −78 °C; TIBA, reflux, 24 h.

reactions. Various reagents like (1,3-dichlorotetrafluoroacetone, 1,4-diiodoperfluorobutane and 1,2-dibromotetrafluoroethane) failed to afford the fluorinated carbon chain to **19**. Compound **20** was dissolved in DMF, treated with 1,2-dibromo-1-chloro-1,2,2-trifluoro-ethane (**81**) and triethylamine or NaH as bases to give alkylated **117** as product. Attempts, linking 2-(4-methoxyphenyl)-*N*-methyl-ethanamine (**110**) with **117** to obtain the desired alkylated **114,** however, failed. Similarly, attempts to prepare **115** using 2-(3,4-dimethoxyphenyl)-*N*-methyl-ethanamine (**111**) were unsuccessful. This may be due to a β-elimination during the reaction or an inability of the amines **110** and **111** to form donor-acceptor complexes with perfluoroalkyl iodides and bromides (Scheme 3B) [46]. By applying sonication in an ultrasonic bath the desired product 9-(1,1,2,2,3,3-hexafluoro-3-iodo-propyl)carbazole (**112**) could be obtained in good yield (Scheme 3B) using **20**, 1,1,2,2,3,3,4,4-octafluoro-1,4-diiodo-butane (**118**) and $AgNO_3$ (to obtain AgI) dissolved in DMF and deprotonation with *n*-BuLi. Due to poor stability of **112** (containing iodine) it was used in the following reaction step without purification. Deprotonated **110** combined with a suspension of fluorinated **112** in DMF was added and placed in an ultrasonic bath to give NB 32 (**113**). Applying the same reaction scheme to obtain the dimethoxy analogue **116** using **111** was, however, unsuccessful (Scheme 3B).

4.3.7. Synthesis of 1,2,3,4-tetrahydrocarbazole derivatives

Pharmacologically active pyrazinocarbazoles were synthesized by oxidation of tetrahydrocarbazole (**119**) with I_2O_5 to give 2,3,4,9-tetrahydrocarbazol-1-one (**120**) together with a byproduct formed by oxidation on two positions of the unsaturated carbazole ring [47] 2-[(E)-2,3,4,9-tetrahydrocarbazol-1-ylideneamino]ethanol (**121**) was obtained by condensation of carbonyl group of ketone **120** with ethanolamine (R = CH_2) in 60% yield. After chlorinating the hydroxy group of **121** with PCl_5 to give (E)-*N*-(2-chloroethyl)-2,3,4,9-tetrahydrocarbazol-1-imine (**122**), cyclization was achieved by heating of **122** in DMF/H2O with K_2CO_3 yielding 73% of the tetracyclic product 2,4,5,6-Tetrahydro-1*H*-pyrazino[3,2,1-jk]carbazol (**123**). Reduction of **123** (NaBH4 in MeOH) afforded (2,3,3a,4,5,6-hexahydro-1*H*-pyrazino[3,2,1-jk]carbazole) (**124**) and after deprotonating, addition of **7**, TIBA and heating, NB 43 (**125**) was obtained (Scheme 3C). Reduction of **122** to the corresponding amine with NaBH4 was also tried prior to the cyclization to obtain **124**. The yield of **124**, however, was 25% higher compared to the method originally used. To obtain NB 44 (**130**), the same procedure was applied starting with **120** and propanolamine (R=$(CH_2)_2$) to give 3-[(E)-2,3,4,9-tetrahydrocarbazol-1-ylideneamino]propan-1-ol (**126**). Cyclization of chlorinated **127** was more difficult than cyclization of **122** with a shorter carbon chain. The yield of the following reduction step proved to be independent of the ring size of the starting material (Scheme 3C).

*4.3.8. Synthesis of symmetric dicarbazole derivative NB 45 (**132**)*

1,4-Bis(2-bromoethyl)-2,5-dimethoxy-benzene (**131**) was prepared to obtain access to a carbazole derivative of **23** with dimer like structure. An analogue to **23** with a big planar linker and cationic binding structure was synthesized to test the hypothesis whether biological activity is based on DNA-intercalation. To obtain **140**, 4-dibromo-2,5-dimethoxy-benzene (**139**) was treated with propargylbromid in a cross-coupling reaction using regioselective

Please cite this article in press as: M. Blaess, et al., NB 06: From a simple lysosomotropic aSMase inhibitor to tools for elucidating the role of lysosomes in signaling apoptosis and LPS-induced inflammation, European Journal of Medicinal Chemistry (2017), https://doi.org/10.1016/j.ejmech.2017.09.021

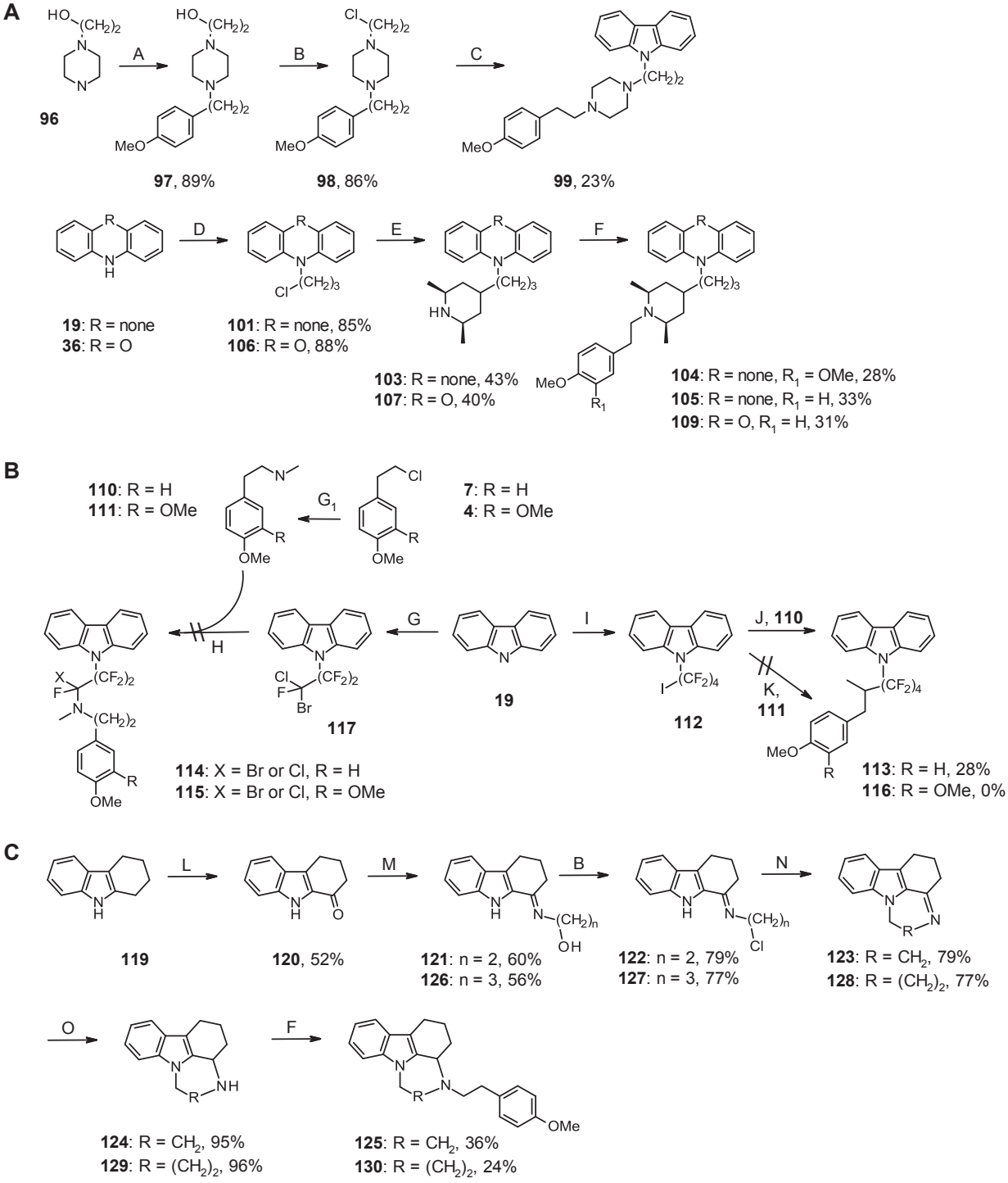

Scheme 3. Synthesis of compounds containing piperazine, dimethyl piperazine residues (A), NB 32 (**113**) (B) and 1,2,3,4-tetrahydrocarbazole derivatives (C). Reagents and conditions: (A) *n*-BuLi, dry toluene, −78 °C; **7** in dry toluene, TBAI, reflux, 48 h; (B) PCl_5, $CaCO_3$, dry toluene, 0 °C - RT, 5 h; (C) **19**, *n*-BuLi, dry toluene, −78 °C; TBAI, reflux, 24 h; (D) *n*-BuLi, dry toluene, −78 °C; 1-bromo-3-chloropropane, reflux, 24 h; (E) 2,6-dimethylpiperazine, K_2CO_3, DMF/H_2O, 80 °C, 4 h; (F) *n*-BuLi, dry toluene, −78 °C; **4** or **7** in toluene, TBAI, reflux, 48 h; (G_1) Methylamine in EtOH, TIBA, 70 °C, 7 h; (G) Triethylamine or NaH, 2-chloro-1,2-dibromo-1,1,2-trifluoroethane (**115**), dry DMF, ultrasound, 72 h; (H) Triethylamine, NaH, 2-(4-Methoxy-phenyl-ethyl)methylamine (**110**) or 2-(3,4-dimethoxy-phenyl-ethyl)methylamine (**111**) in dry DMF; (I) *n*-BuLi, dry DMF, −78 °C; $I(CF_2)_4I$, $AgNO_3$, 60–80 °C, 72 h; (J) *n*-BuLi, dry DMF, −78 °C; **110**, $AgNO_3$, 60–80 °C, 72 h; (K) *n*-BuLi, dry DMF, −78 °C; **111**, $AgNO_3$, 60–80 °C, 72 h. Attempts to obtain the desired alkylated compounds **114** and **115** using Method **H** were not successful. Treatment of **112** with **111** using method **K** to achieve **116,** also failed. (L) I_2O_5, THF/H_2O, 1–2 h, RT; (M) $H_2N(CH_2)_nOH$, MeOH, 60 °C, 5 h; (N) K_2CO_3, DMF/H_2O; (O) $NaBH_4$, MeOH.

Pd(0)-catalyzators as $Pd(P(C_6H_5)_3)_4$ [48] or $Pd(P(C_6H_5)_3)_2Cl_2$ [49] along with CuI. The Pd[0] catalyzed coupling (Heck reaction), was more successful for furans, than for other aromats [50]. Next we tried to utilize lithium-di(benzo)-cuprate [51,52] by treating **139** with *t*-BuLi, dimethylsulfid, CuI and 1-bromo-2-chloroethane in THF to obtain **140** [53]. **139** was treated with *n*-BuLi in THF, $ZnCl_2$ [50], $Pd[P(C_6H_5)_3]_4$ and 1-bromo-2-chloro-ethane (**141**) to achieve the desired product **131**. Both reactions, however, were

Please cite this article in press as: M. Blaess, et al., NB 06: From a simple lysosomotropic aSMase inhibitor to tools for elucidating the role of lysosomes in signaling apoptosis and LPS-induced inflammation, European Journal of Medicinal Chemistry (2017), https://doi.org/10.1016/j.ejmech.2017.09.021

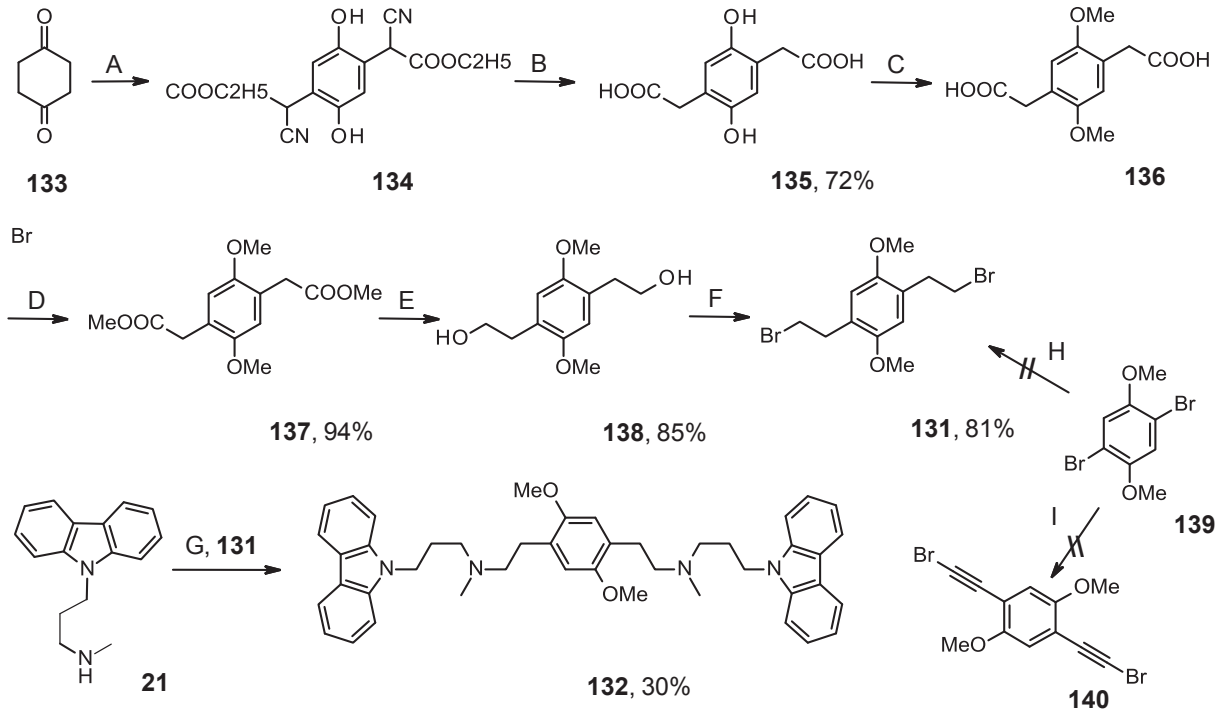

Scheme 4. Synthesis of 1,4-bis(2-bromoethinyl)-2,5-dimethoxy-benzene (**140**) and 3-carbazol-9-yl-*N*-[2-[4-[2-[3-carbazol-9-ylpropyl(methyl)amino]ethyl]-2,5-dimethoxy-phenyl] ethyl]-*N*-methyl-propan-1-amine (**132**) (NB 45). Reagents and conditions: (A) 1) ethyl cyanoacetate, *p*-benzochinone, EtOH, 40 °C, 30 min, 2) NH_4OH, H_2O, RT, 2 h; (B) HCl/H_2O, reflux, 20 h; (C) dimethyl sulphate, 10% NaOH, 50 °C, 2 h; (D) thionylchloride, MeOH, RT, overnight; (E) $LiAlH_4$, THF, RT, 1 h; (F) CBr_4, PPh_3, CH_2Cl_2, RT, 4 h; (G) *n*-BuLi, dry toluene, −78 °C; **131**, TBAI, reflux, 48 h. Unsuccessful attempts to achieve **131**: (H) dry THF, *t*-BuLi, dimethylsulfide, CuI, 50 °C, 30 h, $Cl(CH_2)_2Br$, RT, 24 h or dry THF, *n*-BuLi, ZnCl, $Pd(PPh_3)_4$, $Cl(CH_2)_2Br$, 50 °C, 24 h. (I) $Pd(PPh_3)_2Cl2$ or $Pd(PPh_3)_4$, diisopropylamine, CuI, 60 °C, 15 h, $CH{\equiv}CCH_2Br$, dry THF, reflux, 24 h.

unsuccessful. Starting with *p*-benzochinone (**133**) and ethyl cyanoacetate in ethanol [54,55] (Scheme 4), **131** was successfully synthesized. 2-[4-(carboxymethyl)-2,5-dimethoxy-phenyl]acetic acid (**136**), obtained as a side product due to uncompleted reaction, was reacted with thionylchloride and methanol to give methyl 2-[2,5-dimethoxy-4-(2-methoxy-2-oxo-ethyl)phenyl]acetate (**137**). Reduction with $LiAlH_4$ gave 2-[4-(2-hydroxyethyl)-2,5-dimethoxy-phenyl]ethanol (**138**) in 85% yield. Subsequent bromination was performed using CBr_4 and $P(C_6H_5)_3$ in dichloromethane to yield **131**. Finally, **131** was added to deprotonated **21** to afford NB 45 (**132**). The reaction produced more than 50% of the methylated form of **131** as a byproduct.

4.4. Synthesis and experimental procedures of NB compounds

Only the last step of the synthesis of each NB compound is described here. Syntheses of intermediates (compounds II/III according to Scheme 1/Table 2) are described in the supplementary data.

4.4.1. ***Desipramine*** *3-(5,6-Dihydrobenzo[b][1]benzazepin-11-yl)-N-methyl-propan-1-amine (**2**)*

Method **B**, reactant: imipramine (**1**). **1** (2.0 g, 6.33 mmol) was dissolved in 1,2-dichloroethane (80 mL), **58** (2.70 g, 12.66 mmol) and ACE-Cl (1.36 g, 9.50 mmol) were added. The reaction mixture was refluxed 1 h, methanol (50 mL) was added and refluxed additional 2 h. After purification, a red/orange solid was obtained: **2** (1.43 g, 85%). ^{1}H NMR (360 MHz, $CDCl_3$): δ 1.95–2.07 (tt, 2H, J = 6.74 Hz, $CH_2CH_2CH_2$), 2.40 (s, 3H, CH_3), 2.85–2.89 (t, 2H, J = 7.12 Hz, CH_2NH), 3.12 (s, 4H, $2CH_2$), 3.81–3.84 (t, 2H, J = 6.74 Hz, -NCH_2), 6.35–6.60 (b, 1H, NH), 6.89–6.93 (m, 2H, *CH*-Ar), 7.03–7.14 (m, 6H, *CH*-Ph). ^{13}C NMR (90.6 MHz, $CDCl_3$): δ 24.04 ($CH_2CH_2CH_2$), 32.11 ($2CH_2$), 32.76 (CH_3NH), 47.43 (CH_2N), 47.72 (CH_2NH), 119.75, 123.04, 126.63, 180.03 (4CH-Ar), 134.19 (*C-C*), 147.65 (C-N). IR (KBr): $\tilde{\nu}$(cm^{-1}) 3398 (m, NH), 2926 (s, CH_2), 2824 (s, CH_3), 2776 (s), 1576 (s), 1487 (s), 1384 (m), 1226 (m, N), 938 (m), 753 (m). MS (EI, 130 °C): *m/z* (%) 266 (27) [M^+], 235 (55) [M^+- $NHCH_3$], 208 (33) [M^+- $C_2H_4NHCH_3$], 193 (33) [iminodibenzyl]. HRMS $C_{18}H_{22}N_2$: found 266.1789 [calcd. 266.1783].

4.4.2. ***NB 01*** *3-(5,6-Dihydrobenzo[b][1]benzazepin-11-yl)-N-[2-(3,4-dimethoxyphenyl)ethyl]-N-methyl-propan-1-amine (**5**)*

Method **C**, reactant: **2**. **2** (0.45 g, 1.69 mmol) was dissolved in THF/toluene (20/10 mL), *n*-BuLi (1.27 mL, 2.03 mmol), **4** (0.37 g, 1.86 mmol) and TIBA (0.69 g, 1.86 mmol) were added. The mixture was refluxed overnight. Processing and final purification by silica gel column chromatography (chloroform-methanol 99:1 (*v/v*)) yielded a yellow oil: **5** (NB 01) (0.28 g, 38%). ^{1}H NMR (360 MHz, $CDCl_3$): δ 1.74–1.79 (tt, 2H, J = 6.74 Hz, $CH_2CH_2CH_2$), 2.21 (s, 3H, CH_3), 2.46–2.51 (t, 2H J = 6.96 Hz, CH_2Ph), 2.53–2.57 (m, 2H, CH_2NMe), 2.61–2.66 (m, 2H, CH_2NMe), 3.16 (s, 4H, $2CH_2$), 3.74–3.78 (t, 4H, J = 6.74 Hz, CH_2N), 3.84 (s, 6H, $2OCH_3$), 6.61–6.66 (m, 2H, *CH*-Ar), 6.74–6.76 (m, 1H, *CH*-Ar), 6.88–6.92 (m, 4H, *CH*-Ar), 7.06–7.12 (m, 4H, *CH*-Ar). ^{13}C NMR (90.6 MHz, $CDCl_3$): δ 25.06 ($CH_2CH_2CH_2$), 28.12 ($2CH_2$), 32.99 (CH_2Ph), 44.02 (CH_3N), 47.98 (-NCH_2), 54.84 (CH_2NMe), 5.48, 55.54 ($2OCH_3$), 58.18 (CH_2NMe), 110.82, 110.85, 119.18 (3CH-Ar), 110.73, 111.97, 116.39, 126.28, 128.62 (5CH-Ar), 131.34 (*C-C*), 131.68 (*C*-Ar), 132.45 (C-N), 147.33, 148.49 (2COMe). IR (Film): $\tilde{\nu}$(cm^{-1}) 2958 (s, OCH_3), 2874 (s, OCH_3), 2672 (m), 1670 (m), 1471 (s), 1380 (m), 1028 (m), 859 (m), 796 (s), 750 (m). MS (EI, 132 °C): *m/z* (%) 430 (30) [M^+], 279 (50) [M^+- $CH_2Ph(OMe)_2$], 208 (21) [M^+- $C_3H_7NC_2H_4Ph(OMe)_2$], 193 (16) [iminodibenzyl]. HRMS $C_{24}H_{34}N_2O_2$: found 430.3624 [calcd. 430.2620].

Please cite this article in press as: M. Blaess, et al., NB 06: From a simple lysosomotropic aSMase inhibitor to tools for elucidating the role of lysosomes in signaling apoptosis and LPS-induced inflammation, European Journal of Medicinal Chemistry (2017), https://doi.org/10.1016/j.ejmech.2017.09.021

4.4.3. ***NB 02*** *3-(5,6-Dihydrobenzo[b][1]benzazepin-11-yl)-N-[2-(4-methoxyphenyl)ethyl]-N-methyl-propan-1-amine (**8**)*

Method **C**, reactant: **2**. **2** (0.40 g, 1.50 mmol) was dissolved in dry THF/toluene (2:1 (*v/v*), 20 mL), *n*-BuLi (1.13 mL, 1.81 mmol), **4** (0.29 g, 1.65 mmol) in toluene (10 mL) and TIBA (0.61 g, 1.65 mmol) were added and the mixture refluxed overnight. After processing, the crude product was purified by silica gel column chromatography (chloroform-methanol 99:1(*v/v*)) to give a brown oil: **8** (NB 02) (0.232 g, 39%). ^{1}H NMR (360 MHz, $CDCl_3$): δ 1.98–2.06 (tt, 2H, J = 6.74 Hz, $CH_2CH_2CH_2$), 2.21 (s, 3H, CH_3), 2.40–2.45 (t, 2H J = 6.96 Hz, CH_2Ph), 2.49–2.54 (m, 2H, CH_2NMe), 2.59–2.66 (m, 2H, CH_2NMe), 3.15 (s, 4H, $2CH_2$), 3.75–3.80 (t, 2H, J = 6.74 Hz, CH_2N), 3.77 (s, 3H, OCH_3), 6.77–6.80 (m, 2H, CH-Ar), 6.87–6.93 (m, 4H, CH-Ar), 7.04–7.11 (m, 4H, CH-Ar), 7.19–7.23 (m, 2H, CH-Ar). ^{13}C NMR (90.6 MHz, $CDCl_3$): δ 25.06 ($CH_2CH_2CH_2$), 28.18 ($2CH_2$), 32.89 (CH_2Ph), 44.12 (CH_3), 47.50 (-NCH_2), 54.95 (CH_2NMe), 55.32 (OCH_3), 58.12 (CH_2NMe), 112.01, 116.32, 126.08, 128.50 (4CH-Ar), 114.06, 128.92 (2CH-Ar), 131.68 (C-Ar), 131.42 (C-C), 132.83 (C-N), 158.52 (COMe). IR (Film): $\tilde{\nu}$(cm^{-1}) 2933 (s, CH_2), 2837 (m, OCH_3), 1612 (m), 1595 (m), 1512 (s), 1247 (s), 1126 (m), 825 (s), 751 (m). MS (EI, 132 °C): *m/z* (%) 400 (26) [M^+], 279 (50) [M^+- CH_2PhOMe], 208 (28) [M^+- $C_3H_7NC_2H_4$PhOMe], 193 (49) [iminodibenzyl]. HRMS $C_{27}H_{32}N_2O$: found 400.2521 [calcd. 400.2515].

4.4.4. ***NB 15*** *N-[2-(5,6-dihydrobenzo[b][1]benzazepin-11-yl)ethyl]-2-(3,4-dimethoxyphenyl)-N-methyl-ethanamine (**13**)*

Method **C**, reactant: **12**. **12** (0.25 g, 0.99 mmol) was dissolved in THF (30 mL), *n*-BuLi (6.82 mL, 1.06 mmol), **4** (0.22 g, 1.06 mmol) and TIBA (0.40 g, 1.06 mmol) were added. Resulting mixture was refluxed overnight. After processing and purification, **13** (NB 15) (0.115 g, 28%) was obtained as a brown oil. ^{1}H NMR (360 MHz, $CDCl_3$): δ 2.42 (s, 3H, CH_3), 2.71–2.78 (m, 4H, NCH_2CH_2Ph), 3.02–3.10 (t, 2H, J = 6.97 Hz, CH_2NMe), 3.13 (s, 4H, $2CH_2$), 3.85 (s, 6H, $2OCH_3$), 3.97–4.01 (t, 2H, J = 6.97 Hz, -NCH_2), 6.66–6.70 (m, 2H, CH-Ar), 6.90–6.96 (m, 4H, CH-Ar), 7.07–7.17 (m, 4H, CH-Ar), 7.32–7.36 (m, 2H, CH-Ar). ^{13}C NMR (90.6 MHz, $CDCl_3$): δ 32.25 ($2CH_2$), 32.91 (CH_2Ph), 42.72 (CH_3), 49.39 (-NCH_2), 55.11 55.30 ($2OCH_3$), 55.67 (CH_2NMe), 60.15 (CH_2NMe), 113.76, 122.99, 126.43, 129.51 (4CH-Ar), 120.09, 130.50 (2CH-Ar), 132.31 (C-Ar), 134.62 (C-C), 142.29 (C-N), 147.99, 148.78 (2COMe). IR (Film): $\tilde{\nu}$(cm^{-1}) 2932 (s), 2842 (s), 2749 (s), 1679 (m), 1588 (s), 1488 (s), 1466 (s), 1262 (m), 1237 (s), 1143 (m), 814 (m), 765 (s). MS (EI, 110 °C): *m/z* (%) 416 (6) [M^+], 265 (22) [M^+- CH_2Ph$(OMe)_2$], 222 (8) [M^+- $C_2H_5NC_2H_4$Ph$(OMe)_2$], 208 (100) [M^+- $C_3H_7NC_2H_4$Ph$(OMe)_2$], 193 (18) [iminodibenzyl]. HRMS $C_{27}H_{32}N_2O_2$: found 416.2467 [416.2464].

4.4.5. ***NB 16*** *N-[2-(5,6-dihydrobenzo[b][1]benzazepin-11-yl)ethyl]-2-(4-methoxyphenyl)-N-methyl-ethanamine (**14**)*

Method **C**, reactant: **12**. **12** (0.28 g, 1.11 mmol) was dissolved in THF (30 mL), deprotonated by *n*-BuLi (7.64 mL, 1.22 mmol), treated with **7** (0.21 g, 1.22 mmol) in toluene and TIBA (0.45 g, 1.22 mmol) and the reaction mixture refluxed overnight. Processing and purification yielded a brown oil: **14** (NB 16) (0.128 g, 30%). ^{1}H NMR (360 MHz, $CDCl_3$): δ 2.31 (s, 3H, CH_3), 2.54–2.65 (m, 4H, NCH_2CH_2Ph), 3.08–3.13 (t, 2H, J = 7.31 Hz, CH_2NMe), 3.15 (s, 4H, $2CH_2$), 3.77 (s, 3H, OCH_3), 3.86–3.91 (t, 2H, J = 7.31 Hz, -NCH_2), 6.78–6.81 (m, 2H, CH-Ar), 6.89–6.95 (m, 4H, CH-Ar), 7.03–7.10 (m, 4H, CH-Ar), 7.12–7.16 (m, 2H, CH-Ar). ^{13}C NMR (90.6 MHz, $CDCl_3$): δ 32.15 ($2CH_2$), 32.91 (CH_2Ph), 42.61 (CH_3), 49.29 (-NCH_2), 55.21 (OCH_3), 55.56 (CH_2NMe), 60.07 (CH_2NMe), 113.75, 122.99, 126.40, 129.50 (4CH-Ar), 120.03, 129.50 (2CH-Ar), 132.31 (C-Ar), 134.32 (C-C), 148.29 (C-N), 157.86 (COMe). IR (Film): $\tilde{\nu}$(cm^{-1}) 2932 (s), 2842 (s), 1676 (m), 1587 (s), 1488 (s), 1457 (m), 1247 (m), 1176 (m), 1111 (m), 824 (m), 760 (s). MS (EI, 128 °C): *m/z* (%) 386 (7) [M^+], 265 (33) [M^+- CH_2PhOMe], 222 (9) [M^+- $C_2H_5NC_2H_4$PhOMe], 208 (39) [M^+- $C_3H_7NC_2H_4$PhOMe], 193 (19) [iminodibenzyl]. HRMS $C_{26}H_{30}N_2O$: found 386.2361 [calcd. 386.2358].

4.4.6. ***NB 04*** *3-(2-Chlorophenothiazin-10-yl)-N-[2-(4-methoxyphenyl)ethyl]-N-methyl-propan-1-amine (**17**)*

Method **C**, reactant: **16**. **16** (0.35 g, 1.15 mmol) was dissolved in a dry mix of THF/toluene (2:1 (*v/v*), 30 mL). *n*-BuLi (0.72 mL, 1.15 mmol), **7** (0.22 g, 1.27 mmol) in toluene (10 mL) and TIBA (0.47 g, 1.27 mmol) were added constantly stirring. The mixture was refluxed 48 h and resulting product was purified as a light brown oil: **17** (NB 04) (0.18 g, 36%). ^{1}H NMR (360 MHz, $CDCl_3$): δ 1.87–1.95 (tt, 2H, J = 6.73 Hz, $CH_2CH_2CH_2$), 2.27 (s, 3H, CH_3), 2.50–2.54 (t, 2H, J = 6.73 Hz, CH_2Ph), 2.55–2.57 (m, 2H, CH_2NMe), 2.61–2.64 (m, 2H, CH_2NMe), 3.77 (s, 3H, OCH_3), 3.84–3.87 (t, 2H, J = 6.73 Hz, -NCH_2), 6.79–6.81 (m, 2H, CH-Ar), 6.86–6.92 (m, 4H, CH-Ar), 7.00–7.06 (m, 2H, CH-Ar), 7.10–7.16 (m, 2H, CH-Ar), 7.19–7.21 (m, 1H, CH-Cl). ^{13}C NMR (90.6 MHz, $CDCl_3$): δ 24.65 ($CH_2CH_2CH_2$), 32.83 (CH_2Ph), 42.36 (NCH_3), 45.14 (-NCH_2), 54.41 (CH_2NMe), 55.24 (OCH_3), 59.90 (CH_2NMe), 113.75, 115.95, 122.21, 122.85, 127.24, 127.38, 127.86 (7CH-Ar), 115.88, 129.56 (2CH-Ar), 123.59, 125.01 (2C-S), 132.54 (C-Ar), 33.22 (C-Cl), 144.58, 146.58 (2C-N), 157.84 (COMe). IR (KBr): $\tilde{\nu}$(cm^{-1}) 2932 (s, OMe), 2852 (s, OMe), 2794 (m), 1567 (s), 1461 (s), 1408 (m), 1246 (s), 1127 (s), 824 (m, CCl), 745 (s). MS (EI, 125 °C): *m/z* (%) 438/404 (14/11) [M^+], 317/319 (31/24) [M^+- CH_2Ph$(OMe)_2$], 232/234 (20/16) [phenothiazine hydrochloride]. HRMS $C_{25}H_{27}ClN_2OS$: found 438.1539 [calcd. 435.1533].

4.4.7. ***NB 03*** *3-(2-Chlorophenothiazin-10-yl)-N-[2-(3,4-dimethoxyphenyl)ethyl]-N-methyl-propan-1-amine (**18**)*

Method **C**, reactant: **16**. **16** (0.29 g, 1.45 mmol) was dissolved in dry a mix of THF/toluene (2:1 (*v/v*), 30 mL). *n*-BuLi (0.82 mL, 1.31 mmol), **4** (0.29 g, 1.45 mmol) in toluene (10 mL) and TIBA (0.53 g, 1.45 mmol) were added constantly stirring. The mixture was refluxed for 48 h and resulting product was purified by column chromatography (chloroform-methanol, 99:1 (*v/v*)) to give a light brown oil: **18** (NB 03) (0.23 g, 37%). ^{1}H NMR (250 MHz, $CDCl_3$): δ 2.02–2.13 (dt, 2H, J = 6.78 Hz, $CH_2CH_2CH_2$), 2.39 (s, 3H, CH_3), 2.66–2.69 (t, 2H, J = 6.78 Hz, CH_2NH), 2.72–2.77 (m, 4H, 2 CH_2CH_2Ph), 3.84 (s, 3H, OCH_3), 3.86 (s, 3H, OCH_3), 3.92–3.97 (t, 2H, J = 6.78 Hz, -NCH_2), 6.63–6.68 (m, 2H, CH-Ar), 6.75–6.78 (m, 1H, CH-Ar), 6.89–6.98 (m, 4H, CH-Ar), 7.01–7.04 (m, 1H, CH-Ar), 7.10–7.15 (m, 1H, CH-Ar), 7.17–7.21 (m, 1H, CH-Cl). ^{13}C NMR (63 MHz, $CDCl_3$): δ 24.52 ($CH_2CH_2CH_2$), 33.29 (CH_2Ph), 42.22 (NCH_3), 44.94 (-NCH_2), 54.24 (CH_2NMe), 55.68 (OCH_3), 55.76 (OCH_3), 59.77 (CH_2NMe), 111.11, 111.86, 120.36 (CH-Ph), 115.72, 115.76,122.69, 127.24, 127.31, 127.69 (CH-Ar), 123.38, 124.63 (C-S), 132.97 (C-Ph), 133.03 (C-Cl), 144.39, 146.38 (C-N), 147.10, 148.63 (COMe). IR (KBr): $\tilde{\nu}$(cm^{-1}) 2956, 2872, 2694, 1667, 1471, 1408, 1246, 1027, 855, 785. MS (EI, 125 °C): *m/z* (%) = 468/470 (22/9) [M^+], 317/319 (63/24) [M^+- CH_2Ph$(OMe)_2$], 232/234 (10/5) [phenothiazine hydrochloride]. HRMS: $C_{26}H_{29}ClN_2O_2S$: found 468.1642 [calcd. 468.1638].

4.4.8. ***NB 05*** *3-Carbazol-9-yl-N-[2-(3,4-dimethoxyphenyl)ethyl]-N-methyl-propan-1-amine (**22**)*

Method **C**, reactant: **21. 21** (0.90 g, 3.78 mmol) was dissolved in dry THF/toluene (2:1 (*v/v*), 20 mL), *n*-BuLi (2.36 mL, 3.78 mmol), **4** (0.71 g, 4.16 mmol) in toluene (10 mL) and TIBA (1.53 g, 4.16 mmol) were added and the reaction mixture refluxed overnight. Crude product was purified by column chromatography (chloroform-methanol 99:1 (*v/v*)) to afford a yellow oil: **22** (NB 05) (0.59 g, 39%). ^{1}H NMR (250 MHz, $CDCl_3$): δ 1.98–2.09 (tt, 2H, J = 6.78 Hz, $CH_2CH_2CH_2$), 2.29 (s, 3H, CH_3), 2.39–2.44 (t, 2H, J = 6.78 Hz, CH_2Ph),

Please cite this article in press as: M. Blaess, et al., NB 06: From a simple lysosomotropic aSMase inhibitor to tools for elucidating the role of lysosomes in signaling apoptosis and LPS-induced inflammation, European Journal of Medicinal Chemistry (2017), https://doi.org/10.1016/j.ejmech.2017.09.021

2.53–2.59 (m, 2H, CH_2NMe), 2.69–2.75 (m, 2H, CH_2NMe), 3.83 (s, 3H, OCH_3), 3.85 (s, 3H, OCH_3), 4.32–4.38 (t, 2H, J = 6.78 Hz, -NCH_2), 6.72–6.80 (m, 2H, C*H*-Ar), 7.17–7.22 (m, 3H, C*H*-Ar), 7.39–7.48 (m, 4H, C*H*-Ar), 8.07–8.10 (m, 2H, C*H*-Ar). ^{13}C NMR (90.6 MHz, $CDCl_3$): δ 26.57 ($CH_2CH_2CH_2$), 33.46 (CH_2Ph), 40.63 (-NCH_2), 41.86 (CH_3), 54.79 (CH_2NMe), 55.86, 55.95 (2OCH_3), 59.64 (CH_2NMe), 108.80, 118.77, 120.29, 125.58 (4CH-Ar), 111.31, 112.07, 120.58 (3CH-Ar), 122.84 (*C*-*C*), 133.11 (*C*-Ar), 140.49 (C-N), 147.39, 148.87 (2COMe). IR (KBr): $\tilde{\nu}$(cm^{-1}) 2958 (s), 2874 (s), 1652 (m), 1516 (m), 1471 (s), 1381 (m), 1326 (s), 1110 (m), 896 (m), 747 (m). MS (EI, 65 °C): *m/z* (%) 402 (2) [M^+], 251 (75) [M^+- $CH_2Ph(OMe)_2$], 180 (34) [M^+- $C_3H_7NC_2H_4Ph(OMe)_2$], 166 (2) [carbazole]. HRMS $C_{26}H_{30}N_2O_2$: found 402.2309 [calcd. 402.2307].

4.4.9. ***NB 06*** *3-Carbazol-9-yl-N-[2-(4-methoxyphenyl)ethyl]-N-methyl-propan-1-amine (**23**)*

Method **C**, reactant: **21**. **21** (0.30 g, 1.26 mmol) dissolved in toluene (30 mL) and deprotonated with *n*-BuLi (1.80 mL, 2.94 mmol). **7** (0.24 g, 1.39 mmol) in 10 mL toluene and TIBA (0.51 g, 1.39 mmol) were added and reaction mix was refluxed 48 h; the suspension was diluted with toluene and washed and the concentrated product purified by column chromatography to yield a yellow oil: **23** (NB 06) (0.19 g, 41%). ^{1}H NMR (360 MHz, $CDCl_3$): δ 1.96–2.04 (tt, 2H, J = 6.73 Hz, $CH_2CH_2CH_2$), 2.27 (s, 3H, CH_3), 2.36–2.40 (t, 2H, J = 6.73 Hz, CH_2Ph), 2.52–2.56 (m, 2H, CH_2NMe), 2.68–2.74 (m, 2H, CH_2NMe), 3.75 (s, 3H, OCH_3), 4.29–4.33 (t, 2H, J = 6.73 Hz, -NCH_2), 6.81–6.84 (m, 2H, C*H*-Ar), 7.08–7.11 (m, 2H, C*H*-Ar), 7.39–7.46 (m, 4H, C*H*-Ar), 8.07–8.11 (m, 2H, C*H*-Ar). ^{13}C NMR (90.6 MHz, $CDCl_3$): δ 25.92 ($CH_2CH_2CH_2$), 32.07 (CH_2Ph), 40.32 (-NCH_2), 41.44 (CH_3), 54.50 (CH_2NMe), 55.26 (OCH_3), 59.03 (CH_2NMe), 108.72, 118.90, 120.33, 127.08 (4CH-Ar), 113.93, 129.61 (2CH-Ar), 122.85 (*C*-*C*), 131.45 (*C*-Ar), 140.37 (C-N), 158.11 (COMe). IR (KBr): $\tilde{\nu}$(cm^{-1}) 2949 (s), 2835 (s), 1597 (m), 1512 (s), 1484 (s), 1453 (s), 1326 (m), 1247 (s), 1153 (m), 1037 (m), 824 (m), 750 (s). MS (EI, 65 °C): *m/z* (%) 372 (2) [M^+], 251 (37) [M^+- CH_2PhOMe], 180 (20) [M^+- $C_3H_7NC_2H_4PhOMe$], 166 (2) [carbazole]. HRMS $C_{25}H_{28}N_2O$: found 372.2203 [calcd. 372.2202].

4.4.10. ***NB 30*** *3-Carbazol-9-yl-N-[(4-methoxyphenyl)methyl]-N-methyl-propan-1-amine (**25**)*

Method **C**, reactant: **21**. **21** (0.30 g, 1.26 mmol) dissolved in dry toluene (30 mL), *n*-BuLi (1.80 mL, 2.94 mmol), 1-(chloromethyl)-4-methoxy-benzene (**24**) (1.19 mL, 1.39 mmol) in toluene (10 mL) and TBAI (0.51 g, 1.39 mmol) were added and the resulting mix was refluxed 48 h. The suspension then was diluted with toluene and washed and the crude product purified by column chromatography (chloroform-methanol 99:1 (*v/v*)) to give a yellow syrup: **25** (NB 30) (0.151 g, 33%). ^{1}H NMR (360 MHz, $CDCl_3$) δ 2.02–2.10 (tt, 2H, J = 6.73 Hz, $CH_2CH_2CH_2$), 2.17 (s, 3H, CH_3), 2.40–2.44 (t, 2H, J = 6.73 Hz, CH_2NMe), 3.43 (s, 2H, CH_2Ph), 3.79 (s, 3H, OCH_3), 4.35–4.39 (t, 2H, J = 6.97 Hz, -NCH_2), 6.82–6.87 (m, 2H, C*H*-Ar), 7.19–7.26 (m, 2H, C*H*-Ar), 7.29–7.36 (m, 4H, C*H*-Ar), 7.42–7.48 (m, 2H, C*H*-Ar), 8.07–8.09 (m, 2H, C*H*-Ar). ^{13}C NMR (90.6 MHz, $CDCl_3$), δ 26.38 ($CH_2CH_2CH_2$), 40.64 (CH_2NMe), 41.66 (CH_3N), 54.27 (CH_2Ph), 55.19 (OCH_3), 61.36 (-NCH_2), 108.67, 118.73, 120.25, 125.57 (4CH-Ar), 113.65, 130.21 (2CH-Ph), 122.79 (*C*-*C*), 131.99 (*C*-Ph), 140.39 (C-N), 158.75 (COMe). IR (Film): $\tilde{\nu}$(cm^{-1}) 2951 (s), 2835 (s, OMe), 1611 (m), 1512 (s), 1484 (s), 1326 (m), 1249 (s), 1121 (m), 816 (m), 750 (s), 724 (m). MS (EI, 135 °C): *m/z* (%) 358 (24) [M^+], 237 (28) [M^+- CH_2PhOMe], 180 (49) [M^+- $C_3H_8NCH_2PhOMe$], 167 (16), 166 (18) [carbazole]. HRMS $C_{24}H_{26}N_2O$: found 358.2049 [calcd. 358.2045].

4.4.11. ***NB 25*** *N-(2-carbazol-9-ylethyl)-2-(4-methoxyphenyl)-N-methyl-ethanamine (**28**)*

Method **C**, reactant: **27**. **27** (0.25 g, 1.12 mmol) was dissolved in THF (30 mL), *n*-BuLi (0.84 mL, 1.34 mmol), **7** (0.21 g, 1.23 mmol) in 10 mL toluene and TBAI (0.45 g, 1.23 mmol) were added, the reaction mixture then was refluxed 48 h. Processing and purification afforded a yellow oil: **28** (NB 25) (0.098 g, 25%). ^{1}H NMR (360 MHz, $CDCl_3$): δ 2.43–2.47 (t, 2H, J = 6.68 Hz, CH_2Ph), 2.25 (s, 3H, CH_3), 2.62–2.66 (m, 2H, CH_2NMe), 2.69–2.73 (m, 2H, CH_2NMe), 3.69 (s, 3H, OCH_3), 4.24–4.28 (t, 2H, J = 6.68 Hz, -NCH_2), 6.65–6.69 (m, 2H, C*H*-Ar), 7.02–7.06 (m, 2H, C*H*-Ar), 7.38–7.47 (m, 4H, C*H*-Ar), 8.10–8.14 (m, 2H, C*H*-Ar). ^{13}C NMR (90.6 MHz, $CDCl_3$): δ 32.17 (CH_2Ph), 40.96 (-NCH_2), 45.46 (CH_3), 55.25 (OCH_3), 54.55 (CH_2NMe), 59.12 (CH_2NMe), 108.74, 118.82, 119.93, 126.01 (4CH-Ar), 113.99, 129.43 (2CH-Ar), 122.67 (*C*-*C*), 130.94 (*C*-Ar), 140.32 (C-N), 158.41 (COMe). IR (Film): $\tilde{\nu}$(cm^{-1}) 2933 (s, CH_3), 2835 (s, OMe), 1675 (m), 1627 (m), 1598 (m), 1512 (s), 1453 (s), 1350 (m), 1246 (s), 1153 (m), 1121 (m), 824 (m), 740 (s), 680 (s). MS (EI, 120 °C): *m/z* (%) 358 (7) [M^+], 237 (49) [M^+- CH_2PhOMe], 194 (23) [M^+- $CH_3NC_2H_4PhOMe$], 180 (18) [M^+- $C_2H_5NC_2H_4PhOMe$], 167 (8), 166 (6) [carbazole]. HRMS $C_{24}H_{26}N_2O$: found 358.2049 [calcd. 358.2045].

4.4.12. ***NB 29*** *9-[(4-methoxyphenyl)methyl]carbazole (**30**)*

Method **C**, reactant: **19**. **19** (0.30 g, 1.79 mmol) was dissolved in dry THF (30 mL), *n*-BuLi (1.35 mL, 2.15 mmol), **24** (0.27 mL, 1.97 mmol) in 10 mL toluene and TBAI (0.73 g, 1.97 mmol) were added. The reaction mixture then was refluxed 48 h, processing and purification by column chromatography afforded a light yellow solid: **30** (NB 29) (0.19 g, 41%). ^{1}H NMR (360 MHz, $CDCl_3$): δ 2.78 (s, 2H, -NCH_2), 3.69 (s, 3H, OCH_3), 6.66–6.70 (m, 2H, C*H*-Ph), 6.95–6.99 (m, 2H, C*H*-Ar), 7.18–7.21 (m, 2H, C*H*-Ar), 7.27–7.38 (m, 4H, C*H*-Ar), 8.06–8.09 (m, 2H, C*H*-Ar). ^{13}C NMR (90.6 MHz, $CDCl_3$): δ 45.83 (-NCH_2), 55.03 (OCH_3), 108.86, 119.07, 120.28, 125.74 (4CH-Ar), 114.02, 127.95 (2CH-Ar), 128.53 (*C*-*C*), 144.44 (C-N), 158.84 (COMe). IR (KBr): $\tilde{\nu}$(cm^{-1}) 2833 (s, OMe), 1612 (m), 1511 (s), 1485 (s), 1248 (s), 849 (m), 750 (s), 722 (s). MS (EI, 65 °C): *m/z* (%) 287 (100) [M^+], 256 (10) [M^+-OMe], 242 (18) [M^+- CH_2OMe], 241 (45), 180 (20) [M^+- PhOMe], 166 (6), 167 (11) [carbazole]. HRMS $C_{20}H_{17}NO$: found 287.1314 [calcd. 287.1310].

4.4.13. ***NB 35*** *N-[2-(3,4-dimethoxyphenyl)ethyl]-N-methyl-N′,N′-diphenyl-propane-1,3-diamine (**34**)*

Method **C**, reactant: **33**. **33** (0.30 g, 1.25 mmol) was dissolved in THF/toluene (3:1 (*v/v*), 40 mL), treated with *n*-BuLi (2.5 M in *n*-hexane) (0.60 mL, 1.50 mmol), **4** (0.30 g, 1.50 mmol) in 10 mL toluene and TIBA (0.55 g, 1.50 mmol). The reaction mixture was refluxed overnight; processing and purification afforded a yellow oil: **34** (NB 35) (0.123 g, 24%). ^{1}H NMR (250 MHz, $CDCl_3$): δ 1.77–1.85 (tt, 2H, J = 7.28 Hz, $CH_2CH_2CH_2$), 2.29 (s, 3H, CH_3), 2.43–2.49 (t, 2H, J = 7.28 Hz, CH_2NMe), 2.59–2.78 (m, 4H, CH_2CH_2Ph), 3.72–3.78 (t, 2H, J = 7.28 Hz, -NCH_2), 3.85 (s, 6H, 2CH_3), 6.69–6.77 (m, 4H, C*H*-Ar), 6.79–6.87 (m, 2H, C*H*-Ar), 6.90–6.99 (m, 4H, C*H*-Ar), 7.00–7.04 (m, 1H, C*H*-Ar), 7.15–7.21 (m, 2H, C*H*-Ar). ^{13}C NMR (90.6 MHz, $CDCl_3$): δ 25.09 ($CH_2CH_2CH_2$), 32.29 (CH_2Ph), 42.96 (CH_3), 50.04 (-NCH_2), 54.87 (CH_2NMe), 55.72 (OCH_3), 55.81 (OCH_3), 59.57 (CH_2NMe), 111.24, 111.99, 121.04 (3CH-Ar), 120.87, 121.14, 129.24 (3CH-Ar), 132.95 (*C*-Ar), 147.24 (COMe), 147.95 (C-N), 148.76 (COMe). IR (Film): $\tilde{\nu}$(cm^{-1}) 2950 (s), 2835 (s), 2792 (m), 1677 (m), 1589 (s), 1504 (s), 1455 (s), 1365 (m), 1262 (s), 1237 (s), 1142 (m), 747 (s), 698 (s). MS (EI, 130 °C): *m/z* (%) 404 (11) [M^+], 253 (34) [M^+- CH_2PhOMe], 182 (19) [M^+-$C_2H_4NCH_3C_2H_4PhOMe$], 168 (7) [diphenylamine]. HRMS $C_{26}H_{32}N_2O_2$: found 404.2462 [calcd. 404.2464].

Please cite this article in press as: M. Blaess, et al., NB 06: From a simple lysosomotropic aSMase inhibitor to tools for elucidating the role of lysosomes in signaling apoptosis and LPS-induced inflammation, European Journal of Medicinal Chemistry (2017), https://doi.org/10.1016/j.ejmech.2017.09.021

4.4.14. **NB 34** *N-[2-(4-methoxyphenyl)ethyl]-N-methyl-N′,N′-diphenyl-propane-1,3-diamine (**35**)*

Method **C**, reactant: **33**. **33** (0.30 g, 1.25 mmol) was dissolved in THF/toluene (3:1 (*v/v*), 40 mL), deprotonated with *n*-BuLi (2.5 M in hexane) (0.60 mL, 1.50 mmol), treated with **7** (0.26 g, 1.50 mmol) and TBAI (0.55 g, 1.50 mmol). The mixture was refluxed overnight; processing and purification afforded a yellow oil: **35** (NB 34) (0.119 g, 25%). ^{1}H NMR (250 MHz, $CDCl_3$): δ 1.78–1.86 (tt, 2H, J = 6.97 Hz, $CH_2CH_2CH_2$), 2.27 (s, 3H, CH_3), 2.41–2.46 (t, 2H, J = 6.97 Hz, CH_2Ph), 2.51–2.56 (m, 2H, CH_2NMe), 2.66–2.71 (m, 2H, CH_2NMe), 3.72–3.75 (t, 2H, J = 6.97 Hz, -NCH_2), 3.77 (s, 3H, CH_3), 6.80–6.82 (m, 2H, C*H*-Ar), 6.91–6.95 (m, 2H, C*H*-Ar), 6.97–7.00 (m, 2H, C*H*-Ar), 7.07–7.09 (m, 2H, C*H*-Ar), 7.22–7.28 (m, 2H, C*H*-Ar). ^{13}C NMR (90.6 MHz, $CDCl_3$): δ 25.16 ($CH_2CH_2CH_2$), 32.90 (CH_2Ph), 42.13 (CH_3), 50.15 (-NCH_2), 54.99 (CH_2NMe), 55.24 (OCH_3), 59.76 (CH_2NMe), 113.96, 129.58 (2CH-Ar), 120.96, 121.12, 129.24 (3CH-Ar), 132.48 (*C*-Ar), 148.03 (C-N), 157.87 (*C*OMe). IR (Film): $\tilde{\nu}$(cm^{-1}) 2932 (s), 2851 (m), 2792 (m), 1647 (m), 1589 (s), 1512 (s), 1496 (s), 1363 (m), 1246 (s), 1110 (m), 747 (s), 698 (s). MS (EI, 110 °C): *m/z* (%) 374 (5) [M^+], 253 (27) [M^+-CH_2PhOMe], 209 (16) [M^+-$CH_3NC_2H_4$PhOMe], 182 (20) [M^+-$C_2H_4NCH_3C_2H_4$PhOMe], 168 (3) [diphenylamine]. HRMS $C_{25}H_{30}N_2O$: found 374.2368 [calcd. 374.2358].

4.4.15. **NB 37** *N-[2-(3,4-dimethoxyphenyl)ethyl]-N-methyl-3-phenoxazin-10-yl-propan-1-amine (**39**)*

Method **C**, reactant: **38**. **38** (0.50 g, 1.97 mmol) was dissolved in THF (40 mL), deprotonated with *n*-BuLi (1.48 mL, 2.36 mmol), treated with **4** (0.44 g, 2.17 mmol) in 10 mL toluene and TIBA (0.80 g, 2.17 mmol); the mixture was refluxed 48 h, processing and purification yielded a red oil: **39** (NB 37) (0.19 g, 23%). ^{1}H NMR (360 MHz, $CDCl_3$): δ 1.80–1.88 (tt, 2H, J = 6.73 Hz, $CH_2CH_2CH_2$), 2.36 (s, 3H, CH_3), 2.52–2.56 (t, 2H, J = 6.73 Hz, CH_2Ph), 2.63–2.67 (m, 2H, CH_2NH), 2.75–2.79 (m, 2H, CH_2NH), 3.52–3.56 (t, 2H, J = 6.73 Hz, -NCH_2), 3.85 (s, 3H, OCH_3), 6.51–6.53 (m, 2H, C*H*-Ar), 6.61–6.68 (m, 4H, C*H*-Ar), 6.73–6.79 (m, 4H, C*H*-Ar), 7.10–7.13 (m, 1H, C*H*-Ar). ^{13}C NMR (90.6 MHz, $CDCl_3$): δ 22.72 ($CH_2CH_2CH_2$), 33.29 (CH_2Ph), 41.71 (-NCH_2), 41.99 (CH_3), 54.72 (CH_2NMe), 55.79, 55.85 ($2OCH_3$), 59.56 (CH_2NMe), 111.27, 111.97, 120.50 (3CH-Ar), 111.32, 115.26, 120.70, 123.55 (4CH-Ar), 132.61 (*C*-Ar), 133.25 (C-N), 144.89 (C-O), 147.37, 148.84 (2*C*OMe). IR (Film): $\tilde{\nu}$(cm^{-1}) 2953 (s), 2936 (s), 2795 (m), 1628 (m), 1592 (m), 1516 (m), 1489 (s), 1464 (s), 1380 (m), 1270 (s), 1237 (s), 1142 (m), 840 (s), 780 (s). MS (EI, 154 °C): *m/z* (%) 418 (29) [M^+], 267 (33) [M^+- $CH_2Ph(OMe)_2$], 196 (36) [M^+-$C_3H_7NC_2H_4Ph(OMe)_2$], 183 (11), 182 (13) [phenoxazine]. HRMS $C_{26}H_{30}N_2O_3$: found 418.2260 [calcd. 418.2256].

4.4.16. **NB 20** *N-[2-(4-methoxyphenyl)ethyl]-N-methyl-3-phenoxazin-10-yl-propan-1-amine (**40**)*

Method **C**, reactant: **38**. **38** (0.30 g, 1.18 mmol) was dissolved in toluene (40 mL), *n*-BuLi (0.89 mL, 1.42 mmol), 2-(4-methoxyphenyl)ethyl chloride (**7**) (0.22 g, 1.30 mmol) in 10 mL toluene and TIBA (0.48 g, 1.30 mmol) were added. The mixture was stirred 48 h under reflux. After processing and purification a light yellow syrup was obtained: **40** (NB 20) (0.161 g, 35%). ^{1}H NMR (360 MHz, $CDCl_3$): δ 1.94–2.02 (tt, 2H, J = 6.73 Hz, $CH_2CH_2CH_2$), 2.49 (s, 3H, CH_3), 2.75–2.79 (t, 2H, J = 7.68 Hz, CH_2NMe), 2.82–2.90 (m, 4H, CH_2CH_2Ph), 3.56–3.61 (t, 2H, J = 6.73 Hz, -NCH_2), 3.77 (s, 3H, OCH_3), 6.53–6.55 (m, 2H, C*H*-Ar), 6.61–6.68 (m, 4H, C*H*-Ar), 6.77–6.84 (m, 4H, C*H*-Ar), 7.10–7.13 (m, 2H, C*H*-Ar). ^{13}C NMR (90.6 MHz, $CDCl_3$): δ 23.22 ($CH_2CH_2CH_2$), 32.75 (CH_2Ph), 41.85 (CH_3), 41.98 (-NCH_2), 54.25 (CH_2N), 55.65 (OCH_3), 58.89 (CH_2N), 111.72, 115.83, 121.02, 123.96 (4CH-Ar), 114.01, 129.59 (2CH-Ar), 130.92 (*C*-Ar), 133.12 (C-N), 145.34 (C-O), 158.98 (*C*OMe). IR (Film): $\tilde{\nu}$(cm^{-1}) 2959 (s, CH_3), 2861 (s, OMe), 2360 (s), 1692 (m), 1592 (m), 1514 (s), 1466 (s), 1380 (s), 1272 (s), 1179 (m), 1035 (s, COC), 823 (s), 745 (s). MS (EI, 136 °C): *m/z* (%) 388 (16) [M^+], 267 (17) [M^+- CH_2PhOMe], 196 (30) [M^+-$C_3H_7NC_2H_4$PhOMe], 183 (12), 182 (14) [phenoxazine]. HRMS $C_{25}H_{28}N_2O_2$: found 388.2150 [calcd. 388.2151].

4.4.17. **NB 40** *N-[2-(3,4-dimethoxyphenyl)ethyl]-N-methyl-3-phenothiazin-10-yl-propan-1-amine (**44**)*

Method **C**, reactant: **43**. **43** (0.50 g, 1.85 mmol) was dissolved in THF (40 mL), treated with *n*-BuLi (1.39 mL, 2.22 mmol), **4** (0.35 g, 2.04 mmol) in toluene (10 mL) and TIBA (0.75 g, 2.04 mmol). The mixture was refluxed overnight. After processing and purification a yellow oil was obtained: **44** (NB 40) (0.26 g, 32%). ^{1}H NMR (360 MHz, $CDCl_3$): δ 1.91–1.98 (tt, 2H, J = 6.68 Hz, $CH_2CH_2CH_2$), 2.27 (s, 3H, CH_3), 2.52–2.58 (m, 4H, CH_2CH_2Ph), 2.61–2.67 (m, 2H, CH_2NMe), 3.83 (s, 3H, OCH_3), 3.84 (s, 3H, OCH_3), 3.89–3.92 (t, 2H, J = 6.68 Hz, -NCH_2), 6.64–6.66 (m, 2H, C*H*-Ar), 6.74–6.78 (m, 3H, C*H*-Ar), 6.85–7.91 (m, 2H, C*H*-Ar), 7.15–7.23 (m, 4H, CH-Ar). ^{13}C NMR (90.6 MHz, $CDCl_3$): δ 24.54 ($CH_2CH_2CH_2$), 33.15 (CH_2Ph), 42.23 (CH_3), 44.90 (-NCH_2), 54.40 (CH_2NMe), 55.74 (OCH_3), 55.81 (OCH_3), 59.63 (CH_2NMe), 111.14, 111.91, 120.40 (3CH-Ar), 115.52, 122.34, 127.13, 127.34 (4CH-Ar), 125.11 (C-S), 132.86 (*C*-Ar), 145.17 (C-N), 147.18, 148.68 (2*C*OMe). IR (Film): $\tilde{\nu}$(cm^{-1}) 2951 (s), 2835 (s), 2795 (m), 1592 (m), 1516 (s), 1459 (s), 1336 (m), 1261 (s), 1237 (s), 1156 (m), 1045 (s), 854 (m), 752 (s). MS (EI, 146 °C): *m/z* (%) 434 (6) [M^+], 283 (31) [M^+-$CHPh(OMe)_2$], 212 (28) [M^+- $C_2H_4NC_2H_4Ph(OMe)_2$], 198 (6) [thiodiphenylamine]. HRMS $C_{26}H_{30}N_2O_2S$: found 434.2033 [calcd. 434.2028].

4.4.18. **NB 39** *N-[2-(4-methoxyphenyl)ethyl]-N-methyl-3-phenothiazin-10-yl-propan-1-amine (**45**)*

Method **C**, reactant: **43**. **43** (0.50 g, 1.85 mmol) was dissolved in THF (40 mL) and deprotonated with *n*-BuLi (1.39 mL, 2.22 mmol). **7** (0.35 g, 2.04 mmol) dissolved in toluene (10 mL) and TIBA (0.75 g, 2.04 mmol) were added. The mixture was refluxed overnight; after processing and purification a yellow oil was obtained: **45** (NB 39) (0.23 g, 31%). ^{1}H NMR (360 MHz, $CDCl_3$): δ 1.97–2.05 (tt, 2H, J = 6.65 Hz, $CH_2CH_2CH_2$), 2.32 (s, 3H, CH_3), 2.57–2.66 (m, 4H, CH_2CH_2Ph), 2.67–2.70 (m, 2H, CH_2NMe), 3.76 (s, 3H, OCH_3), 3.90–3.96 (t, 2H, J = 6.65 Hz, -NCH_2), 6.77–6.79 (m, 2H, C*H*-Ar), 6.80–6.92 (m, 4H, C*H*-Ar), 6.99–7.03 (m, 2H, C*H*-Ar), 7.12–7.19 (m, 4H, C*H*-Ar). ^{13}C NMR (90.6 MHz, $CDCl_3$): δ 24.02 ($CH_2CH_2CH_2$), 32.01 (CH_2Ph), 41.98 (CH_3), 44.84 (-NCH_2), 52.41 (CH_2NMe), 55.18 (OCH_3), 59.25 (CH_2NMe), 113.80, 129.53 (2CH-Ph), 115.67, 122.51, 127.25, 127.45 (4CH-Ar), 125.32 (C-S), 131.49 (C-Ar), 144.10 (C-N), 157.95 (*C*OMe). IR (Film): $\tilde{\nu}$(cm^{-1}) 2933 (s), 2835 (s), 2795 (m), 1687 (m), 1593 (m), 1513 (s), 1463 (s), 1338 (m), 1248 (s), 1178 (m), 1038 (s), 825 (m), 753 (s). MS (EI, 212 °C): *m/z* (%) 404 (4) [M^+], 283 (28) [M^+-CHPhOMe], 270 (21) [M^+- C_2H_4PhOMe], 212 (15) [M^+-$C_2H_4NC_2H_4$PhOMe], 198 (5) [thiodiphenylamine]. HRMS $C_{25}H_{28}N_2OS$: found 404.1923 [calcd. 404.1922].

4.4.19. **NB 07** *2-(3,4-dimethoxyphenyl)-N-methyl-N-(2-phenothiazin-10-ylethyl)ethanamine (**48**)*

Method **C**, reactant: **47**. **47** (0.45 g, 1.78 mmol) was dissolved in THF (30 mL), BuLi (1.21 mL, 1.93 mmol), **4** (0.39 g, 1.93 mmol) in 10 mL toluene and TIBA (0.71 g, 1.93 mmol) were added. The mixture was refluxed 48 h, the crude compound purified by column chromatography (chloroform-methanol, 99:1 (*v/v*)) to give a light brown oil: **48** (NB 07) (0.24 g, 33%).

^{1}H NMR (360 MHz, $CDCl_3$): δ 2.32–2.36 (m, 2H, CH_2Ph), 2.42 (s, 3H, CH_3), 2.89–2.93 (t, 2H, J = 6.97 Hz, CH_2NMe), 3.32–3.37 (t, 2H, J = 6.97 Hz, CH_2NMe), 3.78 (s, 6H, $2OCH_3$), 4.03–4.08 (t, 2H, J = 6.97 Hz, -NCH_2), 6.85–6.91 (m, 2H, C*H*-Ar), 6.93–7.01 (m, 4H, C*H*-Ar), 7.11–7.18 (m, 4H, C*H*-Ar), 7.25–7.28 (m, 2H, C*H*-Ar). ^{13}C NMR (62.9 MHz, $CDCl_3$): δ 31.03 (CH_2Ph), 43.88 (CH_3), 45.89

Please cite this article in press as: M. Blaess, et al., NB 06: From a simple lysosomotropic aSMase inhibitor to tools for elucidating the role of lysosomes in signaling apoptosis and LPS-induced inflammation, European Journal of Medicinal Chemistry (2017), https://doi.org/10.1016/j.ejmech.2017.09.021

(-NCH_2), 54.56 (CH_2NMe), 55.27 (OCH_3), 55.39 (OCH_3), 60.68 (CH_2NMe), 113.85, 115.61, 122.56, 127.57 (4*C*H-Ar), 115.35, 129.85 (2*C*H-Ar), 124.92 (C-S), 131.06 (*C*-Ar), 145.23 (C-N), 148.51 (*C*OMe), 149.30 (*C*OMe). IR (KBr): $\tilde{\nu}$(cm^{-1}) 2931 (s), 2872 (s), 2705 (m), 2627 (m), 1593 (m), 1463 (s), 1307 (m), 1255 (m), 1128 (m), 840 (m), 750 (s). MS (EI, 65 °C): *m/z* (%) 420 (17) [M^+], 270 (8), 269 (56) [M^+- $CH_2N(OMe)_2$], 213 (71), 212 (36) [M^+- $C_2H_5NC_2H_4Ph(OMe)_2$], 199 (24), 93 (40) [thiodiphenylamine]. HRMS $C_{25}H_{28}N_2O_2S$: found 420.2879 [calcd. 420.1871].

4.4.20. ***NB 08*** *2-(4-methoxyphenyl)-N-methyl-N-(2-phenothiazin-10-ylethyl)ethanamine (**49**)*

Method **C**, reactant: **47**. **47** (0.65 g, 2.54 mmol) was dissolved in THF (40 mL), BuLi (1.75 mL, 2.793 mmol), **7** (0.48 g, 2.79 mmol) in 15 mL toluene and TIBA (1.03 g, 2.79 mmol) were added and the mixture was refluxed 48 h. The crude compound was purified by column chromatography (chloroform-methanol, 99:1 (*v/v*)) to give a light brown oil: **49** (NB 08) (0.24 g, 33%). ^{1}H NMR (360 MHz, $CDCl_3$): δ 2.30–2.35 (m, 2H, CH_2Ph), 2.40 (s, 3H, CH_3), 2.88–2.93 (t, 2H, *J* = 6.97 Hz, CH_2NMe), 3.31–3.35 (t, 2H, *J* = 6.97 Hz, CH_2NMe), 3.77 (s, 3H, OCH_3), 4.01–4.05 (t, 2H, *J* = 6.97 Hz, -NCH_2), 6.80–6.86 (m, 2H, C*H*-Ar), 6.88–6.99 (m, 4H, C*H*-Ar), 7.11–7.19 (m, 4H, C*H*-Ar), 7.21–7.25 (m, 2H, C*H*-Ar). ^{13}C NMR (63 MHz, $CDCl_3$): δ 31.03 (CH_2Ph), 43.88 (CH_3), 45.89 (-NCH_2), 54.56 (CH_2NMe), 55.27 (OCH_3), 55.39 (OCH_3), 60.68 (CH_2NMe), 113.85, 115.61, 122.56, 127.57 (*C*H-Ar), 115.35, 129.85 (*C*H-Ph), 124.92 (C-S), 131.06 (*C*-Ph), 145.23 (C-N), 148.51, 149.30 (2*C*OMe). IR (Film): $\tilde{\nu}$(cm^{-1}) 2963, 2896, 2724, 2615, 1633, 1468, 1357, 1263, 1148, 855, 785. MS (EI, 65 °C): *m/z* (%) = 390 (14) [M^+], 270 (14), 269 (41) [M^+- CH_2NOMe], 213 (27), 212 (84) [M^+- $C_2H_5NC_2H_4PhOMe$], 199 (29), 193 (54) [thiodiphenylamine]. HRMS: $C_{24}H_{26}N_2OS$: found 390.1768 [calcd. 390.1766].

4.4.21. ***NB 14*** *N-[3-(5,6-dihydrobenzo[b][1]benzazepin-11-yl) propyl]-2-(4-methoxyphenyl)-N-methyl-acetamide (**51**)*

Method **D**, reactant: **2**. **2** (0.60 g, 2.26 mmol) was dissolved in 1,2-dichloroethane (30 mL). The mixture was stirred 30 min at RT after addition of trimethylamine (0.93 mL, 6.76 mmol); a mixture of **50** (0.35 mL, 2.26 mmol) in 10 mL toluene and TIBA (1.25 g, 3.39 mmol) was added slowly and the solution stirred and refluxed overnight. Reaction was quenched by addition of saturated NH_4Cl and extracted with toluene (40 mL); the organic layer was dried with Na_2SO_4, filtered and solvent evaporated under vacuum. The residue was purified by column chromatography (chloroform-methanol, 99:1 (*v/v*)) to give a red/orange oil: **51** (NB 14) (0.25 g, 25%). ^{1}H NMR (360 MHz, $CDCl_3$): δ 1.73–1.81 (tt, 2H, *J* = 6.73 Hz, $CH_2CH_2CH_2$), 2.80 (s, 3H, CH_3), 3.12 (s, 4H, $2CH_2$), 3.39–3.41 (t, 2H *J* = 6.96 Hz, CH_2NMe), 3.58 (s, 2H, CH_2Ph), 3.66–3.71 (m, 2H, -NCH_2), 3.76 (s, 3H, OCH_3), 6.78–6.82 (m, 2H, C*H*-Ar), 6.87–6.98 (m, 4H, C*H*-Ar), 7.00–7.04 (m, 4H, C*H*-Ar), 7.07–7.3 (m, 2H, C*H*-Ar). ^{13}C NMR (90.6 MHz, $CDCl_3$): δ 26.45 ($CH_2CH_2CH_2$), 32.17 ($2CH_2$), 35.68 (CH_3), 40.46 (CH_2Ph), 45.68 (-NCH_2), 48.14 (CH_2NMe), 55.24 (OCH_3), 114.22, 122.77, 126.41, 129.33 (4*C*H-Ar), 119.85, 130.04 (2*C*H-Ar), 127.28 (*C*-Ar), 134.23 (*C*-*C*), 148.12 (C-N), 158.39 (*C*OMe), 171.24 (C=O). IR (Film): $\tilde{\nu}$(cm^{-1}) 2935 (s), 2837 (s, OMe), 1724 (s, C=O), 1657 (s, NCO), 1567(m), 1514 (s), 1332 (m), 1127 (m), 850 (s), 756 (s). MS (EI, 151 °C): *m/z* (%) 414 (42) [M^+], 235 (14) [M^+- CH_2NCOCH_2-PhOMe], 234 (22), 222 (42) [M^+- $C_2H_5NCOCH_2PhOMe$], 208 (100) [M^+- $C_3H_7NCOCH_2PhOMe$], 194 (34), 193 (49) [iminodibenzyl]. HRMS $C_{27}H_{30}N_2O_2$: found 414.2306 [calcd. 414.2307].

4.4.22. ***NB 17*** *N-[2-(5,6-dihydrobenzo[b][1]benzazepin-11-yl) ethyl]-2-(4-methoxyphenyl)-N-methyl-acetamide (**52**)*

Method **D**, reactant: **12**. **12** (0.40 g, 1.59 mmol) was dissolved in 1,2-dichloroethane (40 mL) and triethylamine (0.26 mL, 1.90 mmol) was added. The mixture was stirred for 30 min. **50** (0.26 mL, 1.75 mmol) in 10 mL toluene and TIBA (0.64 g, 1.75 mmol) were added, stirred and refluxed overnight. After washing with aqueous NH_4Cl and extraction with toluene (40 mL), the organic layer was dried over Na_2SO_4 and concentrated. Purification by column chromatography (chloroform-methanol, 99:1 (*v/v*)) afforded a red/orange oil: **52** (NB 17) (0.21 g, 33%). ^{1}H NMR (360 MHz, $CDCl_3$): δ 2.88 (s, 3H, CH_3), 3.12 (s, 4H, $2CH_2$), 3.50–3.54 (t, 2H, *J* = 6.73 Hz, CH_2NMe), 3.58 (s, 2H, CH_2Ph), 3.76 (s, 3H, OCH_3), 3.90–3.94 (t, 2H, *J* = 6.73 Hz, -NCH_2), 6.76–6.80 (m, 2H, C*H*-Ar), 6.86–6.98 (m, 4H, C*H*-Ar), 7.03–7.08 (m, 4H, C*H*-Ar), 7.11–7.14 (m, 2H, C*H*-Ar). ^{13}C NMR (90.6 MHz, $CDCl_3$): δ 31.99 ($2CH_2$), 37.06 (CH_3), 40.30 (CH_2Ph), 47.69 (CH_2NMe), 48.28 (-NCH_2), 55.21 (OCH_3), 114.08, 123.21, 126.60, 129.71 (4*C*H-Ar), 119.82, 130.24 (2*C*H-Ar), 127.26 (*C*-Ar), 134.66 (*C*-*C*), 148.13 (C-N), 158.29 (*C*OMe), 171.63 (C=O). IR (Film): $\tilde{\nu}$(cm^{-1}) 2926 (s), 2823 (s), 2359 (m), 1711 (m, C=O), 1647 (s), 1512 (s), 1487 (s), 1457 (m), 1247 (s), 1178 (m), 850 (m), 748 (s). MS (EI, 128 °C): *m/z* (%) 400 (6) [M^+], 222 (15) [M^+- CH_3NCOCH_2PhOMe], 221 (82), 209 (20), 208 (100) [M^+- $C_2H_5NCOCH_2PhOMe$], 193 (34) [iminodibenzyl]. HRMS $C_{26}H_{28}N_2O_2$: found 400.2161 [calcd. 400.2151].

4.4.23. ***NB 22*** *N-(3-carbazol-9-ylpropyl)-2-(4-methoxyphenyl)-N-methyl-acetamide (**53**)*

Method **D**, reactant: **21**. **21** (0.30 g, 1.26 mmol) was dissolved in THF (30 mL), triethylamine (0.21 mL, 1.51 mmol) was added at 0 °C. After 30 min stirring, **50** (0.21 mL, 1.39 mmol) in 10 mL toluene and TIBA (0.47 g, 1.39 mmol) were added, stirred and refluxed 48 h. After reaching RT, ethyl acetate (80 mL) was added and washed with aqueous saturated NH_4Cl (20 mL) and brine (10 mL). The organic solvent was evaporated and crude product purified by column chromatography (chloroform-methanol, 99:1 (*v/v*)) to afford a light yellow oil: **53** (NB 22) (0.11 g, 23%). ^{1}H NMR (250 MHz, $CDCl_3$): δ 1.97–2.07 (tt, 2H, *J* = 6.74 Hz, $CH_2CH_2CH_2$), 2.89 (s, 3H, CH_3), 3.21–3.30 (t, 2H, *J* = 6.74 Hz, CH_2NMe), 3.62 (s, 2H, CH_2Ph), 3.70 (s, 3H, OCH_3), 3.75–3.80 (t, 2H, *J* = 6.74 Hz, -NCH_2), 6.80–6.85 (m, 2H, C*H*-Ar), 7.01–7.07 (m, 2H, C*H*-Ar), 7.12–7.21 (m, 4H, C*H*-Ar), 7.38–7.45 (m, 2H, C*H*-Ar), 8.03–8.10 (m, 2H, C*H*-Ar), ^{13}C NMR (90.6 MHz, $CDCl_3$): δ 26.66 ($CH_2CH_2CH_2$), 35.79 (CH_3), 40.14 (CH_2NMe), 42.21 (-NCH_2), 45.82 (CH_2Ph), 55.28 (OCH_3), 108.54, 118.95, 120.38, 125.77 (4*C*H-Ar), 114.06, 129.72 (2*C*H-Ar), 122.40 (*C*-*C*), 126.59 (*C*-Ar), 140.17 (C-N), 158.63 (*C*OMe), 170.29 (C=O). IR (Film): $\tilde{\nu}$(cm^{-1}) 2935 (s, CH_3), 2836 (s, OMe), 2244 (m), 1719 (m, C=O), 1632 (s), 1512 (s), 1463 (s), 1248 (s), 1178 (m), 1034 (s), 855 (m), 745 (s). MS (EI, 157 °C): *m/z* (%) 386 (39) [M^+], 296 (21), 265 (13) [M^+- CH_2PhOMe], 238 (20) [M^+- $COCH_2PhOMe$], 180 (58) [M^+- $C_3H_8NCOCH_2PhOMe$], 167 (18), 166 (20) [carbazole]. HRMS $C_{25}H_{26}N_2O_2$: found 386.1998 [calcd. 386.1994].

4.4.24. ***NB 09*** *N-[3-(2-chlorophenothiazin-10-yl)propyl]-2-(3,4-dimethoxyphenyl)-N-methyl-acetamide (**55**)*

Method **D**, reactant: **16**. **16** (0.35 g, 1.15 mmol) was dissolved in 1,2-dichloroethane (30 mL) and triethylamine (0.45 mL, 3.28 mmol) was added. After 30 min stirring, 2-(3,4-dimethoxyphenyl)acetyl chloride (**54**) (0.35 g, 1.64 mmol) in 10 mL toluene was added and stirred another 2 h at RT before refluxing overnight. The mixture was diluted with toluene (80 mL) and washed with saturated aqueous NH_4Cl (20 mL); the organic layer was dried, filtered, evaporated, and the product was purified by column chromatography (chloroform-methanol, 99:1 (*v/v*)) to give a dark red syrup: **55** (NB 09) (0.29 g, 37%). ^{1}H NMR (250 MHz, $CDCl_3$): δ 1.97–2.08 (tt, 2H, *J* = 6.78 Hz, $CH_2CH_2CH_2$), 2.89 (s, 3H, CH_3N), 3.47–3.53 (t, 2H, *J* = 6.78 Hz, CH_2NMe), 3.61 (s, 2H, CH_2Ph), 3.80 (s, 6H, $2OCH_3$), 3.98–4.03 (t, 2H, *J* = 6.78 Hz, -NCH_2), 6.53–6.64 (m, 2H, C*H*-Ar), 6.71–6.84 (m, 4H, C*H*-Ar), 6.90–6.96 (m, 2H, C*H*-Ar), 7.11–7.16 (m,

Please cite this article in press as: M. Blaess, et al., NB 06: From a simple lysosomotropic aSMase inhibitor to tools for elucidating the role of lysosomes in signaling apoptosis and LPS-induced inflammation, European Journal of Medicinal Chemistry (2017), https://doi.org/10.1016/j.ejmech.2017.09.021

2H, C*H*-Ar). ^{13}C NMR (62.9 MHz, $CDCl_3$): δ 25.29 ($CH_2CH_2CH_2$), 36.27 (CH_3N), 40.86 (*C*H_2NMe), 47.15 (*C*H_2Ph), 47.17 (-N*C*H_2), 55.88 (OCH_3), 111.24, 112.01, 116.15 (3*C*H-Ar), 112.92, 120.86, 121.87, 122.59, 123.07, 127.53, 128.39 (7*C*H-Ar), 123.57, 127.34 (2C-S), 128.47 (*C*-Ar), 133.45 (CCl), 144.46, 146.39 (2C-N), 147.93, 148.81 (2*C*OMe), 171.49 (C=O). IR (KBr): $\tilde{\nu}$(cm^{-1}) 2936 (s), 2836 (s, OMe), 1720 (s, C=O), 1634 (s, NCO), 1592 (m), 1514 (s), 1463 (m), 1318 (m), 1142 (m), 855 (s), 756 (s). MS (EI, 125 °C): *m/z* (%) 438/440 (14/11) [M^+], 317/319 (31/24) [M^+- $CH_2Ph(OMe)_2$], 232/234 (20/16) [thiodiphenylamine chloride]. HRMS $C_{26}H_{27}ClN_2O_3S$: found 482.1432 [calcd. 482.1431].

4.4.25. ***NB 23*** *3-indol-1-yl-N-[2-(4-methoxyphenyl)ethyl]-N-methyl-propan-1-amine (**62**)*

Method **C**, reactant: **61**. **61** (0.30 g, 1.60 mmol) was dissolved in THF (30 mL), *n*-BuLi (1.20 mL, 1.91 mmol), **7** (0.30 g, 1.76 mmol) and TBAI (0.65 g, 1.76 mmol) were added and refluxed overnight. After processing, the solvent was removed. Purification afforded a colorless syrup: **62** (NB 23) (0.151 g, 29%). ^{1}H NMR (250 MHz, $CDCl_3$): δ 1.89–1.97 (tt, 2H, *J* = 6.85 Hz, $CH_2CH_2CH_2$), 2.26 (s, 3H, CH_3), 2.29–2.33 (t, 2H, *J* = 6.85 Hz, C*H*$_2$Ph), 2.50 2.55 (m, 2H, C*H*$_2$NMe), 2.66–2.70 (m, 2H, C*H*$_2$NMe), 3.75 (s, 3H, OCH_3), 4.08–4.11 (t, 2H, *J* = 6.85 Hz, -N*C*H_2), 6.44–6.46 (m, 1H, C*H*-Ar), 6.80–6.98 (m, 4H, C*H*-Ar), 7.05–7.09 (m, 1H, C*H*-Ar), 7.17–7.7.20 (m, 1H, C*H*-Ar), 7.30–7.36 (m, 2H, C*H*-Ar), 7.59–7.62 (m, 1H, C*H*-Ar). ^{13}C NMR (90.6 MHz, $CDCl_3$): δ 27.77 ($CH_2CH_2CH_2$), 32.85 (*C*H_2Ph), 41.84 (CH_3), 43.82(-N*C*H_2), 54.38 (*C*H_2NMe), 55.22 (OCH_3), 59.65 (*C*H_2NMe), 100.81, 109.83, 119.14, 120.86, 121.25, 128.05 (6*C*H-Ar), 109.43, 129.61 (2*C*H-Ar), 128.56 (*C*-*C*), 132.58 (*C*-Ar), 135.94 (C-N), 157.92 (*C*OMe). IR (Film): $\tilde{\nu}$(cm^{-1}) 2933 (s, CH_3), 2834 (s, OMe), 1612 (m), 1512 (s), 1464 (s), 1316 (m), 1247 (s), 1037 (m), 824 (m), 741 (s). MS (EI, 104 °C): *m/z* (%) 322 (11) [M^+], 201 (55) [M^+- CH_2PhOMe], 144 (6) [M^+- $C_2H_5NC_2H_4PhOMe$], 130 (23) [M^+- $C_3H_7NC_2H_4PhOMe$], 116 (11) [indole]. HRMS $C_{21}H_{26}N_2O$: found 322.2045 [calcd. 322.2045].

4.4.26. ***NB 12*** *2-(3,4-dimethoxyphenyl)-N-(1-naphthylmethyl) ethanamine (**64**)*

Method **C**, reactant: 1-naphtylmethanamine (**63**). **63** (0.60 g, 3.82 mmol) was dissolved in THF (50 mL), *n*-BuLi (2.86 mL, 4.58 mmol), **4** (0.84 g, 4.20 mmol) in 10 mL toluene and TIBA (1.55 g, 4.20 mmol) were added. The suspension was diluted with ethyl acetate (100 mL) and washed, the product then purified by column chromatography (chloroform-methanol, 99:1 (*v/v*)) to give a red oil: **64** (NB 12) (0.565 g, 46%). ^{1}H NMR (250 MHz, $CDCl_3$): δ 2.75 (s, 1H, NH), 2.79–2.85 (t, 2H, *J* = 6.84 Hz, C*H*$_2$Ph), 2.97–3.02 (t, 2H, *J* = 6.84 Hz, C*H*$_2$NH), 3.79 (s, 3H, OCH_3), 3.82 (s, 3H, OCH_3), 4.29 (s, 2H, NHC*H*$_2$-Ar), 6.69–6.74 (m, 4H, C*H*-Ar), 7.74–7.48 (m, 4H, C*H*-Ar), 7.73–7.76 (m, 1H, C*H*-Ar), 7.81–7.85 (m, 1H, C*H*-Ar), 7.99–8.03 (m, 1H, C*H*-Ar). ^{13}C NMR (62.9 MHz, $CDCl_3$): δ 32.37 (*C*H_2Ph), 50.66 (CH_2NH), 51.01 (CH_2NH), 55.75 (OCH_3), 55.84 (OCH_3), 111.98, 123.37, 125.24, 126.27, 127.90 (5*C*H-Ar), 120.57, 128.63 (2*C*H-Ar), 131.64 (*C*-Ar), 132.12, 133.74, 134.74 (3*C*-Ar), 147.48, 148.93 (2*C*OMe). IR (Film): $\tilde{\nu}$(cm^{-1}) 3318 (b, NH), 2932 (s), 2831 (s), 2598 (m), 2434 (m), 1674 (m), 1590 (s), 1514 (s), 1417 (m), 1329 (m), 1261 (s), 1027 (m), 855 (m), 778 (s). MS (EI, 100 °C): *m/z* (%) 321 (12) [M^+], 170 (23) [M^+- $CH_2Ph(OMe)_2$], 152 (26), 151 (11) [M^+- $NC_2H_4Ph(OMe)_2$], 142 (13), 141 (100) [naphtaline]. HRMS $C_{21}H_{23}NO_2$: found 321.1732 [calcd. 321.1729].

4.4.27. ***NB 13*** *2-(4-methoxyphenyl)-N-(1-naphthylmethyl) ethanamine (**65**)*

Method **C**, reactant: **63**. **63** (0.60 g, 3.82 mmol) was dissolved in THF (50 mL), deprotonated with *n*-BuLi (2.38 mL, 3.82 mmol), treated **7** (0.72 g, 4.20 mmol) in 20 mL toluene and TIBA (1.55 g, 4.20 mmol). The mixture was refluxed over night, processing and purification yielded a red oil: **65** (NB 13) (0.524 g, 47%). ^{1}H NMR (250 MHz, $CDCl_3$): δ 2.42 (s, 1H, NH), 2.75–2.81 (t, 2H, *J* = 6.84 Hz, C*H*$_2$Ph), 2.93–2.99 (t, 2H, *J* = 6.84 Hz, C*H*$_2$NH), 3.74 (s, 3H, OCH_3), 4.21 (s, 2H, NHC*H*$_2$-Ar), 6.78–6.81 (m, 2H, C*H*-Ar), 7.08–7.11 (m, 2H, C*H*-Ar), 7.37–7.47 (m, 4H, C*H*-Ar), 7.71–7.74 (m, 1H, C*H*-Ar), 7.80–7.85 (m, 1H, C*H*-Ar), 7.99–8.04 (m, 1H, C*H*-Ar). ^{13}C NMR (62.9 MHz, $CDCl_3$): δ 35.39 (*C*H_2Ph), 51.18 (CH_2NH), 51.43 (CH_2NH), 55.18 (OCH_3), 113.88, 125.31, 125.84, 127.62, 128.63 (5*C*H-Ar), 123.57, 129.56 (2*C*H-Ar), 131.77 (*C*-Ar), 132.05, 133.85, 135.89 (3*C*-Ar), 158.04 (*C*OMe). IR (Film): $\tilde{\nu}$(cm^{-1}) 3318 (b, NH), 2932 (s), 2833 (s), 1877 (m), 1611 (m), 1512 (m), 1457 (m), 1246 (s), 1177 (m), 1036 (s), 840 (m), 745 (s); MS (EI, 90 °C): *m/z* (%) 291 (13) [M^+], 171 (5), 170 (41) [M^+- $CH_2Ph(OMe)_2$], 152 (24), 151 (10) [M^+- NC_2H_4PhOMe], 142 (14), 141 (100) [naphtaline]. HRMS $C_{20}H_{21}NO$: found 291.1622 [calcd. 291.1623].

4.4.28. ***NB 10*** *N-[2-(3,4-dimethoxyphenyl)ethyl]-N′-(1-naphthyl) ethane-1,2-diamine (**67**)*

Method **C**, reactant: *N′*-(1-naphthyl)ethane-1,2-diamine (**66**). **66** (0.68 g, 2.62 mmol) was dissolved in THF (40 mL), treated with *n*-BuLi (4.92 mL, 7.87 mmol), **4** (0.81 g, 4.01 mmol) in 10 mL toluene and TIBA (1.48 g, 4.01 mmol). The resulting suspension was diluted with ethyl acetate (100 mL) and washed and the crude product purified by column chromatography (chloroform-methanol, 99:1 (*v/v*)) to give a red oil. **67** (NB 10) (0.83 g, 65%). ^{1}H NMR (250 MHz, $CDCl_3$): δ 2.18 (s, 1H, NH), 2.77–2.81 (t, 2H, *J* = 6.71 Hz, C*H*$_2$Ph), 2.92–2.96 (t, 2H, *J* = 7.38 Hz, C*H*$_2$NH), 3.02–3.05 (t, 2H, *J* = 6.71 Hz, C*H*$_2$NH), 3.34–3.37 (t, 2H, *J* = 7.38 Hz, C*H*$_2$NH-Ar), 3.82 (s, 6H, $2OCH_3$), 5.02 (s, 1H, NH), 6.57–6.59 (m, 1H, C*H*-Ar), 6.72–6.74 (m, 2H, C*H*-Ar), 7.20–7.23 (m, 2H, C*H*-Ar), 7.30–7.33 (m, 1H, C*H*-Ar), 7.41–7.45 (m, 2H, C*H*-Ar), 7.76–7.81 (m, 2H, C*H*-Ar). ^{13}C NMR (62.9 MHz, $CDCl_3$): δ 31.92 (*C*H_2Ph), 40.20 (CH_2NH-naphtaline), 46.46 (CH_2NH), 49.69 (CH_2NH), 55.67, 55.85 ($2OCH_3$), 104.26, 117.70, 122.01, 124.56, 125.58, 126.16, 127.14 (7*C*H-Ar), 111.08, 111.29, 120.67 (3*C*H-Ar), 123.71 (*C*-Ar), 129.14 (*C*-Ar), 134.05 (*C*-Ar), 142.63 (C-NH), 147.68, 148.87 (2*C*OMe). IR (KBr): $\tilde{\nu}$(cm^{-1}) 3348 (b, NH), 2961 (s), 2875 (s), 2772 (m), 1918 (m), 1663 (m), 1582 (m), 1516 (s), 1464 (s), 1381 (m), 1261 (s), 1158 (m), 809 (m), 749 (s). MS (EI, 141 °C): *m/z* (%) 350 (45) [M^+], 200 (11), 199 (76) [M^+- $CH_2Ph(OMe)_2$], 194 (50), 170 (23) [M^+- $CH_2NHC_2H_4Ph(OMe)_2$], 158 (13), 157 (100) [1-naphtylmethylamine]. HRMS $C_{22}H_{26}N_2O_2$: found 350.1997 [calcd. 350.1994].

4.4.29. ***NB 11*** *N-[2-(4-methoxyphenyl)ethyl]-N′-(1-naphthyl) ethane-1,2-diamine (**68**)*

Method **C**, reactant: **66**. **66** (0.524 g, 2.02 mmol) was dissolved in THF (40 mL), *n*-BuLi (3.79 mL, 6.06 mmol), 7 (0.53 g, 3.09 mmol) in 10 mL toluene and TBAI (1.14 g, 3.09 mmol) were added. The mixture was refluxed overnight, diluted with ethyl acetate (100 mL) and washed; crude product was purified by column chromatography (chloroform-methanol, 99:1 (*v/v*)) to yield a red oil: **68** (NB 11) (0.54 g, 60%). ^{1}H NMR (360 MHz, $CDCl_3$): δ 2.19 (s, 1H, NH), 2.76–2.99 (t, 2H, *J* = 6.71 Hz, C*H*$_2$Ph), 2.90–2.94 (t, 2H, *J* = 7.38 Hz, C*H*$_2$NH), 3.10–3.14 (t, 2H, *J* = 6.71 Hz, C*H*$_2$NH), 3.28–3.32 (t, 2H, *J* = 7.38 Hz, C*H*$_2$NH-Ar), 3.84 (s, 3H, OCH_3), 4.98 (s, 1H, NH), 6.66–6.68 (m, 1H, C*H*-Ar), 6.73–6.76 (m, 2H, C*H*-Ar), 7.18–7.22 (m, 2H, C*H*-Ar), 7.31–7.34 (m, 1H, C*H*-Ar), 7.48–7.52 (m, 2H, C*H*-Ar), 7.82–7.85 (m, 2H, C*H*-Ar). ^{13}C NMR (62.9 MHz, $CDCl_3$): δ 31.02 (*C*H_2Ph), 39.99 (*C*H_2NH-naphtaline), 46.75 (CH_2NH), 49.75 (CH_2NH), 55.02 (OCH_3), 104.29, 117.69, 122.45, 124.56, 125.59, 126.18, 127.95 (7*C*H-Ar), 113.88, 129.73 (2*C*H-Ar), 123.80 (*C*-Ar), 128.39 (*C*-Ar), 134.11 (*C*-Ar), 142.73 (C-NH), 158.32 (*C*OMe). IR (KBr): $\tilde{\nu}$(cm^{-1}) 3366 (b, NH), 2872 (s), 1582 (m), 1513 (m), 1473 (s), 1380 (m), 1245 (m), 1179 (m), 922 (m), 881 (m), 765 (s). MS (EI, 141 °C):

Please cite this article in press as: M. Blaess, et al., NB 06: From a simple lysosomotropic aSMase inhibitor to tools for elucidating the role of lysosomes in signaling apoptosis and LPS-induced inflammation, European Journal of Medicinal Chemistry (2017), https://doi.org/10.1016/j.ejmech.2017.09.021

m/z (%) 320 (45) [M^+], 200 (11), 199 (76) [M^+- CH_2PhOMe], 194 (50), 170 (23) [M^+- $CH_2NHC_2H_4PhOMe$], 158 (13), 157 (100) [1-naphtylmethylamine]. HRMS $C_{21}H_{24}N_2O$: found 320.1890 [calcd. 320.1889]. Anal ($C_{21}H_{24}N_2O$): C, H, N.

4.4.30. **NB 27** *3-[(4-methoxyphenyl)methyl]-1H-quinazoline-2,4-dione (**70**)*

Method **C**, reactant: 1*H*-quinazoline-2,4-dione (**69**). **69** (1.0 g, 6.17 mmol) was dissolved in THF (50 mL), *n*-BuLi (3.86 mL, 6.17 mmol) was added over a period of 20 min at −78 °C. Temperature was maintained under 0 °C during addition. After addition temperature was allowed to reach RT and the mixture was stirred 1 h. **24** (1.05 g, 6.79 mmol) in 10 mL toluene and TBAI (2.51 g, 6.79 mmol) were added and the mixture was refluxed overnight. Processing according to method **C** gave yellow crystals, crystallization with toluene afforded white needles: **70** (NB 27) (0.79 g, 45%). ^{1}H NMR (360 MHz, $CDCl_3$): δ 3.73 (s, 3H, OCH_3), 5.21 (s, 2H, -N*CH*$_2$), 6.80–6.90 (m, 2H, CH-Ar), 7.16–7.28 (m, 2H, C*H*-Ar), 7.48–7.54 (m, 3H, C*H*-Ar), 8.18–8.22 (m, 1H, C*H*-Ar), 10.42 (s, 1H, NH). ^{13}C NMR (62.9 MHz, $CDCl_3$): δ 43.52 (-NCH_2), 55.18 (OCH_3), 113.72, 130.62 (2*C*H-Ph), 115.00, 123.25, 128.62, 134.91 (4*C*H-Ar), 123.25 (*C*-Ar), 129.15 (*C*-Ar), 141.08 (C-NH), 150.90 (C=O), 159.06 (*C*OMe), 162.33 (C=O). IR (KBr): $\tilde{\nu}$(cm^{-1}) 3355 (s, NH), 3061 (m, CH), 2859 (s, OMe), 1693 (s, C=O), 1671 (s, C=O), 1455 (s), 1367 (m), 1251 (s), 1181 (m), 1128 (m), 1041 (s), 862 (m), 740 (s). MS (EI, 150 °C): *m/z* (%) 282 (31) [M^+], 253 (8) [M^+- OCH_3], 162 (13) [benzoylene urea]. HRMS $C_{16}H_{14}N_2O_3$: found 282.1003 [calcd. 282.1004].

4.4.31. **NB 28** *1,3-bis[(4-methoxyphenyl)methyl]quinazoline-2,4-dione (**71**)*

Method **C**, reactant: **69**. **69** (1.0 g, 6.17 mmol) in THF (50 mL), *n*-BuLi (8.48 mL, 13.57 mmol), **24** (2.10 g, 13.57 mmol) in 10 mL toluene and TIBA (5.01 g, 13.57 mmol) were added, the mixture stirred and refluxed 48 h. Processing and removal of the solvent afforded yellow crystals, crystallization with toluene yielded white needles: **71** (NB 28) (1.21 g, 49%) as. ^{1}H NMR (360 MHz, $CDCl_3$): δ 3.71 (s, 3H, OCH_3), 3.73 (s, 3H, OCH_3), 4.35 (s, 2H, -NCH_2), 5.24 (s, 2H, -NCH_2), 6.78–6.86 (m, 2H, C*H*-Ar), 7.10–7.15 (m, 1H, C*H*-Ar), 7.19–7.25 (m, 4H, C*H*-Ar), 7.51–7.54 (m, 2H, C*H*-Ar), 8.17–8.20 (m, 1H, C*H*-Ar). ^{13}C NMR (90.6 MHz, $CDCl_3$): δ 44.45 (-NCH_2), 46.72 (-NCH_2), 55.11 (OCH_3), 55.14 (OCH_3), 113.51, 114.24, 128.35, 131.88 (4*C*H-Ar), 122.83, 127.28, 128.76, 134.85 (4*C*H-Ar), 115.71 (C-Ar), 127.29, 129.25 (2*C*-Ar), 139.82 (C-N), 151.31 (C=O), 158.96, 159.00 (2*C*OMe), 161.63 (C=O). IR (KBr): $\tilde{\nu}$(cm^{-1}) 3355 (s, NH), 3061 (m, CH), 2859 (s, OMe), 1693 (s, C=O), 1671 (s, C=O), 1455 (s), 1367 (m), 1251 (s), 1181 (m), 1128 (m), 1041 (s), 862 (m), 740 (s). MS (EI, 170 °C): *m/z* (%) 402 (25) [M^+], 281 (21) [M^+-CH_2PhOMe], 238 (9) [M^+- $CONCH_2$PhOMe], 162 (3) [benzoylene urea]. HRMS $C_{24}H_{22}N_2O_4$: found 402.1587 [calcd. 402.1580].

4.4.32. **NB 26** *4-[(4-methoxyphenyl)methyl]-1,4-benzoxazin-3-one (**73**)*

Method **C**, reactant: 4H-1,4-benzoxazin-3-one (**72**). **72** (0.50 g, 3.35 mmol) was dissolved in THF (40 mL), *n*-BuLi (2.51 mL, 4.02 mmol), **24** (0.50 mL, 3.69 mmol) in 5 mL toluene and TIBA (1.36 g, 3.69 mmol) were added. The mixture was refluxed overnight and after processing and purification by crystallization with toluene, colorless crystals were obtained: **73** (NB 26) (0.244 g, 27%). ^{1}H NMR (250 MHz, $CDCl_3$): δ 3.73 (s, 3H, OCH_3), 4.70 (s, 3H, -NCH_2), 5.09 (s, 2H, CH_2O), 6.82–6.87 (m, 2H, C*H*-Ar), 6.91–6.99 (m, 4H, C*H*-Ar), 7.17–7.22 (m, 2H, C*H*-Ar). ^{13}C NMR (62.9 MHz, $CDCl_3$): δ 44.42 (-NCH_2), 55.28 (OCH_3), 67.75 (CH_2O), 114.33, 128.08 (2*C*H-Ar), 115.73, 116.96, 122.74, 123.93 (4*C*H-Ar), 128.52 (*C*-Ar), 129.19 (C-N), 145.41 (C-O), 159.04 (*C*OMe), 164.67 (C=O). IR (Film): $\tilde{\nu}$(cm^{-1}) 2872 (s, OMe), 1684 (s, C=O), 1515 (m), 1499 (s), 1472 (m), 1282 (m), 1252 (m), 1172 (m), 889 (s), 736 (s). MS (EI, 113 °C): *m/z* (%) 269 (13) [M^+], 134 (10) [M^+- NCH_2PhOCH_3], 121 (100) [M^+- $CH_3NCH_2PhOCH_3$]. HRMS $C_{16}H_{15}NO_3$: found 269.1055 [calcd. 269.1052].

4.4.33. **NB 33** *N-benzyl-N-[2-(4-methoxyphenyl)ethyl]pyridin-2-amine (**75**)*

Method **C**, reactant: *N*-benzylpyridin-2-amine (**74**). **74** (0.50 g, 2.71 mmol) was dissolved in dry THF (40 mL) and *n*-BuLi (2.03 mL, 3.26 mmol) was added at −78 °C. The mixture was stirred 1 h, **7** (0.51 g, 2.99 mmol) in 10 mL toluene and TIBA (1.10 g, 2.99 mmol) were added. Processing and purification yielded yellow crystals: **75** (NB 33) (0.26 g, 30%) as. ^{1}H NMR (250 MHz, $CDCl_3$): δ 2.83–2.89 (t, 2H, J = 7.64 Hz, C*H*$_2$Ar), 3.68–3.74 (dd, 2H, J = 7.64 Hz, -NCH_2), 3.79 (s, 3H, OCH_3), 4.64 (s, 2H, NC*H*$_2$Ar), 6.45–6.47 (m, 2H, C*H*-Ar), 6.53–6.57 (m, 1H, C*H*-Ar), 7.09–7.13 (m, 4H, C*H*-Ar), 7.18–7.29 (m, 4H, C*H*-Ar), 7.41–7.44 (m, 1H, C*H*-Ar), 8.19–8.21 (m, 1H, C*H*-Ar). ^{13}C NMR (62.9 MHz, $CDCl_3$): δ 32.67 (CH_2Ph), 50.51 (-NCH_2), 51.68 (-NCH_2Ph), 55.12 (OCH_3), 111.62, 113.52, 137.07, 148.00 (4CH-py), 113.78, 129.63 (2*C*H-Ar-OMe), 126.70, 126.81, 128.34 (3CH-Ph), 131.64 (*C*-Ar-OMe), 138.72 (*C*-Ar), 157.89 (*C*OMe), 157.96 (*C*-N). IR (KBr): $\tilde{\nu}$(cm^{-1}) 2889 (s), 1595 (s), 1556 (m), 1493 (s), 1369 (m), 1278 (m), 1242 (s), 1161(m), 1037 (s), 815 (m), 734 (s). MS (EI, 110 °C): *m/z* (%) 318 (15) [M^+], 198 (19), 197 (100) [M^+-CH_2PhOMe], 184 (12) [2-benylaminopyridine]. HRMS $C_{21}H_{22}N_2O$: found 318.1734 [calcd. 318.1732].

4.4.34. **NB 48** *4-[3-[2-(4-methoxyphenyl)ethyl-methyl-amino] propyl]-1,4-benzoxazin-3-one (**78**)*

Method **C**, reactant: **77**. **77** (0.30 g, 1.36 mmol) was dissolved in toluene (30 mL), deprotonated with *n*-BuLi (1.02 mL, 1.64 mmol), treated with **7** (0.25 mL, 1.50 mmol) in toluene (10 mL) and TIBA (0.55 g, 1.50 mmol); the mixture was refluxed 48 h, the suspension diluted with toluene and washed. Solvent then was evaporated and product purified by column chromatography to afford a yellow syrup: **78** (NB 48) (0.096 g, 18%). ^{1}H NMR (250 MHz, $CDCl_3$): δ 2.25–2.30 (tt, 2H, J = 6.78 Hz, $CH_2CH_2CH_2$), 2.82–2.85 (m, 2H, $CH_2N(Me)_2$), 2.91 (s, 3H, CH_3), 4.08–4.11 (t, 2H, J = 6.78 Hz, -NCH_2), 4.59 (s, 2H, CH_2O), 6.64–6.67 (m, 2H, C*H*-Ar), 6.99–7.05 (m, 4H, C*H*-Ar), 7.15–7.18 (m, 2H, C*H*-Ar), 8.72 (b, 1H, NH). ^{13}C NMR (62.9 MHz, $CDCl_3$): δ 24.03 ($CH_2CH_2CH_2$), 32.84 (2CH_3), 38.52 (-NCH_2), 46.82 (CH_2NH), 67.118 (CH_2O), 114.80, 116.84, 122.88, 123.91 (4CH-Ar), 129.19 (C-N), 144.94 (C-O), 164.38 (C=O). IR (Film): $\tilde{\nu}$(cm^{-1}) 3405 (b, NH), 2960 (s, CH_3), 1683 (s, C=O), 1604 (s), 1587 (m), 1505 (s), 1466 (s), 1273 (m), 1242 (m), 1160 (m), 740 (s). MS (EI, 125 °C): *m/z* (%) 220 (13) [M^+], 176 (12) [M^+- CH_3NHCH_3], 149 (26) [2*H*-1,4-benzoxazine-3(4*H*)-one]. HRMS $C_{21}H_{26}N_2O_3$: found 354.1932 [calcd. 354.1934].

4.4.35. *N′-(6,11-dihydro-5H-dibenzo[2,1-b:1′,2′-e][7]annulen-11-yl)propane-1,3-diamine (**83a**)*

Reactant: 5-chlorodibenzosuberane (**82**). To a stirred solution of 1,3-diaminopropane (1.0 g, 13.49 mmol) in toluene (30 mL) *n*-BuLi (2.10 mL, 3.37 mmol, 1.6 M in *n*-hexane) was added at −78 °C over a period of 20 min. The mixture was stirred 1 h at 0 °C before **82** (1.54 g, 6.74 mmol) in toluene (10 mL) and TBAI (2.49 g, 6.74 mmol) were added. After stirring 1 h at RT, the mixture was refluxed overnight. The solution then was cooled, diluted with toluene (70 mL) and washed with saturated NH_4Cl (20 mL). The organic layer was dried and evaporated to give a yellow oil as crude product. Purification by column chromatography (chloroform-methanol, 4:1 (*v/v*)) yielding **83a** (1.47 g, 82%). **83a**: ^{1}H NMR (250 MHz, $CDCl_3$) δ 1.22 (s, 2H, NH_2), 1.50–1.60 (tt, 2H, J = 6.84, 6.34 Hz, $CH_2CH_2CH_2$), 2.55–2.60 (t, 2H, J = 6.84, 6.34 Hz, C*H*$_2$NH), 2.65–2.70 (t, 2H, J = 6.84, 6.34 Hz, C*H*$_2$NH$_2$), 2.89–3.01, 3.63–3.77 (2xm, 4H, C*H*$_2$C*H*$_2$-Ar), 4.77 (s, 1H, C*H*NH), 7.06–7.15 (m, 7H, C*H*-Ar,

Please cite this article in press as: M. Blaess, et al., NB 06: From a simple lysosomotropic aSMase inhibitor to tools for elucidating the role of lysosomes in signaling apoptosis and LPS-induced inflammation, European Journal of Medicinal Chemistry (2017), https://doi.org/10.1016/j.ejmech.2017.09.021

N*H*), 7.22–7.24 (m, 2H, C*H*-Ar). ^{13}C NMR (62.9 MHz, $CDCl_3$): δ 32.26 (2CH_2-Ar), 33.93 ($CH_2CH_2CH_2$), 40.35 (CH_2NH_2), 46.14 (CH_2NH), 69.63 (*C*HNH), 125.70, 127.26, 128.90, 130.28 (4*C*H-Ar), 139.79 (*C*CHC), 140.38 ($C(CH_2)_2C$). IR (Film): $\tilde{\nu}$(cm^{-1}) 3367 (b, NH_2), 3299 (b, NH), 2924 (s), 2854 (m), 1492 (s), 1445 (s), 1361 (m), 1279 (m), 1104 (s), 1024 (m), 757 (s). MS (EI, 170 °C): *m/z* (%) 266 (4) [M^+], 265 (17), 194 (20) [M^+- $NC_3H_6NH_2$], 193 (100) [M^+- $NHC_3H_6NH_2$], 192 (40) [naphthoyl]. HRMS $C_{18}H_{22}N_2$: found 266.1786 [calcd. 266.1783].

If the mixture was diluted with ethyl acetate instead of toluene, the acylated form of the compound *N*-[3-(6,11-dihydro-5*H*-dibenzo [2,1-b:1′,2′-e][7]annulen-11-ylamino)propyl]acetamide **83b** (1.10 g, 61%) was obtained as an ester, as proven by two-dimensional NMR analyses, NOE and HH COSY: **83b**: ^{1}H NMR (360 MHz, $CDCl_3$) δ 1.50–1.57 (tt, 2H, *J* = 6.28 Hz, $CH_2CH_2CH_2$), 1.74 (s, 3H, CH_3), 2.55–2.58 (t, 2H, *J* = 6.28 Hz, CH_2NH), 2.85–2.94, 3.55–3.65 (2m, 4H, CH_2CH_2-Ar), 3.16–3.21 (t, 2H, *J* = 6.28 Hz, CH_2NHCO), 4.68 (s, 1H, C*H*NH), 6.10 (s, 1H, NH), 7.02–7.12 (m, 7H, C*H*-Ar, N*H*), 7.17–7.19 (m, 2H, C*H*-Ar). ^{13}C NMR (90.6 MHz, $CDCl_3$) δ 23.08 (CH_3), 28.91 ($CH_2CH_2CH_2$), 32.45 (2CH_2-Ar), 38.29 (CH_2NHCO), 46.19 (CH_2NH), 69.35 (CHNH), 125.92, 127.59, 128.12, 130.42 (4CH-Ar), 139.73 (*C*CHC), 139.80 ($C(CH_2)_2C$), 169.97 (C=O). HRMS $C_{20}H_{24}N_2O$: found 308.1891 [calcd. 308.1889].

4.4.36. ***NB 41*** *N′-(6,11-dihydro-5H-dibenzo[1,2-a:2′,1′-d][7] annulen-11-yl)-N-[2-(3,4-dimethoxyphenyl)ethyl]propane-1,3-diamine (**84**)*

Method **C**, reactant: **83a**. **83a** (0.25 g, 0.94 mmol) was dissolved in THF (40 mL), *n*-BuLi (0.58 mL, 0.94 mmol), **4** (0.23 g, 1.13 mmol) and TIBA (0.42 g, 1.13 mmol) were added. The mixture was refluxed for 48 h. Processing and purification by column chromatography (chloroform-methanol, 99:1 (*v/v*)) gave a yellow oil as the desired main-product: **84** (NB 41) (0.11 g, 29%) and a prominent by-product: **86** (NB 47) (0.079 g, 19%).

84 (NB 41): ^{1}H NMR (360 MHz, $CDCl_3$): δ 1.22 (s, 1H, NH), 1.49–1.58 (tt, 2H, *J* = 6.74 Hz, $CH_2CH_2CH_2$), 1.90–1.94 (m, 2H, CH_2NHCH), 2.51–2.59 (m, 4H, CH_2CH_2Ph), 2.68–2.74 (m, 4H, 2CH_2NH), 3.10–3.12, 3.56–3.68 (2m, 4H, CH_2CH_2-Ar), 3.80 (s, 6H, 2OCH_3), 4.80 (s, 1H, C*H*), 6.75–6.80 (m, 2H, C*H*-Ar), 7.02–7.06 (m, 3H, C*H*-Ar, NH), 7.09–7.15 (m, 4H, C*H*-Ar), 7.63–7.68 (m, 4H, C*H*-Ar). ^{13}C NMR (90.6 MHz, $CDCl_3$): δ 28.63 ($CH_2CH_2CH_2$), 32.29 (2CH_2-Ar), 33.21 (CH_2Ph), 46.87 (CH_2NHCH), 51.98 (CH_2NH), 55.77, 55.78 (2OCH_3), 55.86 (CH_2NH), 69.70 (CHNH), 113.22, 114.05, 129.65 (3*C*H-Ph), 125.67, 127.23, 129.09, 130.21 (4*C*H-Ar), 132.64 (*C*-Ph), 139.81 (*C*CHC), 140.68 ($C(CH_2)_2C$), 147.31, 148.80 (2*C*OMe). IR (Film): $\tilde{\nu}$(cm^{-1}) 3308 (s, NH), 3217 (s, NH), 2925 (s), 2833 (m), 1659 (m), 1592 (m), 1516 (s), 1493 (s), 1447 (s), 1362 (m), 1261 (m), 1104 (m), 1031 (s), 757 (s). MS (EI, 142 °C): *m/z* (%) 430 (2) [M^+], 279 (8) [M^+-CH_2PhOMe], 208 (5), 207 (16) [M^+- $HC_3H_6NHC_2H_4PhOMe$], 193 (100) [M^+- $NHC_3H_6NH_2$], 192 (21) [naphthoyl]. HRMS $C_{28}H_{34}N_2O_2$: found 430.2626 [calcd. 430.2620].

4.4.37. ***NB 46*** *N′-(6,11-dihydro-5H-dibenzo[1,2-a:2′,1′-d][7] annulen-11-yl)-N-[2-(4-methoxyphenyl)ethyl]propane-1,3-diamine (**85**)*

Method **C**, reactant: **83a**. **83a** (0.25 g, 0.939 mmol) was dissolved in THF (40 mL), *n*-BuLi (0.587 mL, 0.93 mmol), **7** (0.23 g, 1.13 mmol) and TIBA (0.41 g, 1.13 mmol) were added. The mixture was refluxed 48 h, processing and purification gave the desired compound **85** as yellow oil (NB 46) (0.10 g, 25%) and a prominent by-product: **87** (NB 24) (0.074 g, 19%).

85 (NB 46): ^{1}H NMR (360 MHz, $CDCl_3$): δ 1.26 (s, 1H, NH), 1.58–1.66 (tt, 2H, *J* = 6.84 Hz, $CH_2CH_2CH_2$), 1.92–1.96 (m, 2H, CH_2NHCH), 2.54–2.60 (m, 4H, CH_2CH_2Ph), 2.64–2.68 (m, 4H, 2CH_2NH), 2.92–3.04, 3.67–3.79 (2m, 4H, CH_2CH_2-Ar), 3.77 (s, 3H, OCH_3), 4.78 (s, 1H, C*H*), 6.78–6.82 (m, 2H, C*H*-Ar), 7.03–7.07 (m, 3H, C*H*-Ar, NH), 7.09–7.15 (m, 4H, C*H*-Ar), 7.25–7.29 (m, 4H, C*H*-Ar). ^{13}C NMR (90.6 MHz, $CDCl_3$): δ 27.68 ($CH_2CH_2CH_2$), 31.66 (2CH_2-Ar), 32.90 (CH_2Ph), 46.70 (CH_2NHCH), 52.26 (CH_2NH), 55.21 (OCH_3), 56.38 (CH_2NH), 74.84 (CHNH), 113.71, 129.58 (2*C*H-Ph), 125.68, 127.30, 129.47, 130.12 (4*C*H-Ar), 132.65 (*C*-Ph), 139.83 (*C*CHC), 140.73 ($C(CH_2)_2C$), 157.70 (*C*OMe). IR (Film): $\tilde{\nu}$(cm^{-1}) 3098 (b, NH), 3013 (b, NH), 2832 (s, OMe), 1658 (m), 1611 (s), 1463 (m), 1442 (m), 1242 (s), 1037 (s), 822 (m), 757 (s). MS (EI, 139 °C): *m/z* (%) 400 (2) [M^+], 279 (8) [M^+-CH_2PhOMe], 208 (5), 207 (16) [M^+- $HC_3H_6NHC_2H_4PhOMe$], 193 (100) [M^+- $NHC_3H_6NH_2$], 192 (21) [naphthoyl]. HRMS $C_{27}H_{32}N_2O$: found 400.2517 [calcd. 400.2515].

4.4.38. ***NB 47*** *1-(6,11-dihydro-5H-dibenzo[2,1-b:1′,2′-e][7] annulen-11-yl)-3-[2-(3,4-dimethoxyphenyl)ethyl] hexahydropyrimidine (**86**)*

Method **C**, reactant: **83a**. **86** (NB 47) (0.079 g, 19%) is a prominent by-product of the synthesis of **84** (NB 41). Synthesis is described at **84** (NB 41). **86** (NB 47): ^{1}H NMR (360 MHz, $CDCl_3$): δ 1.53–1.61 (tt, 2H, *J* = 6.46 Hz, $CH_2CH_2CH_2$), 2.32–2.36 (t, 2H, *J* = 6.46 Hz, CH_2NCH), 2.52–2.57 (m, 4H, CH_2CH_2Ph), 3.13–3.25, 3.35–3.47 (2m, 4H, CH_2CH_2-Ar), 3.52–3.56 (m, 4H, 2CH_2N), 3.57–3.60 (m, 2H, NCH_2N), 3.81 (s, 6H, 2OCH_3), 4.63 (s, 1H, CH), 6.74–6.78 (m, 2H, C*H*-Ar), 6.95–7.08 (m, 4H, C*H*-Ar, N*H*), 7.99–8.13 (m, 6H, C*H*-Ar). ^{13}C NMR (90.6 MHz, $CDCl_3$): δ 23.63 ($CH_2CH_2CH_2$), 31.73 (2CH_2-Ar), 32.66 (CH_2Ph), 51.02 (CH_2NCH), 53.47 (CH_2N), 55.75, 55.79 (2OCH_3), 57.62 (CH_2N), 73.12 (NCH_2N), 75.10 (CHNH), 113.72, 114.21, 130.06 (3CH-Ph), 125.34, 127.44, 128.99, 131.14 (4*C*H-Ar), 132.55 (*C*-Ph), 139.70 (*C*CHC), 140.03 ($C(CH_2)_2C$), 147.28, 148.68 (*C*OMe). MS (EI, 142 °C): *m/z* (%) 443 (2) [M^+], 279 (8) [M^+-CH_2PhOMe], 208 (5), 207 (16) [M^+- $HC_3H_6NHC_2H_4PhOMe$], 193 (100) [M^+- $NHC_3H_6NH_2$], 192 (21) [naphthoyl]. HRMS $C_{29}H_{34}N_2O_2$: found 442.2624 [calcd. 442.2620].

4.4.39. ***NB 24*** *1-(6,11-dihydro-5H-dibenzo[2,1-b:1′,2′-e][7] annulen-11-yl)-3-[2-(4-methoxy-phenyl)ethyl] hexahydropyrimidine (**87**)*

Method **C**, reactant: **83a**. **87** (NB 24) (0.074 g, 19%) is a prominent by-product of the synthesis of **85** (NB 46). Synthesis is described at **85** (NB 46). ^{1}H NMR (360 MHz, $CDCl_3$) δ 1.59–1.65 (dt, 2H, *J* = 6.28 Hz, $CH_2CH_2CH_2$), 2.38–2.42 (t, 2H, *J* = 6.28 Hz, CH_2NCH), 2.47–2.56 (m, 4H, CH_2CH_2Ph), 2.66–2.70 (m, 4H, 2CH_2N), 2.76–2.88, 3.98–4.10 (2m, 4H, CH_2CH_2-Ar), 3.16–3.20 (m, 2H, NCH_2N), 3.77 (s, 3H, OCH_3), 4.24 (s, 1H, CH), 6.78–6.82 (m, 2H, C*H*-Ar), 6.89–7.06 (m, 4H, C*H*-Ar, NH), 7.96–8.08 (m, 6H, C*H*-Ar). ^{13}C NMR (90.6 MHz, $CDCl_3$): δ 22.53 ($CH_2CH_2CH_2$), 31.80 (2CH_2-Ar), 32.98 (CH_2Ph), 50.89 (CH_2NCH), 52.74 (CH_2N), 55.24 (OCH_3), 56.67 (CH_2N), 73.26 (NCH_2N), 75.05 (CHNH), 113.72, 130.68 (2*C*H-Ph), 125.34, 127.65, 129.33, 130.74 (4*C*H-Ar), 132.55 (*C*-Ph), 139.07 (*C*CHC), 139.85 ($C(CH_2)_2C$), 157.84 (*C*OMe). MS (EI, 139 °C): *m/z* (%) 413 (2) [M^+], 279 (8) [M^+-CH_2PhOMe], 208 (5), 207 (16) [M^+- $HC_3H_6NHC_2H_4PhOMe$], 193 (100) [M^+- $NHC_3H_6NH_2$], 192 (21) [naphthoyl]. HRMS $C_{28}H_{32}N_2O$: found 412.2522 [calcd. 412.2515].

4.4.40. ***NB 38*** *3-(5,6-dihydrodibenzo[2,1-b:1′,2′-e][7]annulen-11-ylidene)-N-[2-(3,4-dimethoxyphenyl)ethyl]-N-methyl-propan-1-amine (**90**)*

Method **C**, reactant: **89**. **89** (0.50 g, 1.90 mmol) was dissolved in THF (40 mL), *n*-BuLi (1.43 mL, 2.28 mmol), **4** (0.42 g, 2.09 mmol) in 10 mL toluene and TIBA (0.77 g, 2.09 mmol) were added. The mixture was refluxed 48 h and a yellow oil was obtained after purification: **90** (NB 38) (0.22 g, 27%). ^{1}H NMR (360 MHz, $CDCl_3$): δ 2.30 (s, 3H, CH_3), 2.35–2.41 (t, 2H, *J* = 7.68 Hz, CH_2CH), 2.61–2.67 (m, 4H, CH_2CH_2Ph), 2.71–2.74 (m, 2H, CH_2NMe), 3.25–3.31 (m, 2H, CH_2-Ar), 3.32–3.38 (m, 2H, CH_2-Ar), 3.83 (s, 6H, 2OCH_3), 5.83–5.87

(t, 1H, $J = 7.45$ Hz, CH), 6.65–6.70 (m, 2H, C*H*-Ar), 6.73–6.76 (m, 1H, C*H*-Ar), 7.01–7.04 (m, 1H, C*H*-Ar), 7.12–7.16 (m, 4H, C*H*-Ar), 7.18–7.20 (m, 2H, C*H*-Ar), 7.26–7.28 (m, 1H, C*H*-Ar). ^{13}C NMR (90.6 MHz, $CDCl_3$): δ 26.62 ($CHCH_2CH_2$), 32.68 ($2CH_2$-Ar), 33.77 (CH_2Ph), 42.71 (CH_3), 55.87, 55.92 ($2OCH_3$), 55.69 (CH_2NMe), 58.99 (CH_2NMe), 111.30, 112.02, 120.57 (3CH-Ar), 126.05, 127.54, 128.57, 130.03 (4CH-Ar), 128.30 (C=CH), 132.21 (*C*-Ar), 137.03, 139.45 (*C*CHC), 139.92, 141.04 ($2C(CH_2)_2C$), 144.28 (*C*-Ar), 147.49, 148.93 (2COMe). IR (Film): $\tilde{\nu}$(cm^{-1}) 2935 (s), 2835 (s), 2790 (m), 1628 (m, C=C), 1592 (m), 1516 (m), 1464 (s), 1418 (m), 1360 (m), 1263 (s), 1237 (s), 1156 (m), 881 (s), 739 (s). MS (EI, 145 °C): *m/z* (%) 427 (3) [M^+], 276 (22) [M^+- $CH_2Ph(OMe)_2$], 209 (12), 208 (100) [M^+- $C_3H_4NC_2H_4Ph(OMe)_2$], 193 (9) [M^+- $C_4H_7NC_2H_4Ph(OMe)_2$], 178 (9) [naphthoyl]. HRMS $C_{29}H_{33}NO_2$: found 427.2510 [calcd. 427.2511].

4.4.41. ***NB 31*** *3-(5,6-dihydrodibenzo[2,1-b:1′,2′-e][7]annulen-11-ylidene)-N-[2-(4-methoxyphenyl)ethyl]-N-methyl-propan-1-amine (**91**)*

Method **C**, reactant: **89**. **89** (0.80 g, 3.04 mmol) was dissolved in THF (50 mL), *n*-BuLi (7.28 mL, 3.65 mmol), **7** (0.62 g, 3.65 mmol) in 10 mL toluene and TIBA (1.35 g, 3.65 mmol) were added. The mixture was refluxed 48 h and the product was purified to yield an orange syrup: **91** (NB 31) (0.38 g, 31%). ^{1}H NMR (360 MHz, $CDCl_3$): δ 2.22 (s, 3H, CH_3), 2.27–2.31 (tt, 2H, $J = 7.72$ Hz, $CHCH_2CH_2$), 2.29–2.33 (dt, 2H, $J = 7.72$ Hz, CH_2NMe), 2.49–2.52 (m, 2H, CH_2-Ar), 2.53–2.55 (m, 2H, CH_2-Ar), 2.62–2.67 (m, 4H, CH_2CH_2Ph), 3.76 (s, 3H, OCH_3), 5.84–5.88 (t, 1H, $J = 7.35$ Hz, C*H*), 6.77–6.79 (m, 2H, C*H*-Ar), 7.01–7.05 (m, 2H, C*H*-Ar), 7.11–7.15 (m, 4H, C*H*-Ar), 7.17–7.20 (m, 2H, C*H*-Ar), 7.25–7.29 (m, 2H, C*H*-Ar). ^{13}C NMR (62.9 MHz, $CDCl_3$): δ 27.22 ($CHCH_2CH_2$), 32.61 ($2CH_2$-Ar), 33.75 (CH_2Ph), 42.03 (CH_3), 55.21 (OCH_3), 56.98 (CH_2NMe), 59.35 (CH_2NMe), 113.73, 129.54 (2CH-Ar), 125.71, 126.95, 127.98, 129.45 (4CH-Ar), 128.62 (C=C), 132.51 (*C*-Ar), 137.03, 139.32 (2CCHC), 140.08, 141.30 ($2C(CH_2)_2C$), 143.47 (*C*-Ar), 157.83 (COMe). IR (Film): $\tilde{\nu}$(cm^{-1}) 2932 (s, CH_3), 2834 (s, OMe), 1612 (m, C=C), 1512 (s), 1486 (s), 1454 (m), 1301 (m), 1247 (s), 1177 (m), 825 (m), 755 (s). MS (EI, 125 °C): *m/z* (%) 397 (14) [M^+], 267 (28) [M^+- CH_2PhOMe], 193 (19) [M^+- $C_4H_7NC_2H_4PhOMe$], 178 (80) [naphthoyl]. HRMS $C_{28}H_{31}NO$: found 397.2407 [calcd. 397.2406].

4.4.42. ***NB 21*** *3-(11,12-dihydro-6H-benzo[c][1]benzazocin-5-yl)-N-[2-(4-methoxyphenyl)ethyl]-N-methyl-propan-1-amine (**95**)*

Method **C**, reactant: **94**. **94** (0.20 g, 0.71 mmol) was dissolved in THF (30 mL), *n*-BuLi (0.49 mL, 0.79 mmol), **7** (0.15 g, 0.86 mmol) and TBAI (0.32 g, 0.86 mmol) were added. The mixture was refluxed overnight; after purification a yellow syrup was obtained: **95** (NB 21) (0.084 g, 28%). ^{1}H NMR (360 MHz, $CDCl_3$): δ 1.60–1.70 (m, 2H, $CH_2CH_2CH_2$), 2.17 (s, 3H, CH_3), 2.33–2.37 (m, 2H, CH_2NMe), 2.43–2.47, 2.59–2.64 (2m, 4H, $2CH_2$-Ar), 3.06–3.10 (m, 2H, -NCH_2), 3.21–3.26 (m, 4H, CH_2CH_2Ph), 3.77 (s, 3H, OCH_3), 4.16 (s, 2H, CH_2-Ar), 6.79–6.85 (m, 3H, C*H*-Ar), 6.99–7.13 (m, 6H, C*H*-Ar). ^{13}C NMR (62.9 MHz, $CDCl_3$): δ 25.60 ($CH_2CH_2CH_2$), 32.59, 33.43 ($2CH_2$-Ar), 34.38 (CH_2Ph), 41.98 (CH_3), 51.55 (-NCH_2), 55.26 (OCH_3), 55.32 (CH_2-Ar), 59.65 (CH_2NMe), 60.89 (CH_2NMe), 113.81, 121.90, 125.96, 126.74, 127.17, 128.90, 129.73, 131.12 (8CH-Ar), 119.68, 130.92 (2CH-Ar), 132.34 (*C*-Ar), 136.32, 137.78 ($2C(CH_2)_2C$), 141.91 (C-N), 150.36 (CCH_2N), 157.92 (COMe). IR (Film): $\tilde{\nu}$(cm^{-1}) 2857 (s, CH_3), 2797 (s, CH_3), 2344 (m), 1612 (m), 1513 (s), 1494 (s), 1353 (m), 1247 (s), 1178 (m), 1037 (s), 825 (m), 759 (s). MS (EI, 130 °C): *m/z* (%) 414 (2) [M^+], 293 (14) [M^+- CH_2PhOMe], 222 (43) [M^+- C_3H_7 NC_2H_4PhOMe], 209 (14), 208 (20) [tetrahydrodibenz[*b,f*]azocine]. HRMS $C_{28}H_{34}N_2O$: found 414.2675 [calcd. 414.2671]. Anal ($C_{28}H_{34}N_2O$): C, H, N.

4.4.43. ***NB 18*** *9-[[4-[2-(4-methoxyphenyl)ethyl]piperazin-1-yl]methyl]carbazole (**99**)*

Modified method **A**, reactant: **19**. **19** (0.15 g, 0.90 mmol) was dissolved in toluene (30 mL), treated with *n*-BuLi (0.67 mL, 1.08 mmol), **98** (0.28 g, 0.99 mmol) and TIBA (0.36 g, 0.99 mmol) and the mixture refluxed overnight. Purification by column chromatography (chloroform-methanol, 99:1 (*v/v*)) afforded a yellow syrup: **99** (0.086 g, 23%). ^{1}H NMR (250 MHz, $CDCl_3$): δ 2.27 (t, 2H, CH_2Ph), 2.55–2.61 (m, 8H, $4CH_2$-piperazine), 2.72–2.83 (m, 4H, $2CH_2N$), 3.79 (s, 3H, OCH_3), 4.42–4.49 (t, 2H, $J = 6.89$ Hz, -NCH_2), 6.81–6.86 (m, 2H, C*H*-Ar), 7.10–7.22 (m, 4H, C*H*-Ar), 7.39–7.50 (m, 4H, C*H*-Ar), 8.08–8.13 (m, 2H, C*H*-Ar). ^{13}C NMR (62.9 MHz, $CDCl_3$): δ 32.58 (CH_2Ph), 41.72 (-NCH_2), 49.96 (CH_2N-), 51.44 (CH_2-piperazine), 52.98 (CH_2-piperazine), 55.43 (OCH_3), 57.45 (CH_2N-), 108.30, 119.01, 119.89, 125.31 (4CH-Ar), 114.23, 129.10 (2CH-Ar), 122.12 (*C*-*C*), 130.86 (*C*-Ar), 139.23 (C-N), 158.33 (COMe). IR (Film): $\tilde{\nu}$(cm^{-1}) 2852 (s, OMe), 2312 (m), 1733 (m), 1647 (m), 1512 (s), 1453 (s), 1326 (m), 1247 (s), 1154 (m), 1037 (m), 848 (w), 738 (s). MS (EI, 154 °C): *m/z* (%) 413 (7) [M^+], 239 (21), 292 (100) [M^+- PhOMe], 234 (15), 180 (14) [M^+- $CH_2NC_4H_8NC_2H_4PhOMe$], 167 (22) [carbazole]. HRMS $C_{27}H_{31}N_3O$: found 413.2466 [calcd. 413.2467].

4.4.44. ***NB 42*** *9-[3-[(3S,5R)-4-[2-(3,4-dimethoxyphenyl)ethyl]-3,5-dimethyl-piperazin-1-yl]propyl]carbazole (**104**)*

Method **C**, reactant: **103**. **103** (0.50 g, 1.56 mmol) was dissolved in toluene (40 mL), *n*-BuLi (1.16 mL, 1.86 mmol), **4** (0.37 g, 1.86 mmol) and TIBA (0.69 g, 1.86 mmol) were added and the mixture refluxed for 48 h. After processing and purification a light yellow volatile oil was obtained: **104** (NB 42) (0.208 g, 28%). ^{1}H NMR (360 MHz, $CDCl_3$): δ 1.12 (s, 3H, CH_3), 1.14 (s, 3H, CH_3), 1.77–1.83 (t, 2H, $J = 10.69$ Hz, CH_2-piperazine), 1.99–2.07 (tt, 2H, $J = 6.84$ Hz, $CH_2CH_2CH_2$), 2.24–2.28 (t, 2H, $J = 6.84$ Hz, CH_2N), 2.62–2.70 (m, 4H, CH_2-piperazine, CH_2Ph), 2.78–2.82 (m, 2H, 2CHMe), 2.96–3.02 (m, 2H, CH_2N), 3.84 (s, 3H, OCH_3), 3.87 (s, 3H, OCH_3), 4.36–4.40 (t, 2H, $J = 6.73$ Hz, -NCH_2), 6.66–6.70 (m, 2H, C*H*-Ar), 6.78–6.80 (m, 1H, C*H*-Ar), 7.19–7.25 (m, 4H, C*H*-Ar), 7.42–7.48 (m, 4H, C*H*-Ar). ^{13}C NMR (90.6 MHz, $CDCl_3$): δ 18.03 ($2CH_3$), 25.86 ($CH_2CH_2CH_2$), 29.02 (CH_2Ph), 40.59 (-NCH_2), 50.04 (CH_2N-), 53.42 (2CHMe), 54.83 (CH_2N-), 55.85, 55.91 ($2OCH_3$), 61.13 (-$N(CH_2)_2$), 108.83, 118.76, 120.26, 125.50 (4CH-Ar), 111.45, 111.94, 120.49 (3CH-Ar), 122.83 (*C*-*C*), 136.02 (*C*-Ar), 140.49 (C-N), 147.38, 148.95 (2COMe). IR (Film): $\tilde{\nu}$(cm^{-1}) 2935 (s, CH_3), 2819 (s, OMe), 2810 (s, OMe), 2316 (m), 1627 (m), 1598 (m), 1510 (s), 1449 (s), 1373 (m), 1249 (s), 1202 (s), 1149 (m), 1039 (m), 752 (s), 724 (s); MS (EI, 153 °C): *m/z* (%) 485 (6) [M^+], 335 (26), 334 (93) [M^+- $CH_2Ph(OMe)_2$], 181 (14), 180 (100) [M^+- $C_2H_4NC_6H_{12}NC_2H_4Ph(OMe)_2$], 167 (4) [carbazole]. HRMS $C_{31}H_{39}N_3O_2$: found 485.3049 [calcd. 485.3042]. Anal ($C_{31}H_{39}N_3O_2$): C, H, N.

4.4.45. ***NB 19*** *9-[3-[(3S,5R)-4-[2-(4-methoxyphenyl)ethyl]-3,5-dimethyl-piperazin-1-yl]propyl]carbazole (**105**)*

Method **C**, reactant: **103**. **103** (0.90 mg, 2.80 mmol) was dissolved in toluene (50 mL), deprotonated with *n*-BuLi (2.10 mL, 3.36 mmol), treated with **7** (0.57 g, 3.36 mmol) and TIBA (1.24 g, 3.36 mmol). The mixture was refluxed for 48 h, processing and purification gave a light yellow volatile oil: **105** (NB 19) (0.42 g, 33%). ^{1}H NMR (250 MHz, $CDCl_3$): δ 1.11 (s, 3H, CH_3), 1.14 (s, 3H, CH_3), 1.75–1.84 (t, 2H, $J = 10.68$ Hz, CH_2-piperazine), 1.98–2.09 (tt, 2H, $J = 6.78$ Hz, $CH_2CH_2CH_2$) 2.24–2.29 (t, 2H, $J = 6.78$ Hz, CH_2N), 2.62–2.70 (m, 4H, CH_2-piperazine, CH_2Ph), 2.77–2.85 (m, 2H, 2CHMe), 2.94–3.01 (m, 2H, CH_2N), 3.78 (s, 3H, OCH_3), 4.37–4.42 (t, 2H, $J = 6.78$ Hz, -NCH_2), 6.83–6.87 (m, 2H, C*H*-Ar), 7.06–7.10 (m, 2H, C*H*-Ar), 7.19–7.25 (m, 4H, C*H*-Ar), 7.44–7.48 (m, 2H, C*H*-Ar), 8.08–8.11 (m, 2H, C*H*-Ar). ^{13}C NMR (62.9 MHz, $CDCl_3$): δ 17.99

Please cite this article in press as: M. Blaess, et al., NB 06: From a simple lysosomotropic aSMase inhibitor to tools for elucidating the role of lysosomes in signaling apoptosis and LPS-induced inflammation, European Journal of Medicinal Chemistry (2017), https://doi.org/10.1016/j.ejmech.2017.09.021

(2CH_3), 25.86 ($CH_2CH_2CH_2$), 28.43 (CH_2Ph), 40.58 (-NCH_2), 50.12 (CH_2N-), 53.40 (2CHMe), 54.82 (CH_2N-), 55.23 (OCH_3), 61.18 (-N(CH_2)$_2$), 108.83, 118.73, 120.24, 125.47 (4CH-Ar), 113.95, 129.42 (2CH-Ar), 122.82 (*C*-*C*), 132.58 (*C*-Ar), 140.48 (C-N), 157.91 (*C*OMe). IR (Film): $\tilde{\nu}$(cm^{-1}) 2935 (s, CH_3), 2814 (s, OMe), 2315 (m), 1627 (m), 1598 (m), 1511 (s), 1454 (s), 1373 (m), 1249 (s), 1207 (s), 1153 (m), 1037 (m), 752 (s), 724 (s). MS (EI, 162 °C): *m/z* (%) 455 (9) [M^+], 335 (26), 334 (100) [M^+- CH_2PhOMe], 181 (13), 180 (79) [M^+-$C_2H_4NC_6H_{12}NC_2H_4$PhOMe], 167 (11) [carbazole]. HRMS $C_{30}H_{37}N_3O$: found 455.2936 [calcd. 455.2937].

4.4.46. ***NB 36*** *10-[3-[(3S,5R)-4-[2-(4-methoxyphenyl)ethyl]-3,5-dimethyl-piperazin-1-yl]propyl]phenoxazine (**109**)*

Method **C**, reactant: **107**. **107** (0.25 g, 0.74 mmol) was dissolved in toluene (30 mL), treated with *n*-BuLi (0.56 mL, 0.89 mmol), **7** (0.15 g, 0.89 mmol) and TIBA (0.33 g, 0.89 mmol). The mixture was refluxed overnight; processing and purification afforded a colorless syrup residue containing **109** (NB 36) (0.11 g, 31%). ^{1}H NMR (360 MHz, $CDCl_3$): δ 1.15 (s, 3H, CH_3), 1.77 (s, 3H, CH_3), 1.79–1.93 (t, 2H, *J* = 10.73 Hz, CH_2-piperazine), 2.35–2.39 (t, 2H, *J* = 6.87 Hz, CH_2Ph), 2.62–2.69 (m, 2H, CH_2N), 2.77–2.87 (tt, 2H, *J* = 7.68 Hz, $CH_2CH_2CH_2$), 2.88–2.95 (m, 2H, 2C*H*-piperazine), 2.97–3.02 (m, 2H, CH_2N), 3.54–3.60 (t, 2H, *J* = 7.68 Hz, -NCH_2), 3.79 (s, 3H, OCH_3), 6.55–6.65 (m, 4H, C*H*-Ar), 6.72–6.74 (m, 2H, C*H*-Ar), 6.75–6.79 (m, 4H, C*H*-Ar), 7.07–7.17 (m, 2H, C*H*-Ar). ^{13}C NMR (90.6 MHz, $CDCl_3$): δ 17.92 (2CH_3), 22.46 ($CH_2CH_2CH_2$), 28.41 (CH_2Ph), 41.72 (-NCH_2), 50.06 (CH_2N), 53.37 (2CH-piperazine), 54.92 (CH_2N), 55.14 (OCH_3), 61.33 ((CH_2)$_2$N), 111.33, 115.18, 120.60, 123.39 (4CH-Ar), 113.86, 128.89 (2CH-Ar), 132.47 (*C*-Ar), 133.24 (C-O), 144.81 (C-N), 157.82 (*C*OMe). IR (Film): $\tilde{\nu}$(cm^{-1}) 3089 (m), 2936 (s), 2811 (m), 2620 (m), 1628 (m), 1612 (m), 1592 (m), 1511 (s), 1489 (s), 1380 (m), 1325 (m), 1272 (s), 1249 (s), 1130 (m), 1040 (m), 739 (s). MS (EI, 184 °C): *m/z* (%) 471 (5) [M^+], 350 (76) [M^+-(OMePhCH_2)], 196 (100) [M^+-$C_2H_4N(C_3H_6)_2NC_2H_4$PhOMe], 182 (12) [phenoxazine]. HRMS $C_{31}H_{39}N_3O_2$: found 485.3047 [calcd. 485.3042].

4.4.47. ***NB 32*** *4-carbazol-9-yl-1,1,2,2,3,3,4,4-octafluoro-N-[2-(4-methoxyphenyl)ethyl]-N-methyl-butan-1-amine (**113**)*

Reactant: **110**. To a stirred solution of **110** (0.10 g, 0.61 mmol) in dry DMF (10 mL), *n*-BuLi (2.0 M in hexane) (0.30 mL, 0.61 mmol) was added over a period of 15 min at −20 °C under an argon atmosphere and light exclusion. The mixture was stirred 30 min at 0 °C before **112** (0.30 g, 0.61 mmol) in 5 mL DMF was added. The mixture was allowed to stay in an ultrasound bath at 60 °C; after 72 h the mixture was diluted with 100 mL ethyl acetate and washed once with 5% NaS_2O_3 and twice with water (60 mL). The organic layer was dried and concentrated. Ultrasonic treatment produced a crude product as a bright yellow oil. The oil was purified by column chromatography under light exclusion (*n*-hexane-ethyl acetate; 29:1 and toluene-ethyl acetate; 19:1). Column fractions were collected and purified once again by HPLC (acetonitril:methanol:25 mM KH_2PO_4, 39:21:40 (*v/v*), 1 mL/min, 40 min) to give a yellow oil **113** (NB 32) (0.091 g, 28%). ^{1}H NMR (360 MHz, $CDCl_3$): δ 2.35 (s, 3H, CH_3), 2.61–2.69 (m, 2H, CH_2Ph), 3.02–3.10 (m, 2H, CH_2NMe), 3.85 (s, 3H, OCH_3), 7.32–7.34, 7.36–7.37 (2m, 2H, CH-Ar), 7.47–7.49, 7.51–7.52 (2m, 2H, CH-Ar), 7.53–7.54, 7.55–7.56 (2m 2H, CH-Ar), 7.73–7.76, 7.80–8.83 (2m, 2H, CH-Ar). ^{13}C NMR (90.6 MHz, $CDCl_3$): δ 35.32 (NCH_3), 35.87 (CH_2Ph), 54.27 (NCH_2), 55.39 (OCH_3), 105.12 (CF_2), 105.83 (CF_2), 113.43, 114.06, 120.32, 121.65, 127.97, 130.02 (6CH-Ph), 111.10 (CF_2), 124.71 (-NCF_2), 126.98 (*C*-*C*), 132.85 (*C*-Ph), 140.24 (C-N), 158.51 (*C*OMe). IR (Film): $\tilde{\nu}$(cm^{-1}) 2983 (s), 2831 (s, OMe), 1716 (m), 1505 (m), 1416 (s), 1335 (m), 1273 (s), 1186 (s), 1128 (m), 1023 (s), 745 (s), 512 (b, CF). MS (EI, 169 °C): *m/z* (%) 530 (100) [M^+], 381 (6) [M^+-C_3H_6PhOMe], 265 (12) [M^+- $C_3H_6F_8$PhOMe], 166 (9) [carbazole]. HRMS $C_{26}H_{22}F_8N_2O$: found: 530.1605 [calcd. 530.1604].

4.4.48. ***NB 43*** *3-[2-(4-Methoxy-phenyl)-ethyl]-2,3,3a,4,5,6-hexahydro-1H-pyrazino[3,2,1-jk]carbazole (**125**)*

Method **C**, reactant: **123**. A 100-mL round-bottomed flask, connected to argon, was charged with **123** (0.30 g, 11.43 mmol) and dry methanol (30 mL). To the mixture $NaBH_4$ (0.108 g, 2.86 mmol) was added in successive portions at −10 °C. The mixture was stirred at −10 °C 1 h before it was allowed to reach RT; after stirring 1 h at RT, solvent was reduced and diluted with water (20 mL), then extracted twice with ethyl acetate (2 × 50 mL). The organic layer was evaporated to give a red oil: **124** (2,3,3a,4,5,6-hexahydro-1*H*-pyrazino[3,2,1-*jk*]carbazole) (0.287 g, 95%). According to method **C** **124** was dissolved in a mixture of THF/toluene (3:5 (*v/v*), 40 mL) and deprotonated by adding *n*-BuLi (1.06 mL, 1.70 mmol, 1.6 M in *n*-hexane) over a period of 30 min at −78 °C. Mixture was stirred 1 h at −78 °C before **7** (0.29 g, 1.70 mmol) and TIBA (0.63 g, 1.70 mmol) were added. After stirring 1 h at RT, refluxing overnight, processing and purification by column chromatography (chloroform-methanol; 99:1 (*v/v*)) gave a red syrup: **125** (NB 43) (0.169 g, 36%). ^{1}H NMR (250 MHz, $CDCl_3$): δ 1.50–1.68 (m, 4H, $CH_2CH_2CH_2$N, CH_2CHN), 2.78–2.82 (m, 2H, CH_2C), 2.97–3.01 (t, 2H, *J* = 7.48 Hz, CH_2Ph), 3.60–3.65 (t, 2H, *J* = 6.78 Hz, CH_2NCH), 3.65–3.71 (t, 2H, *J* = 7.48 Hz, CH_2NCH), 3.79 (s, 3H, OCH_3), 3.81–3.84 (t, 2H, *J* = 6.78 Hz, -NCH_2), 4.28–4.33 (m, 1H, CH), 6.82–6.88 (m, 4H, C*H*-Ar), 7.11–7.13 (m, 2H, C*H*-Ar), 7.15–7.18 (m, 2H, C*H*-Ar). ^{13}C NMR (62.9 MHz, $CDCl_3$): δ 20.92 (CH_2C), 22.69 ($CH_2CH_2CH_2$), 28.34 (CH_2CN), 32.83 (CH_2Ph), 42.75 (-NCH_2), 54.73 (CH_2N), 55.63 (OCH_3), 58.74 (NCH), 63.09 (CH_2N), 109.04, 118.71, 119.71, 121.15 (4CH-Ar), 114.04, 129.81 (2CH-Ar), 108.26, 125.71 (2*C*-*C*), 131.13 (*C*-Ar), 136.33, 137.45 (2*C*-NH), 158.36 (*C*OMe). IR (Film): $\tilde{\nu}$(cm^{-1}) 2945 (s), 2898 (s), 2855 (m), 1668 (m), 1630 (m), 1542 (s), 1486 (m), 1438 (m), 1385 (m), 1268 (m), 1109 (m), 840 (m), 740 (s). MS (EI, 112 °C): *m/z* (%) 346 (22) [M^+], 225 (100) [M^+- CH_2PhOMe], 197 (28) [M^+-$CH_2NC_2H_4$PhOMe], 169 (4), 168 (11) [tetrahydrocarbazole]. HRMS $C_{23}H_{26}N_2O$: found 346.2043 [calcd. 346.2045].

124: MS (EI, 80 °C): *m/z* (%) 212 (54) [M^+], 211 (30), 185 (13), 184 (100) [M^+- C_2H_4], 169 (5) [tetrahydrocarbazole].

4.4.49. ***NB 44*** *4-[2-(4-Methoxy-phenyl)-ethyl]-1,2,3,3a,4,5,6,7-octahydro-[1,4]-diazepino-[3,2,1,jk]carbazole (**130**)*

Method **C**, reactant: **128**. **128** (0.25 g, 1.12 mmol) was dissolved in dry methanol (30 mL) using a 100-mL round bottomed flask under argon atmosphere. $NaBH_4$ (0.084 g, 2.23 mmol) was added in successive portions at −10 °C. The mixture was stirred at −10 °C 1 h and 1 h at RT, solvent reduced, water (20 mL) added and the product extracted with ethyl acetate (2 × 50 mL). Ethyl acetate was evaporated to give a red oil: 1,2,3,3a,4,5,6,7-hexahydro-[1,4]-diazepino-[3,2,1,*jk*]carbazole (**129**) (0.241 g, 96%). According to method **C** **129** (0.241 g, 1.07 mmol) was dissolved in a mixture of THF/toluene (3:5 (*v/v*), 40 mL) and *n*-BuLi (0.80 mL, 1.28 mmol, 1.6 M in *n*-hexane) was added over a period of 30 min at −78 °C permanently stirring. Reaction mixture was stirred 1 h at −78 °C before **7** (0.22 g, 1.28 mmol) and TIBA (0.47 g, 1.28 mmol) were added. After stirring 1 h at RT the mixture was refluxed overnight. Processing and purification by column chromatography (chloroform-methanol; 99:1 (*v/v*)) gave a red syrup: **130** (NB 44) (0.94 g, 24%) as. ^{1}H NMR (250 MHz, $CDCl_3$): δ 1.68–1.76 (m, 2H, $CH_2CH_2CH_2$), 1.98–1.02 (m, 2H, CH_2CHN), 2.16–3.00 (m, 2H, CH_2Ph), 2.66–2.70 (m, 2H, CH_2NCH), 3.08–3.12 (m, 2H, CH_2C), 3.38–3.48 (2m, 4H, $CH_2CH_2CH_2$N, CH_2NCH), 3.75 (s, 3H, OCH_3), 3.82–3.86 (t, 2H, *J* = 6.78 Hz, -NCH_2), 4.15–4.19 (m, 1H, CH), 6.76–6.79 (m, 2H, C*H*-Ar), 7.04–7.07 (m, 2H, C*H*-Ar), 7.12–7.18 (m, 2H, C*H*-Ar), 7.45–7.48 (m, 2H, C*H*-Ar). ^{13}C NMR (62.9 MHz, $CDCl_3$): δ 21.22 (CH_2C), 23.16 ($CH_2CH_2CH_2$), 24.18 ($CH_2CH_2CH_2$), 29.91

(CH_2CN), 34.98 (CH_2Ph), 44.95 (-NCH_2), 54.12 (CH_2N), 55.22 (OCH_3), 57.64 (NCH), 63.80 (CH_2N), 108.73, 118.30, 118.47, 121.04 (4CH-Ar), 113.75, 129.53 (2CH-Ar), 113.11, 126.69 (2C-C), 132.44 (C-Ar), 136.56, 138.02 (2C-NH), 157.92 (COMe). IR (Film): $\tilde{\nu}$(cm^{-1}) 2945 (s), 2899 (s), 2855 (m), 1668 (m), 1630 (m), 1587 (s), 1544 (s), 1485 (m), 1428 (m), 1354 (m), 1268 (m), 1113 (m), 840 (m), 745 (s). MS (EI, 142 °C): *m/z* (%) 360 (14) [M^+], 240 (18), 239 (100) [M^+- CH_2PhOMe], 211 (14) [M^+- NC_2H_4PhOMe], 196 (27) [M^+- $CH_2NC_2H_4PhOMe$], 169 (5) [tetrahydrocarbazole]. HRMS $C_{24}H_{28}N_2O$: found 360.2202 [calcd. 360.2202].

129: MS (EI, 72 °C): *m/z* (%) 266 (82) [M^+], 225 (50), 199 (15), 198 (100) [M^+- C_2H_3NH], 170 (11), 169 (17) [tetrahydrocarbazole].

4.4.50. ***NB 45*** *3-carbazol-9-yl-N-[2-[4-[2-[3-carbazol-9-ylpropyl(methyl)amino]ethyl]-2,5-dimethoxy-phenyl]ethyl]-N-methyl-propan-1-amine (**132**)*

Method **C**, reactant: **21**. **21** (0.40 g, 1.68 mmol) was dissolved in toluene (50 mL), deprotonated with *n*-BuLi (1.26 mL, 2.02 mmol). After 1 h stirring, **131** (0.0296 g, 0.84 mmol) was added. The mixture was refluxed 48 h, processing and purification gave a light yellow oil: **132** (NB 45) (0.251 g, 22%) as. ^{1}H NMR (360 MHz, $CDCl_3$): δ 1.99–2.07 (2tt, 4H, J = 6.73 Hz, $2CH_2CH_2CH_2$), 2.24 (s, 6H, $2CH_3$), 2.29–2.33 (t, 4H, J = 6.73 Hz, $2CH_2NMe$), 3.10–3.15 (m, 4H, $2CH_2Ph$), 3.53–3.58 (m, 4H, $2CH_2NMe$), 3.78 (s, 6H, $2OCH_3$), 4.29–4.33 (t, 4H, J = 6.97 Hz, 2-NCH_2), 6.64 (m, 2H, CH-Ph), 7.21–7.26 (m, 6H, CH-Ar), 7.44–7.47 (m, 6H, CH-Ar), 8.09–8.11 (m, 4H, CH-Ar). ^{13}C NMR (90.6 MHz, $CDCl_3$): δ 26.89 ($2CH_2CH_2CH_2$), 31.74 ($2CH_2Ph$), 40.68 (2-NCH_2), 45.37 ($2CH_3$), 55.95 ($2CH_2NMe$), 56.07 ($2OCH_3$), 56.63 ($2CH_2NMe$), 108.74, 118.77, 120.30, 125,62 (4CH-Ar), 113.65 (CH-Ar), 122.85 (2C-C), 130.02 (2C-Ar), 140.50 (2C-N), 149.81 (COMe). MS (EI, 226 °C): *m/z* (%) 666 (1.87) [M^+], 252 (7), 251 (34) [M^+- $CH_2Ph(OMe)_2C_2H_4N(CH_3)C_3H_6NC_{12}H_8$], 167 (3) [carbazole]. HRMS $C_{44}H_{50}N_4O_2$: found 666.3941 [calcd. 666.3934].

4.5. Cell culture and cell culture experiments

4.5.1. Monocytes/macrophages

Peripheral blood mononuclear cells (PBMC) used in cell culture experiments were isolated from fresh buffy coats using Histopaque (Sigma-Aldrich, Deisenhofen, Germany) and cultured in six-well plates (9.6 cm^2, Greiner bio-one, Frickenhausen, Germany) for six to seven days in a humidified incubator (37 °C, 5% CO_2) with RPMI-1640 medium (PAA, Cölbe, Germany) supplemented with 2 mM L-glutamine, 50 units/mL penicillin 50 μg/mL streptomycin (Sigma-Aldrich, Deisenhofen, Germany) and 10% fetal calf serum (FCS) (Greiner bio-one, Frickenhausen, Germany). Before and during incubation with compounds, supplemented RPMI-1640 Medium with a reduced content of 1% of human albumin (Schering, Berlin, Germany) was used.

Mono-Mac-6: Human acute monocytic leukemia cells Mono-Mac-6 (ACC 124, DSMZ, Braunschweig, Germany) were cultured in CELLSTAR® suspension culture flasks (Greiner bio-one, Frickenhausen, Germany) using RPMI-1640 medium (PAA, Cölbe, Germany) containing 10% fetal calf serum (FCS) (Greiner bio-one, Frickenhausen, Germany), 2 mM L-glutamine + non-essential amino acids + 1 mM sodium pyruvate + 10 μg/mL human insulin (Sigma-Aldrich, Deisenhofen, Germany). All test compounds (NB compounds) were dissolved in 10 mM stock solutions; ceramides were dissolved in a 10 mM ethanol/DMSO stock solution; same concentrations of solvents were present in control samples. Appropriate dilutions in ethanol/cell culture medium and volumes were applied to cells at the beginning of incubation.

4.5.2. Preparation and identification of human low density lipoprotein (LDL)

Isolation was carried out from a pool of whole blood samples of healthy donors anticoagulated with heparin according to Havel [56] or Himber [57] using a Optima XL 100K centrifuge (Beckman Coulter, Munich). Concentrations refer to protein concentrations (apoB, 500 kDa) determined by the modified method of Lowry [58]. LDL was pooled from three donors for each preparation, sterilized by filtration through a 0.2 μm membrane filter and stored at 4 °C under argon (up to 2 weeks). Aliquot for longtime storage at −80 °C aliquots of LDL were combined with a cryo preservation buffer (40% Sucrose, 50 mM TRIS-HCl pH 7,4, 150 mM sodium chloride und 240 μM EDTA) 1:1 (V/V) [59]. mmLDL was obtained by Fe-catalyzed oxidation (20 μM Fe^{3+}, 20 °C, 48 h) according to Watson [60]. If a frozen aliquot was used, LDL is dialyzed using a dialysis buffer containing 20 mM Tris (pH 7.4), 150 mM sodium chloride, 0.1 mM EDTA prior to modification. Peroxide content as determined according to El-Saadani [61] typically increased by 30 nmol/mg to 800–1000 nmol/mg; electrophoretic mobility was only marginally enhanced by this procedure.

4.5.3. Apoptosis

Five or six days after isolation, PBMC were transferred to Nunc® 4-well dishes for IVF (Fisher Scientific, Schwerte, Germany). Prior to incubation, PBMC were cultivated in RPMI-1640 without phenol red (PAA Laboratories, Cölbe or Invitrogen, Karlsruhe, Germany) and pre-treated 30 min with 2 μM of each test compound and thereafter treated 4 h with mmLDL (27 μg/mL) or TNFalpha (3 ng/mL) (only selected compounds). YO-PRO®-1 iodide (491/509) (0.1 mM in DMSO/PBS-buffer, staining apoptotic cells) and Hoechst 33342 (0.1 mM in DMSO/PBS-buffer, staining DNA in nuclei) (Molecular Probes, Leiden, Netherlands or MobiTec, Göttingen, Germany) for apoptosis/number of cells was applied to medium at the end of incubation time. Percentage of apoptotic cells was determined on a Nikon Eclipse FS 100 equipped with an EPI-filter block 340–380 nm or 450–490 nm (Nikon Instruments Europe, Düsseldorf, Germany).

4.6. aSMase activity assay

4.6.1. Cell culture

Six to eight days after isolation PMBC were transferred to CELLSTAR® cell culture 24-well plates (1,9 cm^2, Greiner bio-one, Frickenhausen, Germany) and cultivated in 500 μL full supplemented RPMI-1640 medium (PAA, Cölbe, Germany). After medium exchange (200 μL) prior to incubation, PBMC were pre incubated 30 min with the test compounds (diluted in not supplemented medium) in final concentrations of 50, 25, 10, 2 and 0.5 μM. Then 27 μg/mL mmLDL was added and incubated for 2 h. Each 24-well plate (testing 4 compounds simultaneously), contained a control and mmLDL (stimulus) in duplicates, each test compound once in 50 μM and the stimulus plus the test compound in four concentrations. After incubation, cells were scraped off, centrifuged, washed twice with ice-cold PBS and finally lysated in 40 μL ice-cold lysis-buffer for aSMase (ALB, 250 mM sodium acetate, 0,2% Triton X-100). For best results, the suspension was pipetted a few times through a pipette-tip and incubated 10 min on ice; cells debris was carefully removed by centrifugation; supernatant was transferred in a fresh tube avoiding carryover of any cell debris and shock frozen in liquid nitrogen for long time storage at −80 °C.

4.6.2. Enzyme activity

For aSMase enzyme activity measurement a modified method based on a protocol of Sandhoff and Quintern for ^{3}H-sphingomyelin as substrate was used [62]. Protein content (three aliquots, each

Please cite this article in press as: M. Blaess, et al., NB 06: From a simple lysosomotropic aSMase inhibitor to tools for elucidating the role of lysosomes in signaling apoptosis and LPS-induced inflammation, European Journal of Medicinal Chemistry (2017), https://doi.org/10.1016/j.ejmech.2017.09.021

5 μL) was determined by the modified bicinchoninic acid assay method of Lowry [58] using bovine serum albumin (BSA) as calibrator. To assess intrinsic activity of the lysate obtained two activity measurements of a control lysate (250–400 μg/mL protein) were carried out (30 min incubation period at 37 and 45 °C) out and the turnover (max. 10%) of BODIPY® FL C_5-sphingomyelin to BODIPY® FL C_5–ceramide (Molecular Probes, Leiden, Netherlands) was measured using a HPLC separation and quantification method (see Supplementary data); the resulting amount of BODIPY® FL C_5–ceramide is equivalent to generated ceramide. To determine enzyme activity in a 96er-Well (Greiner bio-one, Frickenhausen, Germany), the following components were combined on ice: normalized cell lysate replenished to 10 μL with ALB, 8 μL acidic reaction-buffer (ARB, 250 mM sodium acetate, 1 mM EDTA) and 2 μL of BODIPY® FL C_5-sphingomyelin solution (62,5 μg/mL) in ARB. Depending on the intrinsic activity of the reference sample, an incubation between 30 and 45 min at 37 °C or, if necessary, at RT was performed. Enzymatic activity was stopped by adding 150 μL methanol containing BODIPY® FL C_5-pentanoic acid (42 ng/mL), used as an internal standard in HPLC separation.

4.6.3. Cell lysate aSMase activity assay

Cell lysates of untreated or mmLDL (27 μg/mL) stimulated PBMC were prepared and aSMase activity was determined as described in section enzyme activity. BODIPY® FL C_5-labeled sphingomyelin (Molecular Probes, Leiden, Netherlands) in ARB (62.5 μg/mL) was added and aSMase turnover was adjusted to about 10% (30 min incubation time, 37 °C). 500 μM stock solutions of each test compound in ARB were prepared and 1, 10, and 100 μM of compounds (3 μL) added to the reaction mixture consisting of 5 μL cell lysate, 5 μL ALB and 5 μL ARB. After 30 min pre-incubation at 37 °C, 2 μL BODIPY® FL C_5-labeled sphingomyelin (Molecular Probes, Leiden, Netherlands) in ARB (62.5 μg/mL) was added and 60 min incubated at 37 °C. Enzymatic activity was stopped by adding 150 μL methanol containing BODIPY® FL C_5-pentanoic acid (42 ng/mL).

4.6.4. HPLC separation and turnover quantification

Samples were transferred into brown 1.5 mL HPLC vials, 600 μL methanol containing BODIPY® FL C_5-pentanoic acid (21 ng/mL) and 90 μL 100 mM Tris-HCl pH 7.5 were added and mixed well. 50 μL of the mixture were injected into a HPLC-column (Merck LiChrosphere RP 18, 125 mm/4 mm) using an auto sampler Spark Promis II (Spark, Friedrichsdorf, Germany) and separated on an isocratic solvent system. Mobile phase: 90% methanol and 10% 100 mM Tris-HCl pH 7.5 (V/V), flow rate: 2 mL/min, Merck Hitachi HPLC-pump L6200 A (Merck, Darmstadt, Germany), fluorescence detection with a Shimadzu RF–535 fluorescence detector (Shimadzu, Duisburg, Germany) at experimentally determined wavelengths of 505 nm (excitation) and 512 nm (emission) (BODIPY® FL C_5-pentanoic acid in mobile phase). Reference for BODIPY®-FL-C_5-Fluorophor solution in methanol: 505 ± 3 nm (excitation) and 512 ± 4 nm (emission) [63]. Retention volumes: BODIPY® FL-C_5-pentanoic acid (calibrator) – 1.4 mL; BODIPY® FL C_5–ceramide (product) – 4.3 mL; BODIPY® FL C_5-sphingomyelin (substrate) – 9.3 ml. The resulting amount of BODIPY® FL C_5 –ceramide is proportional to enzyme activity at conversion rates of less than 15% of substrate and can be calculated using fluorescence (AUC); activity of a particular compound is given as median ± *SE*, determined as triplicates.

4.7. Ceramide quantification

4.7.1. Cell culture

Six to eight days after isolation PMBC were transferred to CELLSTAR® cell culture 6-well plates (9.6 cm^2, Greiner bio-one, Frickenhausen, Germany) and cultivated in 2 mL full supplemented RPMI-1640 medium (PAA, Cölbe, Germany). After medium exchange (1 mL) prior to incubation, PBMC were pre-incubated 30 min with 10 μM NB 06 (**23**) (diluted in unsupplemented medium) if **23** is applied. Macrophages then were treated 4 h with TNFalpha (3 ng/mL) and mmLDL (54 μg/mL) (Fig. 1A and B) or 4 h with 10 μM exogene C_6-ceramide and 10 μM C_2-dihydroceramide (Fig. 1C and D). Lipid extraction, purification and ceramide quantification was performed by HPLC-analysis as described in the section *ceramide quantification* using 7-(diethylamino)coumarin-3-carbonyl azide for ceramide labeling and 100 pmol C_8-ceramide as internal standard [28].

4.7.2. Lipid extraction

Lipid extraction was performed according to the method of Bligh and Dyer [64]. After incubation, cells were isolated and washed twice with ice-cold PBS, 500 μL ice-cold PBS added, cells scraped off the plates (after addition of PBS), transferred to 1.5 mL tubes (Eppendorf, Hamburg, Germany), centrifuged, the PBS supernatant carefully removed, re-suspended in 150 μL methanol and cellular lipids extracted or the pellet stored at −80 °C. The resulting crude lipid extract was split in 50 μL (lipid phosphate quantification) and 100 μL (ceramide analysis). Phosphate quantification was performed according to Jenkins and Hannun [65]. To separate ceramides from other (sphingo-)lipids, the crude extract was separated on a 0.2 mm silica gel 60 F_{254} coated TLC plate (Merck, Darmstadt, Germany) using a 6:4:1 (*v/v*) chloroform/methanol/water mixture as mobile phase. Exogenous ceramides were used as TLC-plate marker and detected separately in an iodine chamber. Ceramide bands (cellular lipids) were scraped off from the plate and transferred to Poly-Prep Columns (BIO-RAD, Munich, Germany), eluted with chloroform (3 × 250 μL) and finally with 250 μL methanol. Glycerolipid/monoacylglycerol impurities were removed by alkaline hydrolysis in 0.03 M NaOH in 90% ethanol at 37 °C for 30 min. After neutralization, a 2nd Bligh and Dyer lipid extraction was performed. Finally the organic phase was dried over water free sodium sulphate and evaporated to dryness.

4.7.3. Ceramide labeling and HPLC separation

An optimized HPLC method [28] was used based on conditions of Moersel [66] and Balestrieri [67] to achieve best performance in terms of sensitivity and ceramide species separation. Solutions containing 100 pmol reference C_8-ceramide (sample calibration) and ceramides obtained from cellular lipid extracts (equivalent to 5–10 nmol lipid phosphate) or 5, 10, 25, 50, 100, 250 and 500 pmol C_{16}-Ceramide (calibration curve) were transferred to sealed borosilicate glass vials with 100 μL inset (VWR, Darmstadt, Germany), solvents evaporated (SpeedVac Concentrator, Eppendorf, Hamburg, Germany), residue re-suspended in 10 μL 0.3 mg/mL 7-(diethylamino)coumarin-3-carbonyl azide (DECCA) in toluene and heated (6 h, 80 °C) under shaking. After cooling to room temperature and solvent evaporation (SpeedVac Concentrator, Eppendorf, Hamburg, Germany), the orange-red residue was dissolved in 50 μL acetonitrile HPLC grade and subjected to HPLC separation. Labeled cellular ceramides were separated on a LiChrospher 100 (5 μm) 250-4 RP-18 HPLC-Column (Merck, Darmstadt, Germany) with 10 μL injection volume (auto sampler Spark Promis II (Spark, Friedrichsdorf, Germany) with a gradient solvent system: acetonitrile-methanol-ethyl acetate composition (*v/v*): 0.0–10.0 min: isocratic 50:45:5; 10.0–15.0 min to 45:50:5; 15.0–20.0 min to 40:50:10; 20.0–60.0 min to 30:50:20; 60.0–65.0 to return to starting conditions; 65.0–80.0 equilibration at starting conditions prior to subsequent injection (flow rate: 1 mL/min, Merck Hitachi HPLC-pump L6200 A (Merck, Darmstadt, Germany), fluorescence detection with a Shimadzu RF–535 fluorescence detector (Shimadzu,

Please cite this article in press as: M. Blaess, et al., NB 06: From a simple lysosomotropic aSMase inhibitor to tools for elucidating the role of lysosomes in signaling apoptosis and LPS-induced inflammation, European Journal of Medicinal Chemistry (2017), https://doi.org/10.1016/j.ejmech.2017.09.021

Duisburg, Germany) at an experimentally determined excitation wavelength of 380 nm and emission wavelength of 475 nm).

4.8. Oligoncleotide array

4.8.1. Cell culture

Mono-Mac-6 cells (10×10^6 cells) were incubated 1, 2, 4 or 6 h with 1 ng/mL LPS (*E. coli* serotype 0111:B4) (Sigma-Aldrich, Deisenhofen, Germany), w/o 5 μM **23** (NB 06) (pre-incubation 30 min) or with 5 μM **23** (NB 06) alone (without LPS). Cells were pre incubated 30 min with 5 μM **23** (NB 06) (diluted in not supplemented medium) if **23** was applied.

4.8.2. totalRNA sample preparation

Mono-Mac-6 cells were collected, washed once with ice-cold PBS, thoroughly lysed in 3 mL lysis buffer and total RNA was extracted using RNeasy® Mini Spin Columns (Qiagen, Hilden, Germany) or TriPure® Isolation Reagent (Roche Diagnostics, Mannheim, Germany) according to manufactures instructions. RNA yield was determined spectrophotometrically on a NanoDrop ND-1000 Spectro-Photometer (NanoDrop Technologies, Wilmington, USA) by measuring absorbance at 260 and 280 nm. All RNA samples used for microarray analysis were analyzed by an ethidium bromide-stained RNA agarose gel or on a Bioanalyzer® 2100 (Agilent Technologies, Boeblingen, Germany) to confirm purity and integrity of RNA.

4.8.3. Oligoncleotide array hybridization

Experiments were performed using the Lab-Arraytor® inflammation microarray oligonucleotide microarray (SIRS-Lab, Jena Germany), comprising 800 probes (each spotted as triple replicates) addressing 780 transcripts corresponding to inflammation as well as 20 reliable control probes (see associated content/supplementary data: “Microarray Experiment Description” online according to Minimal Information about a Microarray Experiment guidelines (MIAME), Gene Expression Data Society MGED) [68]. 10 μg totalRNA were reverse transcribed using Superscript-II reverse transcriptase (Invitrogen, Karlsruhe, Germany) in the presence of aminoallyl-dUTP (Sigma-Aldrich, Deisenhofen, Germany) and labeled using the DYOMICS DY-547/647-S-NHS system (DYOMICs, Jena, Germany). DYOMICS DY-547-S-NHS labeled cDNA from untreated control cells were co-hybridized with DYOMICS DY-647-S-NHS labeled cDNA obtained from the same amount of total RNA isolated from treated cells. After 10 h incubation at 42 °C in a hybridization apparatus (HS 400, TECAN, Crailsheim, Germany) using a formamide-based hybridization buffer system arrays were washed according to the manufacturer's instructions, dried and hybridization signal intensities were read out immediately using an Axon 4000B scanner (Axon Instruments, Foster City, USA). Microarray data pre-processing of hybridization signals included i) spot detection and background subtraction, ii) spot flagging according to defined signal-to-noise threshold values, iii) normalization and transformation of signals obtained from different channels. For the former two steps, GenePix® 5.0 Analysis Software 5.0 (Axon Instruments, Foster City, USA) was used; for the third step we applied the approach from Huber and colleagues [69,70].

4.9. Quantitative real-time PCR

4.9.1. cDNA synthesis

First-strand complementary DNA (cDNA) synthesis was performed with 2 μg of isolated totalRNA from Mono-Mac-6 cells (also used for hybridization experiments) according to the manufacturer's instructions. After adjusting total RNA volume to 11 μL, 1 μL oligo-d$(T)_{12\text{-}18}$-primer solution (2.5 μg/μL) was added, denatured at 70 °C in a PTC-200 DNA Engine (Bio-Rad, Munich, Germany) for 10 min and chilled on ice for 5 min. 8 μL RT-Mix (4 μL reaction-buffer 5x, 1 μL RiboLock® RNAse-inhibitor 20 U/μL), 1 μL Revert Aid Reverse Transcriptase® (200 U/μL), 2 μL 10 mM dNTP stock solution (10 mM dATP, 10 mM dGTP, 10 mM dCTP, 10 mM dTTP) (Thermo Scientific Molecular Biology, St. Leon-Rot, Germany) were added, mixed and incubated 60 min at 42 °C. Reverse Transcriptase was then inactivated by incubation at 70 °C for 5 min.

4.9.2. Quantitative real-time PCR

Real-time PCR was performed in a Rotor-Gene® RG-6000 (Qiagen, Hilden, Germany) equipped with a 72-well carousel and 0.1 mL strip tubes and caps (Qiagen, Hilden, Germany). Reaction volume (10 μL, containing 30 ng cDNA) consists of 4 μL diluted cDNA-solution (7.5 ng/μL), 1 μL 0.1 μM gene specific forward and reverse primer solution (1 pMol each) (Biomers, Ulm, Germany) and QuantiTect® SYBR Green PCR Kit (Qiagen, Hilden, Germany). According to manufacturer recommendations, a cycling program with an initial activation step (94 °C, 15 min) followed by 45 cycles of denaturation (94 °C, 30 s), annealing (55 °C, 30 s) and elongation (72 °C, 30 s) was executed. Fluorescence acquisitions in the SYBR® green and ROX® (internal reference dye) channels were performed at the end of the annealing step. Melting protocol ranged from 50 °C to 95 °C following a stepwise increment of 1.0 °C held for 5 s. Each sample as well as a negative template control (NTC) was amplified in triplet for each of the primer pairs assayed. Raw data (ct-values) were extracted using Rotor-Gene software® (version 2.3.1) (Qiagen, Hilden, Germany).

4.9.3. Primer design, synthesis, data read out and sequences

Gene specific primers (18–22 bp length) were designed by use of Primer 3 software version 0.4.0 (MIT Center for Genome Research) (http://frodo.wi.mit.edu/cgi-bin/primer3/primer3_www.cgi) to obtain an annealing temperature of 55 °C and an amplicon length between 50 and 150 bp (up to 250 bp if necessary) [71]. Gene- and species-specificity was tested using NCBI nucleotide database, nucleotide blast, interrogation mode “blastn” (National Center for Biotechnology Information, Bethesda).

4.9.4. Raw data extraction, normalization software/reference genes

Raw data extraction and calculation of relative gene expression of genes investigated was performed using Delta Delta CT application in the Rotor-Gene software® (version 2.3.1) (Qiagen, Hilden, Germany). Primer efficiency was determined for each primer by a cleaned up PCR-product dilution series (QIAquick® PCR Purification Kit, Qiagen, Hilden, Germany). GAPDH was chosen as a reference gene for normalization of relative gene expression of each gene. It was selected as the most stable gene of all tested genes by “NormFinder”-algorithm [72]. Stability value was calculated as 0.352 ± 0.083.

4.9.5. Primer sequences

Each primer is characterized by the following characteristic features: symbol/gene/gene bank Accession/primer sequence forward (5′–3′) (fw), reverse (5′–3′) (rev) and amplicon size. Genes of interest displayed: **CXCL2**: C-X-C motif chemokine ligand 2 (CXCL2); NM_002089.3; fw: GAC CAG AAG GAA GGA GGA AGC; rv: TCA AAC ACA TTA GGC GCA AGC; 124 bp. **IL23A**: Interleukin 23, alpha subunit p19 (IL23A); NM_016584.2; fw: ACG CGC TGA ACA GAG AGA AT; rv: CAG CAG CAT TAC AGC TCT GC; 139 bp. **IL6**: Interleukin 6, NM_000600.4 (transcript variant 1); fw: CTG CGC AGC TTT AAG GAG TT; rv: GAG GTG CCC ATG CTA CAT TT; 69 bp. T**NFalpha**: Tumor Necrosis Factor alpha; NM_000594.3; fw: ATG AGC ACT GAA AGC ATG ATC C; rev: GAG GGC TGA TTA GAG AGA GGT C; 217 bp. Reference Gene for normalization: **GAPDH**:

Please cite this article in press as: M. Blaess, et al., NB 06: From a simple lysosomotropic aSMase inhibitor to tools for elucidating the role of lysosomes in signaling apoptosis and LPS-induced inflammation, European Journal of Medicinal Chemistry (2017), https://doi.org/10.1016/j.ejmech.2017.09.021

Glyceraldehyd-3-Phosphat-dehydrogenase; NM_002046.5; fw: CTC TGC TCC TCC TGT TCG AC; rev: CAA TAC GAC CAA ATC CGT TGA C; 116 bp.

4.9.6. Statistics

Preprocessing and statistical analysis of microarray gene expression data was performed using the statistical software R in combination with Bioconductor [73,74] and our R package "SLmisc" [40]. For more detailed information about microarray statistical data evaluation we refer to associated content/supplementary data. Statistical significance was investigated using one-way ANOVA in combination with post-hoc t-Tests and Bonferroni's correction for multiple testing, $P < 0.0001$ (1-way ANOVA); significantly different was considered if $P < 0.05$. For more details refer to supplementary data section.

4.10. Calculation of lipophilicity (log P - value)s

Values were calculated using ACD/log P Version 1.0 under Windows 98. Confidence level (p-value) of figures given here is 95%.

Abbreviations used

apc, percentage of apoptotic cells; aSMase, acid spingomyelinase; ACE-Cl, 1-chloroethyl chloroformate; LPS, lipopolysaccharide; mLDL, modified low density lipoprotein; mmLDL, minimally modified low density lipoprotein; *n*-BuLi, *n*-Butyllithium; nSMase, neutral sphingomyelinase; PBMC, peripheral blood mononuclear cells; RT, room temperature; TIBA, triisobutylalumane.

Author contributions

N.B. synthesized compounds; H.P.D. designed compounds; M.B. performed ceramide quantification, aSMase quantification and method development, quantitative RT-PCR, apoptosis and hybridization experiments, individual syntheses; M.K. performed statistical analysis of quantification and hybridization experiments; R.K. supported apoptosis experiments and writing the manuscript; G.A.B. performed analysis of apoptosis experiments; R.A.C. supported cell culture, quantitative real-time PCR and hybridization experiments; M.B. and H.P.D. wrote the manuscript.

Author disclosure statement

The authors declare no competing financial interest. This research did not receive any specific grant from funding agencies in the public, commercial, or not-for-profit sectors.

Acknowledgement

We gratefully acknowledge contributions to discussion and process optimization by former Ph.D. students Dr. Stefan Mueller and graduate students Tobias Nohe and Alexander Schaeffer. We thank Edith Walther for tremendous technical support in cell culture and sample preparation, Heiko Rudy and Peter Weyrich for performing mass spectrometry and analytical chemistry, Dr. Julien Landré for his experimental advice in quantitative real-time PCR and primer design, Petra and Peter Bauer organizing the "sea view office", the staff at Apotheke im Markt, Heidelberg, and especially Victoria Letté for their support during the preparation of the manuscript.

Appendix A. Supplementary data

Supplementary data associated with this article can be found in the online version, at https://doi.org/10.1016/j.ejmech.2017.09.021. These data include MOL files and InChiKeys of the most important compounds described in this article.

References

[1] B. Huppertz, H.-G. Frank, P. Kaufmann, The apoptosis cascade - morphological and immunohistochemical methods for its visualization, Anat. Embryol. 200 (1999) 1–18.
[2] D. Steinberg, A. Lewis, Conner memorial lecture: oxidative modification of LDL and Atherogenesis, Circulation 95 (1997) 1062–1071.
[3] M.P.J. de Winther, K.W. van Dijk, L.M. Havekes, M.H. Hofker, Macrophage scavenger receptor class A: a Multifunctional receptor in Atherosclerosis, Arterioscler. Thromb. Vasc. Biol. 20 (2000) 290–297.
[4] H.P. Deigner, R. Claus, G.A. Bonaterra, C. Gehrke, N. Bibak, M. Blaess, M. Cantz, J. Metz, R. Kinscherf, Ceramide induces aSMase expression: implications for oxLDL-induced apoptosis, FASEB J. 15 (2001) 807–814.
[5] A. Loidl, E. Sevcsik, G. Riesenhuber, H.P. Deigner, A. Hermetter, Oxidized Phospholipids in minimally modified low density Lipoprotein induce Apoptotic signaling via activation of acid Sphingomyelinase in arterial smooth muscle cells, J. Biol. Chem. 278 (2003) 32921–32928.
[6] L. Monney, R. Olivier, I. Otter, B. Jansen, G.G. Poirier, C. Borner, Role of an acidic compartment in tumor-necrosis-factor-alpha-induced production of ceramide, activation of caspase-3 and apoptosis, Eur. J. Biochem. 251 (1998) 295–303.
[7] B.J. Pettus, C.E. Chalfant, Y.A. Hannun, Ceramide in apoptosis: an overview and current perspectives, Biochim. Biophys. Acta Mol. Cell Biol. Lipids 1585 (2002) 114–125.
[8] J.R. Van Brocklyn, J.B. Williams, The control of the balance between ceramide and sphingosine-1-phosphate by sphingosine kinase: oxidative stress and the seesaw of cell survival and death, Comp. Biochem. Physiol. Part B Biochem. Mol. Biol. 163 (2012) 26–36.
[9] M.N. Nikolova-Karakashian, K.A. Rozenova, Ceramide in stress response, Adv. Exp. Med. Biol. 688 (2010) 86–108.
[10] S.A. Saddoughi, B. Ogretmen, Diverse functions of ceramide in cancer cell death and proliferation, Adv. Cancer Res. 117 (2013) 37–58.
[11] B. Stancevic, R. Kolesnick, Ceramide-rich platforms in transmembrane signaling, FEBS Lett. (584) (2010) 1728–1740.
[12] M. Blaess, H. Le, R. Claus, M. Kohl, H.-P. Deigner, Stereospecific induction of apoptosis in tumor cells via endogenous C_{16}-ceramide and distinct transcripts, Cell Death Discov. 1 (2015) 15013.
[13] T. Kolter, K. Sandhoff, Lysosomal degradation of membrane lipids, FEBS Lett. 584 (2010) 1700–1712.
[14] H.B. Simpson, F.R. Schneier, R.B. Campeas, R.D. Marshall, B.A. Fallon, S. Davies, D.F. Klein, M.R. Liebowitz, Imipramine in the treatment of social phobia, J. Clin. Psychopharmacol. 18 (1998) 132–135.
[15] J. Kornhuber, P. Tripal, M. Reichel, L. Terfloth, S. Bleich, J. Wiltfang, E. Gulbins, Identification of new functional inhibitors of acid Sphingomyelinase using a Structure–Property–Activity relation model, J. Med. Chem. 51 (2008) 219–237.
[16] M. Kölzer, N. Werth, K. Sandhoff, Interactions of acid sphingomyelinase and lipid bilayers in the presence of the tricyclic antidepressant desipramine, FEBS Lett. 559 (2004) 96–98.
[17] S. Albouz, F. Le Saux, D. Wenger, J.J. Hauw, N. Baumann, Modifications of sphingomyelin and phosphatidylcholine metabolism by tricyclic antidepressants and phenothiazines, Life Sci. 38 (1986) 357–363.
[18] R. Hurwitz, K. Ferlinz, K. Sandhoff, The Tricyclic antidepressant Desipramine causes proteolytic degradation of lysosomal sphingomyelinase in human fibroblasts, Biol. Chem. Hoppe-Seyler 375 (1994) 447–450.
[19] M. Masson, B. Spezzatti, J. Chapman, C. Battisti, N. Baumann, Calmodulin antagonists chlorpromazine and W-7 inhibit exogenous cholesterol esterification and sphingomyelinase activity in human skin fibroblast cultures, Similarities between drug-induced and niemann-pick type C lipidoses, J. Neurosci. Res. 31 (1992) 84–88.
[20] J. Kornhuber, P. Tripal, M. Reichel, C. Mühle, C. Rhein, M. Muehlbacher, T.W. Groemer, E. Gulbins, Functional inhibitors of acid Sphingomyelinase (FIASMAs): a novel pharmacological group of drugs with broad clinical applications, Cell. Physiol. Biochem. 26 (2010) 9–20.
[21] R.A. Olofson, D.E. Abbott, Tests of a piperidino mask for the protection of functionalized carbon sites in multistep syntheses, J. Org. Chem. 49 (1984) 2795–2799.
[22] A.D. McNaught, A. Wilkinson, Compendium of Chemical Terminology - the Gold Book, Blackwell Science, Oxford, 1997.
[23] R.L. Thomas, C.M. Matsko, M.T. Lotze, A.A. Amoscato, Mass spectrometric identification of increased C_{16} Ceramide levels during Apoptosis, J. Biol. Chem. 274 (1999) 30580–30588.
[24] X. He, N. Okino, R. Dhami, A. Dagan, S. Gatt, H. Schulze, K. Sandhoff, E.H. Schuchman, Purification and characterization of recombinant, human acid ceramidase. Catalytic reactions and interactions with acid

sphingomyelinase, J. Biol. Chem. 278 (2003) 32978–32986.
[25] S. Ohkuma, B. Poole, Fluorescence probe measurement of the intralysosomal pH in living cells and the perturbation of pH by various agents, Proc. Natl. Acad. Sci. U. S. A. 75 (1978) 3327–3331.
[26] G.L. Chen, S.L. Sutrina, K.L. Frayer, W.W. Chen, Effects of lysosomotropic agents on lipogenesis, Arch. Biochem. Biophys. 245 (1986) 66–75.
[27] S. Cassell, J. Edwards, D.T. Brown, Effects of lysosomotropic weak bases on infection of BHK-21 cells by Sindbis virus, J. Virol. 52 (1984) 857–864.
[28] M. Blaess, R.A. Claus, H.-P. Deigner, HPLC separation and ultrasensitive optical quantification of ceramide species applying 7-(diethylamino)coumarin-3-carbonyl azide derivatisation, J. Chromatogr. B Anal. Technol. Biomed. Life Sci. 986–987 (2015) 123–128.
[29] M. Kohl, R-Package "SLmisc: Miscellaneous Functions for Analysis of Gene Expression Data at SIRS-lab GmbH", 2007. https://cran.r-project.org/src/contrib/Archive/SLmisc/.
[30] R. Tibshirani, G. Walther, T. Hastie, Estimating the number of clusters in a data set via the gap statistic, J. R. Stat. Soc. Ser. B Stat. Methodol. 63 (2001) 411–423.
[31] J.W. Griffith, C.L. Sokol, A.D. Luster, Chemokines and Chemokine receptors: positioning cells for host defense and immunity, Annu. Rev. Immunol. 32 (2014) 659–702.
[32] E. Magrini, A. Mantovani, C. Garlanda, The dual complexity of PTX3 in health and disease: a balancing act? Trends Mol. Med. 22 (2016) 497–510.
[33] R. Kurumbail, Cyclooxygenase enzymes: catalysis and inhibition, Curr. Opin. Struct. Biol. 11 (2001) 752–760.
[34] H.F. Tiano, C.D. Loftin, J. Akunda, C.A. Lee, J. Spalding, A. Sessoms, D.B. Dunson, E.G. Rogan, S.G. Morham, R.C. Smart, R. Langenbach, Deficiency of either cyclooxygenase (COX)-1 or COX-2 alters epidermal differentiation and reduces mouse skin tumorigenesis, Cancer Res. 62 (2002) 3395–3401.
[35] L. Yang, R.M. Froio, T.E. Sciuto, A.M. Dvorak, R. Alon, F.W. Luscinskas, ICAM-1 regulates neutrophil adhesion and transcellular migration of TNF-alpha-activated vascular endothelium under flow, Blood 106 (2005) 584–592.
[36] B. Memari, M. Bouttier, V. Dimitrov, M. Ouellette, M.A. Behr, J.H. Fritz, J.H. White, Engagement of the aryl hydrocarbon receptor in mycobacterium tuberculosis–infected macrophages has pleiotropic effects on innate immune signaling, J. Immunol. 195 (2015) 4479–4491.
[37] F. Schaper, S. Rose-John, Interleukin-6: biology, signaling and strategies of blockade, Cytokine Growth Factor Rev. 26 (2015) 475–487.
[38] T. Hehlgans, K. Pfeffer, The intriguing biology of the tumour necrosis factor/tumour necrosis factor receptor superfamily: players, rules and the games, Immunology 115 (2005) 1–20.
[39] J. Wolf, S. Rose-John, C. Garbers, Interleukin-6 and its receptors: a highly regulated and dynamic system, Cytokine 70 (2014) 11–20.
[40] R. Salomão, P.S. Martins, M.K.C. Brunialti, M. da L. Fernandes, L.S.W. Martos, M.E. Mendes, N.E. Gomes, O. Rigato, TLR signaling pathway in patients with sepsis, Shock 30 (Suppl 1) (2008) 73–77.
[41] H. Manchanda, N. Seidel, M. Blaess, R. Claus, J. Linde, H. Slevogt, A. Sauerbrei, R. Guthke, M. Schmidtke, Differential Biphasic Transcriptional host response associated with coevolution of hemagglutinin quasispecies of influenza A virus, Front. Microbiol. 7 (2016) 1167.
[42] K.E. Nograles, J.G. Krueger, Anti-cytokine therapies for psoriasis, Exp. Cell Res. 317 (2011) 1293–1300.
[43] R.S. Vardanyan, V.J. Hruby, Antidepressants, in: Synthesis of Essential Drugs, Elsevier, Amsterdam, 2006, pp. 103–116.
[44] R.J. Bridgewater, C.W. Shoppee, 353. Steroids and walden inversion. Part XI. Acetolysis of the coprostanyl halides, J. Chem. Soc. 241 (1953) 1709–1715.
[45] S.M. Husbands, S. Izenwasser, T. Kopajtic, W.D. Bowen, B.J. Vilner, J.L. Katz, A.H. Newman, Structure–Activity relationships at the Monoamine transporters and σ receptors for a novel series of 9-[3-(cis -3, 5-Dimethyl-1-piperazinyl)-propyl]carbazole (Rimcazole) analogues, J. Med. Chem. 42 (1999) 4446–4455.
[46] N. Cheetham, I. McNaught, A. Pullin, Donor-acceptor complexes formed by perfluoro-organo bromides and iodides with nitrogen and other bases. IV. Analysis of the infrared spectra of CF3I.N(CH3)3 and CF3Br.N(CH3)3 and related complexes, Aust. J. Chem. 27 (1974) 987–1007.
[47] K.J. Rajendra Prasad, C.S. Vijayalakshmi, Synthesis of 4-Methyl-1-oxo-tetrahydrocarbazole, Indian J. Chem. 33B (1994) 481–482.
[48] K. Sonogashira, Y. Tohda, N. Hagihara, A convenient synthesis of acetylenes: catalytic substitutions of acetylenic hydrogen with bromoalkenes, iodoarenes and bromopyridines, Tetrahedron Lett. 16 (1975) 4467–4470.
[49] T. Bach, L. Krüger, Sequential Pd(0)-catalyzed reactions for the construction of multiple substituted furans. A short synthesis of the F5 furan fatty acid1a, Tetrahedron Lett. 39 (1998) 1729–1732.
[50] A. Pelter, M. Rowlands, G. Clements, Cross-coupling reactions for the preparation of 2-Arylfurans, 2-Benzylfuran and 2-Cinnamylfuran, Synthesis 01 (1987) 51–53.
[51] E. Negishi, A.O. King, N. Okukado, Selective carbon-carbon bond formation via transition metal catalysis. 3. A highly selective synthesis of unsymmetrical biaryls and diarylmethanes by the nickel- or palladium-catalyzed reaction of aryl- and benzylzinc derivatives with aryl halides, J. Org. Chem. 42 (1977) 1821–1823.
[52] M. Iyoda, M. Sakaitani, H. Otsuka, M. Oda, Synthesis of riccardin B by nickel-catalyzed intramolecular cyclization, Tetrahedron Lett. 26 (1985) 4777–4780.
[53] Y. Kojima, S. Wakita, N. Kato, Syntheses of 3-substituted furans via lithium di(3-furyl)cuprate—the application of lithium di(3-furyl)cuprate to the total synthesis of dendrolasin, Tetrahedron Lett. 20 (1979) 4577–4580.
[54] M.W. Haenel, A. Flatow, V. Taglieber, H.A. Staab, Neue synthese von [3.3] paracyclophanen. Diastereomere donor-akzeptor-[3.3]paracyclophane, Tetrahedron Lett. 18 (1977) 1733–1736.
[55] J.H. Wood, C.S. Colburn, L. Cox, H.C. Garland, 2,5-Dihydroxy-p-benzenediacetic acid and related compounds from p-benzoquinone1, J. Am. Chem. Soc. 66 (1944) 1540–1542.
[56] R.J. Havel, H.A. Eder, J.H. Bragdon, The distribution and chemical composition of ultracentrifugally separated lipoproteins in human serum, J. Clin. Invest 34 (1955) 1345–1353.
[57] J. Himber, E. Bühler, D. Moll, U.K. Moser, Low density lipoprotein for oxidation and metabolic studies. Isolation from small volumes of plasma using a tabletop ultracentrifuge, Int. J. Vitam. Nutr. Res. 65 (1995) 137–142.
[58] G.L. Peterson, A simplification of the protein assay method of Lowry et al. which is more generally applicable, Anal. Biochem. 83 (1977) 346–356.
[59] S.C. Rumsey, A.F. Stucchi, R.J. Nicolosi, H.N. Ginsberg, R. Ramakrishnan, R.J. Deckelbaum, Human plasma LDL cryopreserved with sucrose maintains in vivo kinetics indistinguishable from freshly isolated human LDL in cynomolgus monkeys, J. Lipid Res. 35 (1994) 1592–1598.
[60] A.D. Watson, J.A. Berliner, S.Y. Hama, B.N. La Du, K.F. Faull, A.M. Fogelman, M. Navab, Protective effect of high density lipoprotein associated paraoxonase. Inhibition of the biological activity of minimally oxidized low density lipoprotein, J. Clin. Invest 96 (1995) 2882–2891.
[61] M. El-Saadani, H. Esterbauer, M. El-Sayed, M. Goher, A.Y. Nassar, G.A. Jürgens, Spectrophotometric assay for lipid peroxides in serum lipoproteins using a commercially available reagent, J. Lipid Res. 30 (1989) 627–630.
[62] L.E. Quintern, K. Sandhoff, Human acid sphingomyelinase from human urine, Methods Enzymol. 197 (1991) 536–540.
[63] R.P. Haugland, in: I.D. Johnson, M.T.Z. Spence, R.P. Haugland (Eds.), The Handbook: a Guide to Fluorescent Probes and Labeling Technologies, tenth ed., Molecular Probes, Eugene, 2005 p Chapter 13.3.
[64] E.G. Bligh, W.J. Dyer, A rapid method of total lipid extraction and purification, Can. J. Biochem. Physiol. 37 (1959) 911–917.
[65] G.M. Jenkins, Y.A. Hannun, Sphingolipids as messengers of cell death, in: G.P. Studzinski (Ed.), Apoptosis: a Practical Approach, Oxford Press, New York, 1999, pp. 105–123.
[66] J.-T. Mörsel, D. Schmiedl, Determination of 2-alkylcyclobutanone using fluorescent labeling, Fresenius' J. Anal. Chem. 349 (1994) 538–541.
[67] C. Balestrieri, G. Camussi, A. Giovane, E.L. Iorio, L. Quagliuolo, L. Servillo, Measurement of Platelet-Activating factor Acetylhydrolase activity by quantitative high-performance liquid chromatography determination of Coumarin-Derivatized 1-O-Alkyl-2-sn-lysoglyceryl-3-phosphorylcholine, Anal. Biochem. 233 (1996) 145–150.
[68] A. Brazma, P. Hingamp, J. Quackenbush, G. Sherlock, P. Spellman, C. Stoeckert, J. Aach, W. Ansorge, C.A. Ball, H.C. Causton, T. Gaasterland, P. Glenisson, F.C.P. Holstege, I.F. Kim, V. Markowitz, J.C. Matese, H. Parkinson, A. Robinson, U. Sarkans, S. Schulze-Kremer, J. Stewart, R. Taylor, J. Vilo, M. Vingron, Minimum information about a microarray experiment (MIAME) toward standards for microarray data, Nat. Genet. 29 (2001) 365–371.
[69] W. Huber, A. von Heydebreck, H. Sueltmann, A. Poustka, M. Vingron, Variance stabilization applied to microarray data calibration and to the quantification of differential expression, Bioinformatics 18 (Suppl 1) (2002) S96–S104.
[70] W. Huber, A. von Heydebreck, H. Sueltmann, A. Poustka, M. Vingron, Parameter estimation for the calibration and variance stabilization of microarray data, Stat. Appl. Genet. Mol. Biol. 2 (2003). Article3.
[71] S. Rozen, H. Skaletsky, Primer3 on the WWW for general users and for biologist programmers, Methods Mol. Biol. 132 (2000) 365–386.
[72] C.L. Andersen, J.L. Jensen, T.F. Ørntoft, Normalization of real-time quantitative reverse Transcription-PCR data: a model-based variance estimation approach to identify genes suited for normalization, applied to bladder and colon cancer data sets, Cancer Res. 64 (2004) 5245–5250.
[73] R Development Core Team, R: a Language and Environment for Statistical Computing, R Foundation for Statistical Computing, Vienna, 2014. http://www.R-project.org.
[74] R.C. Gentleman, V.J. Carey, D.M. Bates, B. Bolstad, M. Dettling, S. Dudoit, B. Ellis, L. Gautier, Y. Ge, J. Gentry, K. Hornik, T. Hothorn, W. Huber, S. Iacus, R. Irizarry, F. Leisch, C. Li, M. Maechler, A.J. Rossini, G. Sawitzki, C. Smith, G. Smyth, L. Tierney, J.Y. Yang, J. Zhang, Bioconductor: open software development for computational biology and bioinformatics, Genome Biol. 5 (2004) R80.

Please cite this article in press as: M. Blaess, et al., NB 06: From a simple lysosomotropic aSMase inhibitor to tools for elucidating the role of lysosomes in signaling apoptosis and LPS-induced inflammation, European Journal of Medicinal Chemistry (2017), https://doi.org/10.1016/j.ejmech.2017.09.021